

## ABSTRACT

Central pit craters are impact craters that contain central depressions, either in the crater floor or superposed on a central rise. Examples of these craters have been found broadly distributed on Mars. Using images from the Mars Reconnaissance Orbiter Context Camera and High Resolution Stereo Camera, a set of central pit craters of Hesperian or Amazonian age were found to have interior valleys draining into their central pits. This study characterizes these features and their formation processes.

The networks were found to be sinuous and often have extensive, preserved tributaries. These tributary systems are often dendritic and originate from various elevations, including the tops of crater rims. The fluxes of the interior valleys are similar to those of rivers found on Earth, but are formed within relatively small watersheds.

In addition, other features have been found within these craters during the course of this study. They include alluvial fans on crater walls, paleo-lakes on crater rims and within the central pits, and deltas located at the termini of the valley systems. The formation of these valleys and related features implies that water was an important geomorphologic agent on Mars even during the Hesperian and Amazonian, when Mars is commonly thought to have been largely a frozen, hyperarid planet.

INVESTIGATION OF THE INTERIOR VALLEY NETWORKS OF CENTRAL  
PIT CRATERS ON MARS: CHARACTERISTICS AND FORMATION  
PROCESSES

By  
Samantha E. Peel

Advisors:

M. Darby Dyar  
Caleb I. Fassett

A Thesis Submitted to the Department of Astronomy, Mount Holyoke College, in  
Partial Fulfillment of the Requirements for the Degree of Bachelors of Arts with  
Honors

May, 2012

*For Mom*  
*You trump them all*

## ACKNOWLEDGEMENTS

I would like to thank the geology department for rescuing a lost (future) science major in her freshman year from majoring in the humanities and reminding me of what I really enjoy. Michelle Markley, you will always be my hero for that.

I would also like to thank Darby Dyar for responding to a tentative email sent from an unknown student and allowing that correspondence to grow into a three-year relationship of support and guidance. Your wisdom and kindness cannot be described with words. You're awesome and I could never thank you enough.

Thanks must also go to Caleb Fassett for his willingness to advise me on this thesis. Without you, this simply would not exist. You've guided me through this so wonderfully, I am incredibly grateful.

Al Werner must also be thanked for being willing to take on my thesis as a part of my committee with very little notice. Thank you so much for being willing to do this and for being a wonderful professor.

And finally, I would like to thank my family and friends for all their support. Without you all I just wouldn't be me. And that I never want to imagine.

## TABLE OF CONTENTS

List of Figures .....	v
List of Tables .....	vii
1. Introduction .....	001
2. Background .....	003
2.1 Water on Mars .....	003
2.1.1 Evidence for Water .....	003
2.1.2 Features Related to Fluid Flow in the History of Mars .....	006
2.1.2.1 Gullies .....	006
2.1.2.2 Valley Networks .....	007
2.1.2.3 Deposition Features Related to Fluvial Features .....	008
2.1.3 Models for the Formation of Water Features .....	013
2.2 Central Pit Craters .....	016
2.2.1 Formation Models for Central Pit Craters .....	017
2.2.2 Current Unknowns Concerning Pit Crater Formation .....	019
3. Methods .....	021
3.1 Valley Characteristics .....	022
3.1.1 General Valley Characteristics .....	022
3.1.2 Valley Volumes .....	024
3.2 Pit Fan Measurements .....	025
3.3 Valley and Channel Flux Measurements .....	027
4. Results .....	031
4.1 General Crater Characteristics .....	031

4.2 Erosion, Preservation, and Mantling of Features .....	032
4.3 Features Characteristic of Fluvial Activity .....	033
4.3.1 Valleys Located Outside the Craters .....	034
4.3.2 Valleys on the Craters' Interiors .....	034
4.3.2.1 Crater Wall Tributaries .....	035
4.3.2.2 Central Pit Valley Systems .....	036
4.3.2.3 Pit-Breaching Channels .....	037
4.3.3 Results from Flux Calculations .....	038
4.4 Depositional Features .....	040
4.4.1 Alluvial Fan Features .....	040
4.4.2 Pit Fan Features .....	041
5. Discussion .....	042
5.1 Formative Conditions of the Valleys .....	042
5.1.1 The Case for Precipitation Induced Fluid Flow .....	042
5.2 Depositional Features .....	045
5.2.1 Alluvial Fans .....	045
5.2.2 Pit Fans .....	048
5.3 Timing of Valley Formation (Relative to Crater Emplacement) ....	051
5.4 Valley Formation and its Relation to Central Pit Formation .....	053
5.5 Pit Lakes .....	055
5.5.1 Valley and Channel Flux Implications .....	055
5.5.2 Implications for Chemistry .....	056
6. Conclusions .....	058
7. Figures.....	062
8. Tables.....	094
9. References .....	124

## LIST OF FIGURES

1. Investigated Craters .....	063
2. Map of Investigated Craters .....	064
3. Structural Comparison of Deltas to Alluvial Fans .....	065
4. Central Pit Crater without Interior Valleys .....	066
5. Aeolian Valley Floor Deposits .....	067
6. Measuring Valley Slopes .....	068
7. Example of Valley Cross-Section .....	069
8. Pit Fan Volume Methods .....	070
9. Highly Eroded Linear Features (Crater 4) .....	071
10. Paleo-Lake Depression on Rim of Crater 1 .....	072
11. Alluvial Fans .....	073
12. Bajada Systems in Crater 5: Superposition Relationships .....	074
13. Distributary Channels (Crater 5) .....	075
14. Inverted Terrain and Valley Relationships (Crater 4) .....	076
15. Island Features .....	077
16. Mantling of Valleys .....	078
17. Heavy Mantling of Crater Wall .....	079
18. External Valley Features .....	080
19. External Valley Features Draining into Neighboring Crater .....	081
20. Ice-Associated External Valleys .....	082
21. Drainage Divide Upper Catchment Areas .....	083
22. Multi-Generational Valley System (Crater 5) .....	084

23. Multi-Generation Tributary System (Crater 5).....	085
24. Drainage Pattern Controlled by Terrace Walls .....	086
25. Comparison of Drainage Patterns .....	087
26. Crater 5 Northern Breach Valley .....	088
27. Full Map of Crater 5 with DTM .....	089
28. Crater 2 Floor Depression .....	090
29. High-Flux Erosion of Alluvial Fans .....	091
30. Comparison of Pit Fan Morphologies .....	092
31. Ice-Associated Internal Valley .....	093

## LIST OF TABLES

1. General Valley Results .....	095
2. Pit Data .....	097
3. Valley Fluxes .....	098
4. Channel Fluxes .....	100
5. Valley Flux Type-1 Results .....	102
6. Valley Flux Type-2 Results (Gravel) .....	105
7. Valley Flux Type-2 Results (Sand) .....	107
8. Valley Flux Type-3 Results .....	110
9. Channel Flux Type-1 Results .....	113
10. Channel Flux Type-2 Results (Gravel) .....	115
11. Channel Flux Type-2 Results (Sand) .....	118
12. Channel Flux Type 3 Results .....	120

## 1. INTRODUCTION

The planet Mars has been a source of wonder and discovery for decades. Starting with the Mariner missions, new information about Mars has continuously changed our understanding of geological processes and the nature of planets other than our own. These discoveries have taken us from the knowledge that advanced civilizations of aliens do not inhabit Mars' surface (a popular belief from the time of Schiaparelli and the mis-interpretation of the Italian "canali" (used for both "channels" and "canals") to the discovery of Vallis Marineris by Mariner 9 and the knowledge that Mars still has active processes. Evidence that water has modified the surface of Mars has been recognized in a variety of morphologic types (Carr, 1996). This investigation focuses on a newly identified landform class in which water appears to have played a role: valley networks that drain into the central pits of floor pit craters (Figure 1).

Central pit craters are complex craters that contain a central pit, either central to the crater floor or on the central peak (Barlow, 2010). Mechanisms have been proposed for the formation of central pits including vaporization, impact melt drainage, and collapse of a central peak. These models often implicate the impact process having been modified as a result of the presence of subsurface water or water-ice (Wood et al., 1978; Croft, 1981; Elder et al., 2010).

Pit craters, both of the summit and floor varieties, have been investigated by a number of studies (eg: Smith, 1976; Hodges, 1978; Barlow, 2010). They occur broadly across Mars (Barlow, 2010), as well as across Ganymede and Callisto (Schenk, 1993; Barlow, 2010). The rims of pit craters can exhibit a range of morphologies (Garner and Barlow, 2012). This is the first investigation into valley features that occur interior to the craters.

Five central pit craters have been investigated in detail for this study (Figure 2). Due to the freshness of their ejecta and the crispness of their rims, they are understood to be Hesperian or Amazonian in age. The valley features located on their interiors must therefore also be Hesperian or Amazonian due to superposition, because a feature located on top, or cutting into, another feature must be younger than its host.

Understanding these features allows for a greater understanding of the (regional) state of water in the most recent time periods of Mars. Through the use of Mars Reconnaissance Orbiter Context Camera (CTX) (Malin et al., 2007) images and digital terrain models (DTMs) from Mars Orbiter Laser Altimeter (MOLA) (Zuber et al., 1992) and High Resolution Stereo Camera on Mars Express (HRSC) (Neukum et al., 2004) data, this investigation aims to characterize these valley features, their associated deposits, and host craters in order to further our understanding of the (regional) state of water in Hesperian and Amazonian Mars.

## 2. BACKGROUND

### 2.1 Water on Mars

#### 2.1.1 Evidence for Water

Evidence for water on present-day Mars has been found in the polar ice caps (Titus et al., 2003; Farmer et al., 1977), in rock glaciers and glacial remnant features (Head et al., 2005; Plaut et al., 2009; Squyres, 1978), and in ground-ice features (Mustard et al., 2001; Squyres and Carr, 1986; Carr and Schaber, 1977). Additionally, water has been observed within the atmosphere (Spinrad et al., 1963; Farmer et al., 1977; Smith, 2004) in a cycle that varies on seasonal to orbital timescales (Jakosky and Farmer, 1982; Farmer et al., 1977; Mellon et al., 1995; Smith, 2004).

There is much evidence for water ice as a component of the Martian polar ice caps. Titus et al. (2003) found evidence for water ice in the southern polar region. Using THEMIS (The Mars Odyssey Thermal Emission Imaging System) and TES (Thermal Emission Spectrometer) they determined that an area of high albedo was also an area of thermal inertia that could be matched to that of water ice. Furthermore, comparison to earlier data suggested that the area investigated likely has persisted for multiple decades and could extend for a great distance beneath the CO<sub>2</sub> caps. Additionally, Farmer et al. (1977) found support for water as a

component of the polar caps when they detected maximum water vapor measurements over the polar regions using MAWD (Mars Atmospheric Water Detector) on the Viking Orbiters. A more recent study by Smith (2004) using TES (Thermal Emission Spectrometer) on the Mars Global Surveyor (MGS) supports these findings. Smith (2004) found that sublimation of water ice on the summer pole contributes to the maximum amount of water vapor that is measured in the Mars atmosphere over its seasonal cycle.

Evidence for water ice on the martian surface in features similar to glaciers on Earth has also been extensive. For example, Holt et al. (2008) investigated lobate features in the eastern portion of Hellas Basin. Ice-bearing, lobate features had previously been identified on the basis of their morphology, which is similar to terrestrial glaciers. The amount of ice contained in lobate features remains uncertain (Head et al., 2005; Plaut et al., 2009; Squyres, 1978, 1979). Holt et al. (2008) utilized SHARAD (the Shallow Radar instrument of the Mars Reconnaissance Orbiter) data to investigate the composition of the lobate features in the mid-southern latitudes. They found the features to be predominantly comprised of water ice (due to matches in radar attenuation and dielectric constant), with a thin layer of shielding debris resting above. This conclusion was supported by the work of Plaut et al. (2009) on lobate debris aprons in the mid-northern latitudes.

Ground ice is another possible reservoir for water on Mars and has been used to explain a variety of features (Carr and Schaber, 1977; Mustard et al., 2001; Squyres and Carr, 1986). Mustard et al. (2001) used Mars Orbital Camera (MOC) images to investigate textured terrain caused by interstitial “near-surface ground ice” that has been at least partially eroded in some areas. Squyres and Carr (1986) investigated areas on Mars that exhibited signs of “terrain softening,” which resulted from the slow creep of ice-containing materials at the near-surface. By conducting a census of the planet, they determined that the features were excluded from equatorial regions. Additionally, they found that different characteristics of the ice-flow features occur at different latitudes, probably due to changes in the structural properties of ice with latitude.

Along with these findings, Stewart et al. (2004) found evidence that high water content in the target material of an impact can explain the fluidized nature of impact ejecta for certain craters observed on Mars supporting the earlier conclusions of Carr et al. (1977). Through simulations they determined that subsurface liquid water was not necessary to create the features observed; ice below the surface would be melted by the impact and act to form the fluid nature of the ejecta.

## 2.1.2 Features Related to Fluid Flow in the History of Mars

### 2.1.2.1 Gullies

Gullies are young, elongate flow features on Mars that appear on relatively steep slopes (e.g., crater walls and walls of valleys) and have a distinct morphology: deep-cut alcoves towards the top of slopes with tapered mouths often terminating at a site of sediment deposition (Malin and Edgett, 2000). Malin and Edgett (2000) noted the gullies' similarity to seepage features on Earth and proposed that Mars gullies may be evidence for groundwater seepage at their head alcove. This interpretation is supported by the numerous occurrences where multiple gullies originate from one stratigraphic layer.

Heldmann and Mellon (2004) conducted a study of 106 MOC images to quantitatively compare the physical characteristics of gullies with previously proposed formation methods. They found that models that incorporated a groundwater liquid reservoir as the source of liquid material matched best with their observations. It is important to note that this study omitted potential gully features lacking certain characteristic features, or with ambiguous features.

More recently, Dickson et al. (2007) supported a model proposed by Christensen (2003) that utilizes the melting of accumulated precipitation (e.g. snow) for the formation of gullies. They based their conclusion on a study of 5168 MOC narrow-angle images at a latitudinal range of 30°-40° S. Their identification requirements were more relaxed than those of Heldmann and Mellon (2004) in

that they accepted features as gullies as long as they had “at least two of the three primary morphologic features outlined by Malin and Edgett (2000)”. With these parameters, they were able to examine a subset of gully features that exist in isolated slopes too small to reasonably presume an internal aquifer. These isolated slopes were found to host gullies that often originate at different layers of strata. Furthermore, these gullies were found to exist only within a limited elevation range of -1822 m and 2156 m. More recent studies have supported this snowmelt model as well (Dickson and Head, 2009; Williams et al., 2009).

#### 2.1.2.2 Valley Networks

Valley networks are common on Mars and have been recognized since the Mariner 9 and Viking missions (Mars Channel Working Group, 1983). They have been found to exist preferentially within the cratered southern uplands though they exist in “nearly all geological settings” including in and around craters (Hynek et al., 2010).

Martian valleys are characterized by a V- or U-shaped cross-section (Williams and Phillips, 2001) and usually have steep walls (Pieri, 1980). Pieri (1980) described valleys as having flat floors, mantling from wind and volcanic deposits, and abrupt tributary origins. Additionally, the Mars Channel Working Group (1983) noted that valleys have been seen to range in sizes, spanning from “less than 5 km to nearly 1,000 km”.

Valleys are sometimes preserved as inverted relief (e.g. Burr et al., 2006; Williams and Edgett, 2005). Inverted valleys are formed when less erosion-resistant material around the valley is preferentially eroded, leaving the valley floor material (possibly made of either larger grains or of cemented material) relatively intact as a raised feature (Williams and Edgett, 2005; Pain et al., 2007). Such features have been found in a number of locations including Arabia Terra (Williams and Edgett, 2005) and Dorsa Argentea (Tanaka and Kolb, 2001; Rice and Mollard, 1994) among numerous others.

Most valley networks on Mars are old (Noachian); however there are examples of a few younger fluvial features (Hynek et al., 2010). Such features include those found on the plateau surrounding Valles Marineris (Mangold et al., 2004), on volcanoes (Gulick and Baker, 1989; Dohm and Tanaka, 1999), adjacent to ice features (Dickson et al., 2009; Fassett et al., 2010), and in association with young craters (Morgan and Head, 2009).

#### 2.1.2.3 Deposition Features Related to Mars Fluvial Features

Our understanding of sedimentary depositional features on Earth has been used to relate similar features on Mars to their possible means of formation. For example, deltas are depositional features formed when the water velocity in a channel decreases where the channel meets with a standing body of water, such as a lake, sea or ocean. The morphology of deltas is distinct. When a stream flows into a sea, the rate of flow of the parent stream is reduced, causing the

sedimentary load of the stream to fall out of suspension; its bed load is slowed and eventually halted. The general pattern of sedimentation is that larger particles drop closer to the contact between stream and lake and progressively smaller particles are deposited further out (Ritter et al., 2006). The beds of a delta are divided into topset, foreset and bottomset beds. Topset beds are horizontal beds located on the top of the delta (overlying sediment beneath) that are located at the apex of the fan. Foreset beds are formed from sediment being deposited at the contact between delta and standing water body. Bottomset beds are those that are formed from very fine grained sediments (on Earth, clays are often found here) that is carried out past the main structure of the delta (Ritter et al., 2006).

The sediment deposited in the delta works its way out farther and farther into the standing body of water as it grows outward (progrades), often forming an easily recognizable fan shape such as that seen with the Nile delta. This shape is not always evident, as in the case with the Mississippi delta, which exhibits a more irregular shape. However, irregularly shaped deltas are still recognizable based on other physical criteria (e.g., bedding morphologies). Additionally, deltas often exhibit greater slopes if they have coarser sediment (Ritter et al., 2006).

Support for deltas on Mars has been proposed repeatedly (e.g. Grin and Cabrol, 1997; Fassett and Head, 2005; Mangold and Ansan, 2006; Di Achille, et al., 2007; Pondrelli et al., 2008). Pondrelli et al. (2008) determined that, based on morphology, a fan feature observed in Eberswalde crater was likely a delta. The

fan feature had previously been investigated to determine its nature; however, conclusive evidence relating delta and alluvial fan features remained elusive (Malin and Edgett, 2003; Moore et al., 2003; Jerolmack et al., 2004).

Fassett and Head (2005) investigated a crater that contained fan-shaped sedimentary features. Using MOLA and THEMIS IR data, they determined that the fans' host crater was likely flooded at some point in its past and that the fan features were deltas deposited into a lake from two in-flowing valley networks. The crater was determined to be a lake due to the presence of another valley flowing away from the crater, originating from an altitude higher than that of the fan deposits (significantly higher than the crater floor).

Similarly, Mangold and Ansan (2006) found evidence for a delta forming during the Hesperian in the Tharsis region. Using MOC, THEMIS and MOLA imagery and data, they were able to investigate a crater that showed evidence of being flooded and drained by valley features. Where the valley had flowed into the crater, Mangold and Ansan found a fan-shaped sedimentary deposit with morphology consistent with a deltaic origin.

Alluvial fans are another type of generally fan-shaped depositional features, but with a different means of formation. Alluvial fans are formed when streams flow from a relatively steep slope to a shallower slope; such as from mountain ranges into basins (Ritter et al., 2006). The change in slope causes a drop in water velocity, which results in a decrease in the carrying capacity of sediment for the

stream, and causes sedimentary deposition. To a first order, the shape of alluvial fans is very similar to that of deltas; however, their formational settings (i.e. deposition into a body of water versus deposition onto a dry plain) and structures are quite different. A prime example of these differences is that alluvial fans do not have topset, foreset and bottomset beds. This causes their cross-sections to be visibly different, with alluvial fans generally having steeper deposits of larger grain sediment at their apex with slopes diminishing towards their toes (Ritter et al., 2006; Figure 3). On Earth, alluvial fans are often associated with seasonal rainfall or melt resulting in dry streams during much of the time and occasional dramatic drainage events. Additionally, fans forming close together may merge to form features called bajadas.

Martian alluvial fans have been identified as having formed throughout Mars' history, with ages of (or younger than) Late Noachian (Moore and Howard, 2005), Late Hesperian (or younger) (Williams and Malin, 2008), and Amazonian-Hesperian boundary (Grant and Wilson, 2011) or Amazonian (Williams et al., 2004).

Through examination of the recurrence intervals for floods that form alluvial fan features on Earth, Moore and Howard (2005) determined that fans were likely to form in less than a one thousand year period. Fans might actually take up to hundreds of millennia to form, particularly if the climatic conditions that allowed for the formation of the alluvial fan features were inconsistent. They suggested

that differences in the physical characteristics of the rock and in the climate could explain why alluvial fans are preferentially located in specific regions. Their surveyed area was between 0° and 30°S and they identified large (>10 km) alluvial fan features, most of which are located in Margaritifer Terra, southwestern Terra Sabaea and southwestern Tyrrhena Terra. Based on morphology, they determined that the features were fluvial in origin. They found little evidence of water originating from outside the crater rim, implying that the sediment of the fans originated from the material of the host crater. Additionally, they found no evidence of branching gullies on the fans as would be caused by precipitation, suggesting that if liquid precipitation was the cause of the fan formation, the precipitation must have been restricted to higher elevations. They found complex systems of alluvial fans, including some that were eroded by younger fluvial systems.

Williams and Malin (2008) describe sedimentary forms on Mars in Mojave Crater that bear a striking resemblance to the alluvial fans and bajadas of Earth. The sedimentary fans in Mojave crater formed as a result of fluvial activity associated with a relatively young crater (Late Hesperian or Amazonian). They found two main alluvial fan types: those deposited from high viscosity and minimal viscosity flows. The cause of the viscid flows was uncertain, but the evidence for lower viscosity flows contributing to some of the alluvial fans is very strong based on their morphology. The alluvial fans formed by these sediment-poor flows have “shallow terminal slopes, a tendency to laterally spread more

broadly, and contributory, distributary and/or anastomosing channeled surfaces” (Williams and Malin, 2008). These morphological characteristics suggest that the fans resulted from the flow of liquid water.

Kraal et al. (2008) documented large ( $>40 \text{ km}^2$ ) alluvial fans across Mars using THEMIS images and MOLA DTMs. Their search supported the observation of Moore and Howard (2005) that there was a particular concentration of fans in southern Margaritifer Terra, southwestern Terra Sabaea, and southwestern Tyrrhena Terra. They further found that there was “no recognizable pattern to predict the size of the fan apron relative to the crater size” (Kraal et al., 2008), that they occurred with no clear preference for particular orientations, and with no clear source of water.

Finally, Grant and Wilson (2011) investigated the ages of features within select craters (containing alluvial fan features) through crater counting and analysis of superposition relationships in order to determine the features’ relative ages. Their results suggest that observed alluvial fan deposits could reasonably be considered as young as Amazonian (along with most observed mantling deposits).

### 2.1.3 Models for the Formation of Water Features

Multiple models have been proposed to account for the existence of the many different water-related features on Mars. Major hypotheses include (1) precipitation as rain (Craddock and Howard, 2002) or snow (Carr and Head, 2003; Kite et al., 2011; Williams et al., 2009) as a result of a different climate on

Mars, (2) rain-fall triggered by impacts (Segura et al., 2002; Toon et al., 2010), (3) groundwater mobilization (Malin and Carr 1999; Malin and Edgett, 2000), (4) subsurface ice melt (Stewart et al., 2004), or (5) release of water from hydrated minerals (Montgomery and Gillespie, 2005). More than one of the above hypotheses may have acted in concert on Mars. It is still unclear what mechanism(s) are most likely responsible for the formation of the features observed on the surface of Mars.

There is evidence for the presence of groundwater in Mars' past as a source of water for valley features. Investigations into groundwater as a reservoir for the necessary water volumes to form the observed flow features on Mars's surface have been undertaken. Evidence for the existence of groundwater has been documented repeatedly. Malin and Carr (1999) analyzed channels on Mars and found that they consistently have limited tributaries and no clear watershed boundaries (supporting prior research by Pieri (1980)). Precipitation was excluded as a likely candidate as the source of water due to the lack of valleys exterior to the craters. They suggest that groundwater was the most likely source of water for at least some valleys.

Malin and Edgett (2000) interpreted gullies, found in MOC images, as evidence for groundwater on Mars. Due to the gullies' sinuous nature and their origination at discrete and consistent heights within a host's (e.g. crater) walls,

groundwater was determined to be a likely source, such that water from within the walls escapes from the aquifer at the observed head above.

For the purposes of this study, models of the greatest interest are those that relate valley formation to the impact cratering process itself. A pioneering study by Segura et al. (2002) suggested that flowing water could have been mobilized on early Mars by impacts from large (100+ km) asteroids, due to vaporized water raining out of the atmosphere. Impacts of this size alter the global climate, so rain would not preferentially fall around the crater. This would allow for the widespread formation of valley networks including those within pre-existing craters. This model accounts for the drastic decrease in erosion activity through time because it relies on the large impact events that are common only early in Mars history as the cause of periods of rain and (temporary) warm climate: without maintained impact activity of the necessary magnitude, the required climate for running water ends.

Evidence in support of precipitation as the source of water for martian valley features was found by Mangold et al. (2004), who concluded that precipitation was the most likely water source for flow features observed in the region of Vallis Marineris. The valleys investigated contained internal channels and dendritic patterns that closely resemble valley systems of Earth.

Another proposed method for the formation of water features was submitted by Wang et al. (2005). They investigated liquefaction caused by impacts as a

method for creating the flow features found on the surface of Mars based on data concerning earthquake induced liquefaction on Earth. They derived a formulaic expression for the maximum distance from an impact site that would exhibit liquefaction (dependant on crater diameter). If their model is correct, seismic effects of impact events could have led to groundwater release.

## 2.2 Central Pit Craters

Central pit craters have regularly-shaped pits in the central areas of their floors or central peaks (Figure 3). Central pit craters have been found in many locations on Mars (e.g. Smith, 1976; Hodges, 1978; Barlow, 2010), Ganymede (Schenk, 1993; Croft, 1983; Moore and Malin, 1988), and Callisto (Schenk, 1993; Croft, 1983). Irregular pit craters have also been found on Mercury, but appear to be formed from a different mechanism based on morphological differences.

Central pits on Mars have been recognized in two forms: floor pits and summit pits, for pits located on their parent crater's floor and central peak, respectively (Wood et al., 1978; Hale and Head, 1981; Barlow, 2010). Barlow (2010) found pits in Martian parent craters with diameters ranging from 5 km to 156.9 km, but most were within the range of 10 to 20 km. Additionally, pits were located in craters that exhibit a wide range in ages, suggesting that the conditions that support their formation have existed throughout the lifetime of the planet (Hodges et al., 1978). Barlow (2010) found pit craters in most regions of Mars

(latitudinal range of  $-76^{\circ}$  and  $+70^{\circ}$ ), though they are more numerous within the  $\pm 40^{\circ}$  latitude range.

Another study by Alzate and Barlow (2011) focused on Ganymede pit craters. Ganymede pit craters often occur with rebound features, such as central doming (Barlow, 2010; Alzate and Barlow, 2011; Croft, 1983) not present on Mars. Otherwise, however, the pit craters of the two planets are similar. Alzate and Barlow (2011) determined that the similarity between pit craters on Mars and Ganymede suggests they formed by similar mechanisms. Additionally, they found that pit size was possibly due to excavation into layers of different rheology (weaker material at depth).

### 2.2.1 Formation Models for Central Pit Craters

There have been a number of formation models suggested for the formation of central pit craters. One of the earliest ideas was that material was ejected from the center of the crater through rebound (Hodges, 1978a, 1978b, 1980). Hodges proposed this mechanism based on Viking image data and the interpretation that the raised rim features often present around the pits are composed of material excavated from the body of a former central peak. However, the proposal that pits were an end-member form of peak ring and multi-ring basins is not supported by evidence submitted by others (Wood et al., 1978; Croft, 1981).

Another model utilizing volatile vaporization was proposed by Wood et al. (1978). The model was based on observations of pit craters and their physical

trends. They suggested this method of pit formation due to the identification of water in the Martian subsurface as a possible component of pit formation.

Croft (1981) proposed an alternate method for central pit formation. Heavily brecciated material formed during the impact would be drained into a central area formed by the uplift of the relatively intact units (surrounding the central pit whose walls are formed by the larger intact units), or would drain outward onto the floor of the crater itself. Croft (1981) proposed that in larger craters, massive slabs of intact units that would otherwise form the center of a central peak would collapse downward forming a central pit; thus creating a summit pit instead of a floor pit. This method does not require liquid or frozen water to sublimate in order to form the pits. It is noted, however, that evaporation or flow of liquid water would “[leave] an enhanced central pit” (Croft, 1981). Furthermore, Croft suggests that the domed floors of pit craters on Ganymede be explained by water that was melted by the impact and then refrozen after draining into the fractures formed by the impact.

Senft and Stewart (2009) modeled the impact cratering process for icy satellites using a 5-phase equation of state for water. Their model found that with these new phase considerations, a hot layer of liquid could become trapped within the central floor area of the crater. Furthermore, if rebound of crater material occurred, the hot layer could be released from confinement as a (potentially

explosive) gaseous evacuation, forming features with marked similarity to crater central pits.

A melt drainage model was suggested by Elder et al. (2010) for central pit formation on Ganymede. Based on the estimated void space in the form of fractures for terrestrial impact craters (Pilkington and Grieve, 1992), they estimated the volume of impact-generated fractures for an impact site and determined the duration of drainage time. The lower limit of the amount of water that could be drained was then determined. They found that the amount of drained liquid (water) was comparable to the volume of observed pits, at least to first-order.

### 2.2.2 Current Unknowns Concerning Pit Crater Formation

Barlow (2010) suggests that a formation model utilizing volatile vaporization from the subsurface (Wood et al., 1978) (in agreement with Pierazzo et al. (2005) and Senft and Stewart (2009)) was the best fit for the formational requirements of pit craters on Mars as represented by her observations. This is further supported by the lack of pit craters on the Moon and their presence on the more volatile-rich bodies. The central peak collapse theory of pit formation was not supported by Barlow's (2010) study due to the existence of summit pits. The subsurface water model was also difficult to support with the results found by Barlow (2010) because of its requirement that the subsurface liquid layer remain fairly constant

over time. The lack of variation of crater diameter (and depth) with craters of different ages, contradicts cooling models for the planets.

As stated by Barlow (2010), it is unclear why craters form with and without pits (as well as with different pit types) in the same region and the same time periods. If the conditions for the formation of all the pits are truly the same, all of them should have central pits or none of them should.

Further insights into the possible formation mechanisms of the central pits may be obtained through the analyses of central pit crater interior valley networks presented in this thesis, if the valleys are attributed to pit formation. In addition, analyses of the valleys may determine the relationship between the valley formations and their host craters. Finally, the placement of the pit valleys and their related pits and craters are analyzed to determine how these features fit within the geologic history of Mars.

### 3. METHODS

Five central pit craters with internal valley systems were characterized in this study using the ArcMap Geographic Information System. The central pit craters studied in this investigation were restricted to those found in Mars Reconnaissance Orbiter Context Camera (CTX) images. Topographic information was obtained using Mars Orbiter Laser Altimeter (MOLA) digital terrain models (DTMs) and individual shot points (Zuber et al., 1992), as well as from DTMs derived from stereo images from the High Resolution Stereo Camera (HRSC) (Neukum et al., 2004) and CTX (Moratto et al., 2010). These topographic datasets were used to analyze crater and valley morphometry, particularly valley slopes, fan slopes, pit volumes, valley depths and cross-sections (Table 1 and 2). Data from the Compact Reconnaissance Imaging Spectrometers for Mars (CRISM) was used to investigate the mineralogy of the craters; however, data was only available for crater 2. CRISM data was viewed on the CRISM webpage ([crism-map.jhuapl.edu/](http://crism-map.jhuapl.edu/)).

### 3.1 Valley Characteristics

#### 3.1.1 General Valley Characteristics

The extent of the internal valley networks was mapped using ArcMap. After initial mapping, measurements were taken on their lengths, widths, slopes and watershed areas. Further data were acquired of the pit fan areas, slopes and volumes as well as the pit volumes using CTX images and DTMs (Table 2). The widths were measured after the point where all tributaries had combined to form the main valley.

Valley lengths were also estimated by mapping the valleys and calculating their lengths in the shapefile on which they were mapped (including in these lengths all clear valley tributaries). The valley tributaries were mapped conservatively so that the lengths and subsequent calculations, such as volume, are minimized. The depths of the valleys were approximated as one-tenth the widths of the valleys, consistent with the estimates of Gulick (2001). The widths of the mapped valleys were measured using the ruler tool. Internal channels, which may be a better estimate of the original flow pathway than full valley widths (e.g., Irwin et al., 2005), were separately measured where possible; channel widths were taken as approximately equal to the width of the visible valley floors (Figure 5).

Average slopes of the pit valleys were calculated using the 3D Analyst tool in ArcMap based on the highest resolution DTM available for that crater. For each

located studied, a line was drawn from the visible headwaters of the valley system (highest point of the mapped valley system) to the point where the valley drains into the central pit (Figure 6). The elevation along the line (the topographic profile) was then graphed and the difference in elevation between the uppermost tributaries and the valley's contact with the pit was divided by the length of the valley network investigated to obtain percent slopes (rise over run).

Watershed areas were mapped and measured as polygons in ArcMap for each distinct valley based on topographic contours derived from either HRSC, MOLA, or CTX stereo DTMs (whichever yielded the highest resolution for the crater being investigated).

Pit fan areas were measured by mapping the extent of each pit fan and outlining it as a polygon; areas were then calculated within each shapefile. The pit fan slopes were measured in the same way as the pit valley slopes, with the highest point being defined at the apex of the fan investigated, located at the contact between the valley terminus and the central pit, and the lowest point at the elevation of the pit floor. Pit fan volume measurement methods are discussed in a later section.

Pit volumes were evaluated by assigning a single contour as the maximum elevation of the pit. The volumes of the central pits were then calculated using the best DTM for the area, with the volume measured as the enclosed space between

the plane at the maximum elevation contour and the topography of the interior of the pit. This was accomplished using the ArcMap Surface Volume function.

### 3.1.2 Valley Volumes

After the initial mapping and measurements were completed, valley volumes were estimated in two ways based on either a rectangular or triangular cross-section. Like most valley networks on Mars, these valleys are probably V-shaped valleys with and without fill, based on cross-sectional profiles taken across numerous valleys (Figure 6; see also Williams and Phillips, 2001). Using a V-shaped profile, the valleys were assumed to have a constant depth and width throughout their length. Because the extent of the drainage network for each valley system was determined based on clear connections between tributaries with the trunk valley, the full extent of the valleys may be modestly underestimated.

The lack of connectivity may be caused by older channels being abandoned over time, observational limitations such as shadows, or later geologic features like alluvial fans obscuring upstream tributaries. Pit valley length measurements at worst are believed accurate to a factor of 5, but most of the calculations are good to a factor of 2, taking into account levels of erosion and shadow that obscure their visible extent, as well as the probability that the valleys feeding the alluvial fans were once tributaries of the pit valleys. Shadows in a number of the CTX images, which obscure the extent of the valleys upstream, are the main

source of inaccuracy for valley length measurements for crater 3, in particular. Valleys that clearly flow from areas of shadow are noted in Table 1.

The assumption that the depths of the valleys are one-tenth the measured width is helpful in determining the depths of valleys that are not large enough for their topographic variation to be resolved with the DTMs used. These depth estimates were typically accurate to within 15% the measured values (when resolvable). However, there are examples where the approximated value differs by 30% from the measured value. As such, the accuracy in the depth measurements of the valleys is good to a factor of 1.3 the measured value. The volume estimate is therefore good to a factor of 3.

### 3.2 Pit Fan Measurements

Areas and slopes of the pit fans were measured using ArcMap. The topography of the fan-shaped features, starting at the terminus of the valley systems and ending within the pits, was determined by graphing MOLA point data acquired through the Planetary Data System Mars Orbital Data Explorer website ([ode.rsl.wustl.edu/mars/indextools.aspx?displaypage=molapedr](http://ode.rsl.wustl.edu/mars/indextools.aspx?displaypage=molapedr)). These data were then used to determine the maximum thickness of the pit fans.

Three different values for fan volume were determined, each based on different assumptions and constrained by the observed size of the fans. The first estimate of fan volume comes from assuming that the shape of the fans is an isosceles triangle and that the pit was initially cylindrical in shape with a flat floor

and vertical walls (Figure 8). The volume is calculated as if the maximum widths of the fans lie at the toe and the thickness of the fan is uniform (no tapering at the sides or toe). This yields a calculation where  $V_{pit\ fan} = l * \left(\frac{w}{2}\right) * h_{max}$  where  $V_{pit\ fan}$  is the volume of the fan,  $l$  is the maximum length of the fan from apex to toe,  $w$  is the maximum width of the fan and  $h_{max}$  is the maximum height of the fan (Figure 8).

The second estimate was determined applying the same assumptions as previously described, except that the shape of the fan was assumed to be more fan-shaped than triangular, so that it was a sector of a circle. The equation used for this method is  $V_{pit\ fan} = h_{max} * \pi * r^2 * \frac{\theta}{360}$  where  $V_{pit\ fan}$  is the calculated volume of the pit fan,  $r$  equals the maximum length of the fan,  $\theta$  equals the angle at the apex of the fan formed by its two opposing sides, and  $h_{max}$  is equal to the maximum thickness of the fan (Figure 8). A similar method was used by Weitz et al. (2006), but with additional assumptions concerning the thickness of the fan.

A third volume estimate for the fans was calculated as  $V_{pit\ fan} = A * h_{max}$  where  $V_{pit\ fan}$  is the calculated volume of the pit fan,  $A$  equals the measured area of the fan, and  $h_{max}$  is equal to the maximum thickness of the fan (Figure 8). This method makes all the same assumptions regarding the pit's structure as the previous two methods, except that the shape of the fans is not restricted. This estimate allows for a wider range in pit fan morphology than the previously

described triangular or fan shapes. The maximum thickness was determined using the same method as that described previously (Figure 8).

### 3.3 Valley and Channel Flux Measurements

Fluxes were calculated for both the valley systems and their interior channels. The valley calculations were based on their visible widths where in contact with the floodplain, while channel widths were estimated by the widths of the valley floors. The flux calculations from the channel measurements are probably the best estimate for the actual hydrology of the pit valley systems, as the valleys themselves are highly eroded and their width is likely greater than the width of flow during valley formation. Calculation of the fluxes from valley widths provides a constraint on the maximum possible discharge that occurred within the individual valleys.

Three types of valley and channel flux measurements were utilized for this study. The first equation used to determine flux is the Manning-Chezy equation corrected for martian gravity, with a roughness coefficient equal to 0.0545 (Wilson et al., 2004). One of the assumptions of this equation is that the hydraulic radius  $R$  can be approximated by the channel depth (Wilson et al., 2004), which is the case for valleys whose widths are much greater than their depths. Because the valleys included in this study meet this requirement (Figure 7), this assumption is deemed reasonable.

The second flux calculation applied a version of the Darcy-Weisbach equation, both for gravel and for sand, corrected for Mars (Wilson et al., 2004). The bed roughness functions used for this study were based on the simplified sand and gravel functions determined by Wilson et al (2004). The sand bed calculation was based on the upper regime parameter equation documented in their study. Wilson et al. (2004) present grain size parameters for the landing sites of Viking 1, Viking 2, and Pathfinder. These grain size distributions may not be representative of those transported by the flows in the pit craters. The flux equation for sand used in this study is based on a sand bed channel characterized by a  $D_{50}$  value of 0.005 m: one order of magnitude lower than those found at the landing sites. The gravel equation  $D_{85}$  (0.1 m) value used in this study was within -0.002 of the lowest value found for the landing sites. These grain size parameters may result in a slightly underestimated flux for the valleys and their channels, however this preferred in order to avoid overestimation of flux.

The third flux measurement is that of Irwin et al. (2005), which uses an empirical relationship between the discharge of 2-year recurrence interval floods in the Missouri River basin system on Earth and channel width, because the volume flux of such floods is closely correlated with valley dimensions. Irwin et al. (2005) then applied a correction for how width should be scaled to account for Mars' lower gravity. They note that this calculation is more reliable for channel systems with sandy beds as well as sand and/or silt banks. Because the valleys

feeding the central pit craters in this study may be comprised of material other than sand, this assumption is a possible source of error in this calculation.

This equation was empirically derived for Earth valley systems. It is unclear if this relationship will apply to pit crater valleys that may have formed under much different climate conditions. The equation derived by Irwin et al. (2005) is also noted to be applicable to channels with a ratio of width to depth significantly greater than 1. Because we assumed the valley/channel depths to be equal to  $\frac{1}{10}$  the width of the valleys/channels, their equation (which includes an additional factor to account for the greater widths of martian valleys as compared to those of Earth) is not likely to have a significant error on this account. Additional error may arise from the widening and shallowing of the valleys as a result of post-fluvial erosion and modification. Irwin et al. (2005) noted that in some instances, valleys may be too heavily modified to be able to determine their widths accurately and therefore their discharge. Qualitatively, however, pit valleys are very well preserved, so this is considered to be a minor source of error in our calculations.

After the flux values for each valley were determined, additional calculations were done to answer the questions: (1) How long would it take to fill the central pit of this crater if all its pit valleys were flowing? (2) How long would it take each of the valleys to independently fill their pit? (3) How much water would be drained into a pit in one day or one week with all the valleys active

simultaneously? (4) How much volume would be discharged over these periods of time if only one valley was active? The same questions were then asked using the channel widths. This analysis leads to insights about the length of time over which channel-forming fluxes may have occurred, as well as the likelihood that water might have ponded within the pits. These factors can then be compared with observations of morphology that also provide information to help constrain whether ponding occurred.

Finally, it is important to note that in some of the craters (e.g., crater 4), the level of erosion is so great that it is difficult to determine if some linear features are highly eroded valleys or are unrelated to fluvial activity (Figure 9). Sources of uncertainty for individual valleys are noted in Table 1 where applicable.

## 4. RESULTS

Results have been obtained through analysis of geomorphological characteristics, morphometry, and valley formation processes. These investigations have revealed the presence of alluvial and fluvial systems, two different main classes of fluvial morphologies (sinuous with extensive tributaries and straight with limited tributaries), as well as depressions, interpreted as paleo-lakes within several craters, perched on the crater rim (Figure 10). The measurements and flux calculations done on these systems shed light onto the water requirements of the systems and their possible flow conditions.

### 4.1 General Crater Characteristics

A summary of the measurements characterizing features observed within the craters may be found in Tables 1 and 2. The craters range in diameter from approximately 20 to 40 km and are located at low-to-mid southern latitudes. CRISM data exists for crater 2 with possible mafic and/or iron oxide signatures; no spectral signatures of aqueous alteration were observed. None of the other craters examined was found to have high resolution hyperspectral data available on the CRISM website ([crism-map.jhuapl.edu/](http://crism-map.jhuapl.edu/)). Based on stratigraphy and morphology (freshness of ejecta blanket and crispness of rims (Craddock et al.,

1997)), the craters are of Hesperian or Amazonian age and the features on their interior are therefore also determined to be of Hesperian or Amazonian age.

Two out of five of the craters (craters 4 and 5) have fan-shaped features on their interiors at the contact between the crater walls and floors. These are found both as stand-alone features (Figure 11) and in regions where they merge together (Figure 12). These fans are interpreted as alluvial fans and bajadas based on their geologic settings and morphological characteristics (e.g., fan-shape; slope diminishing towards their toes; tributaries leading to them and distributaries on the surfaces of well-preserved examples (Figure 13)). In the northern half of crater 4, there are a number of eroded alluvial fans (Figure 14). These features have preserved valleys that cut through the fans, as well as high-standing ridges that are likely inverted remnants of channels which flowed towards the pit valley and drained the majority of the northern half of the crater.

#### 4.2 Erosion, Preservation, and Mantling of Features

The degree of preservation varies between craters as well as within the individual craters. Feature erosion ranges from extremely fresh, as for crater 5, to more degraded, as for crater 4, where inverted terrain is common (Figure 14). Inverted terrain is formed from the preferential erosion of material located around the observed feature due to the preserved feature being more erosion resistant. This can be a result of either the feature being made of more erosion-resistant material (e.g., larger grain size than surrounding area) or from some form of

cementation (Pain et al., 2007). Examples of inverted terrain seen in this study include inverted channels and alluvial fans (e.g., Figure 14). These are likely due to wind erosion, because liquid water generally forms channels and streamlined island features as seen in crater 5 (Figure 15).

Surficial mantling units attributed to water-ice (Soderblom et al., 1973; Mustard et al., 2001) have been found on most of the craters investigated. This mantling exhibits a range of coverage from thin uniform veneers that may obscure measurements such as channel widths (Figure 16), to areas where a major section of the crater wall may be obscured (Figure 17).

#### 4.3 Features Characteristic of Fluvial Activity

There are a few types of features that appear to have resulted from the flow of liquid within and surrounding these craters. They include small valleys on crater exteriors, internal valley networks, alluvial fan systems with tributaries on the interior crater walls, and valleys originating from depressions in the crater rim. In one instance, a small (<100 m) valley cuts through a small crater (<800 m in diameter) at the apex of an alluvial fan (crater 5; Figure 13). Additionally, there are features in crater 5 that are interpreted as islands (Figure 15), supporting the valleys' fluvial origin.

#### 4.3.1 Valleys Located Outside the Craters

External valley features have been found around three of the craters (craters 1, 3 and 5) (Figure 18). A few of these features have also been found to drain into nearby craters (Figure 19). Craters 1 and 3 have ice-related features around them from which these valleys appear to emanate. For this reason, it appears possible that external valleys may be genetically linked to ice-bearing features (Figure 20) as seen in similar proglacial streams suggested by Fassett et al. (2010). It is also possible that some small interior valleys post-dating the activity of the pit valleys and alluvial fan systems could relate to the melting of ice, as they also have some similarities with features described by Fassett et al. (2010). The valleys of crater 5 have no association with ice-related features.

#### 4.3.2 Valleys on the Craters' Interiors

Within the craters, there are a number of different valley features. These features include tributaries along the crater walls, valleys to and across alluvial fans, and crater floor valley networks that drain into the central pit.

Areas of depressed topography found in the crater rim regions are interpreted as paleo-lakes (Figure 10). These features have no valleys leading to them, valleys do drain them from a point of breach. Craters 1 and 5 both appear to have these features. Crater 1 has an example of this feature located on its northern rim (Figure 10). Crater 5 has areas of relatively flat terrain on its eastern rim that are the headwaters for tributaries, though they are not all interpreted as lakes due to

the lack of evidence for ponding and a drainage outlet (Figure 21). The fact that these areas are at the headwaters of drainage networks for both crater 5 and two of its neighbor craters suggests precipitation and runoff occurred from this point on the crater rim.

The pit valleys of crater 5 are also interesting in that they support multiple episodes of valley formation. In one system in particular, there is strong evidence for multiple generations of valleys (Figure 22). The oldest valleys in this system are clearly cut by a larger, younger valley, which is itself cut into by smaller (< 100 m wide) valleys. The age relationship between the two oldest valleys (marked by red arrows in Figure 22) is unclear without further cross-cutting relationships. The same limitation also hinders determination of an age relationship between the two youngest valley features (marked by green arrows). A set of tributaries from a different watershed in crater 5 also exhibits a multi-generational nature (Figure 23).

#### 4.3.2.1 Crater Wall Tributaries

The tributaries along the crater walls have drainage patterns that are controlled by the topography of the crater walls. For example, the presence of terraces caused flow to be directed approximately perpendicular to the radius of the crater (Figure 24). Generally, crater wall tributaries run approximately parallel to one another due to the slope of the walls. The origins of these tributaries are not restricted to a particular elevation or stratigraphic layer. Many of these systems

terminate at the apex of the fan-shaped depositional features that are identified as alluvial fans. Some of these valleys may have once been tributaries for the valleys that extend to the central pits, as seen in craters 4 and 5 (Figures 14 and 12, respectively).

There is one small crater (< 800 m in diameter) located at the apex of an alluvial fan in crater 5 that has been cut by a small (< 100 m wide) valley that both leads to and drains it (Figure 13). The valley must be significantly younger than some of the other valleys of the crater due to its fresh morphology and superposition and cross-cutting relationships. In the same area, there are even smaller distributaries that are just barely resolvable at the CTX image resolution (Figure 13).

#### 4.3.2.2 Central Pit Valley Systems

Central pit valley systems are present on the crater floor and drain into the central pit, often ending with depositional features that are approximately fan-shaped. The valley systems range from sinuous to linear, fresh to highly degraded, and have varying complexity in their tributary development, from simple, relatively undeveloped tributaries to more extensive networks (Figure 25). The drainage pattern for the pit valleys that have extensive tributaries is dendritic, while the more linear valleys (limited to crater 4) have very limited tributaries and their linearity may suggest a possible relationship with faulting.

Typical pit valley widths are ~100-450 m and depths are ~15-20 m; typical widths of internal channels are ~50-200 m. Valleys with extensive tributary systems are observed in a number of the craters investigated; particularly well-preserved examples exist in crater 5 (e.g., Figure 25).

The NE pit valley system of crater 4 exhibits a rapid jump in width from its tributaries to the main valley that deposits into the fan. This is likely due to the tributaries (which appear to be the channels of the alluvial fans) being active and draining into the main pit valley at around the same time. The main pit valley appears to curve around the northern edge of the central pit (which is quite elevated above the crater floor) to drain the entire northern half of the crater.

#### 4.3.2.3 Pit-Breaching Channels

In crater 5, there is a valley that flows out of the northern rim of the central pit into a topographic depression on the crater floor, according to MOLA data (Figure 26). This valley appears to be a drainage-divide crossing outlet channel, similar to much larger examples that exist on Mars (e.g., Fassett and Head, 2008). The gradient of topography in the northern half of the crater is also steeper than that of the southern half of the pit and appears to more gradually transition into the crater floor (Figure 27). This suggests that the water level when it breached the northern rim of the pit was already flooding the southern half of the crater floor (Figure 27). The topographically depressed portion of the floor of crater 5 that is fed by the pit outlet valley has a different texture than other areas of the

floor (Figure 26). Finally, the combined flux calculations for crater 5 suggest that flooding of the pit in crater 5 occurred, particularly because multiple valleys were likely to be active simultaneously due to the proximity of their watersheds. These results suggest that the central pit of crater 5 was once a lake that breached and at least partially flooded the crater floor.

There are two southern valleys in the crater that are at lower elevations than the breach of the pit (Figure 27). This suggests that these valleys are either younger than the pit paleo-lake, or were possible turbidity flows, though their extension across the gradual slope of the southern half of the crater would suggest that if they were turbidity flows they were later utilized as regular drainage channels (Figure 27).

Like the pit of crater 5, the pit of crater 2 may have also flooded in its past. A topographically depressed section of the crater floor on the southeast side of the pit appears to be connected to the pit via a valley (Figure 28). There are two valleys in the area, but one was likely an input valley to the pit that drained a discrete watershed further to the south.

#### 4.3.3 Results of Flux Calculations

Flux calculation results can be found in Tables 3 through 12. The maximum flux results based on valley morphometry yield a flux for the valleys consistent with large valleys found on Earth (e.g., the Mississippi has a discharge up to  $4 \times 10^4 \text{ m}^3/\text{s}$  and the Amazon has a discharge up to  $2 \times 10^5 \text{ m}^3/\text{s}$  (US Army Corp. of

Engineers<sup>1</sup>; Richey et al., 1989)) but with watersheds that are obviously much smaller than those rivers. In addition, the amount of water that is required to be produced over the watersheds per day in order to generate the smallest flux calculations is still very high (Tables 3 and 4), and hard to reconcile with our current understanding of the post-Noachian martian climate.

The length of time it would take for the host pit to fill based on one valley and all valleys flowing has been calculated and shows an average time requirement of 60 days for individual valleys and 8 days for the valleys flowing simultaneously. Using the flux calculation derived by Irwin et al. (2005), this calculation yields the lowest flux values and therefore the maximum time requirements. The results for channel-based fluxes show that 200 days, on average, would be necessary for individual channels to fill the associated pit and 19 days for all channels flowing concurrently. The average amount of water drained into a central pit in one Earth day with all valleys flowing is approximately  $54.1 \times 10^9$  cubic meters, using the highest flux results (those of Wilson et al., 2004 for sand beds): the lowest result for this calculation ( $79.79 \times 10^8 \text{ m}^3$ ) is more than twice the volume of the pit they drain into. With only one valley flowing, the average volume of water contributed to the central pit in one (Earth) day is 3.5 times the volume of the pit. Complimentary results for channels show that the average total amount of water drained into a central pit is  $9.53 \times 10^9$  cubic meters with all channels flowing (lowest value being 0.48 times the volume of the associated pit) and 0.74 times

---

<sup>1</sup> <http://www.mvn.usace.army.mil/cgi-bin/wcmanual.pl?01100>

the pit volume with only one channel active at a time. These results demonstrate that filling of the central pit can happen quickly based on even the lowest estimated fluxes.

#### 4.4 Depositional Features

There are a variety of depositional forms related to the valley features on the craters examined here. In particular, these include alluvial fans and pit fans.

##### 4.4.1 Alluvial Fan Features

Two of the craters (craters 4 and 5) contain features identified as alluvial fans and bajada systems (Figure 12) based on morphology: they are all generally fan shaped with a clear tapering towards the toe of the fan. The fans' apices are typically located at the termination of tributary valleys, at the contact between crater wall and floor. The alluvial fans of crater 4 are inverted (Figure 14) but are still interpreted as alluvial fans due to their positions at the contact between crater wall and floor. Other alluvial fans in crater 4 that are not inverted, predominantly have inverted channels on their surfaces that are interpreted as having once been distributaries (Figure 14).

A number of alluvial fan features within crater 5 terminate atop the apparent headwaters of pit valley systems located on the crater floor. Some depositional features in the northeastern region of crater 4 appear to have been eroded by higher valley flux as does an example within crater 5 (Figure 29).

#### 4.4.2 Pit Fan Features

Fan-shaped features located within the central pits, or “pit fans”, are depositional features with the apices of the fans at the termini of their parent valleys. They are present within four of the five craters investigated: crater 3 is the exception, possibly due to the shallowness of its pit which is less than one half the pit depth of the other craters investigated (Table 2). The pit fans exhibit average slopes of  $\sim 2^\circ$ ,  $5^\circ$  and  $11^\circ$  (where measureable). Their morphology is often a fairly symmetrical fan shape, though some variation does exist (Figure 30). Due to their presence at the end of parent valleys, their morphology, and their location within a significant depression where water may have ponded, these features are interpreted to be delta features. In craters 2 and 5 in particular, the pit fans are thought to be deltas due to the evidence that the central pit was a paleo-lake as described earlier.

The pit fan features exhibit a range of forms, even within a single crater (crater 4). In crater 4, there are two fan-shaped depositional deposits (Figure 30). These deposits are marked by different morphologies in that the NE fan appears to have a gentler slope than the southern fan, as well as a different level of erosion: the NE fan is marked by a highly pocked surface and gradual slope to the pit floor, while the southern fan is shorter, has what appears to be scouring from wind erosion, and an erosional scarp at its toe.

## 5. DISCUSSION

### 5.1 Formative Conditions of the Valleys

Understanding the formative conditions of the valley networks within pit craters is an important goal of this investigation. In this section, evidence that may constrain these conditions is examined.

#### 5.1.1 The Case for Precipitation-Induced Fluid Flow

Areas of depression found on crater rims (craters 1 and 5; Figure 10) show evidence for having been flooded and then breached on their lowest sides, forming lakes. In addition, there are valleys that originate in areas that represent drainage divides, flowing both toward the interior of the craters and toward the exterior (Figure 21). Two possible sources of water for these features are springs (groundwater) and precipitation (either snow or rain). If a spring was the source of water at these locations, it would require a perched and confined aquifer, despite the lack of a clear recharge mechanism, because these lakes are located at the highest elevations of their craters, either at or near the peak of the crater rim. Additionally, if the source were a spring, the groundwater that fed the spring would have to be under pressure in order to come out at the crest of the crater rims. However, the elevations of the headwaters of the valleys originating within

the craters (and exterior to the craters) do not appear to be restricted to particular elevations or strata. Instead, their headwaters form at all elevations including across the crater floor. This suggests that groundwater is likely not the source of water for these features, and is therefore unlikely to be the source of water for the crater rim lakes. Precipitation as a source for water does not require any correlation with a particular layer of strata or elevation. For this reason, as well as the dendritic nature of the pit valleys, precipitation is supported as the source for liquid water in this study.

Valley features occasionally appear exterior to the craters in association with ice-related features/mantling (Figure 20). In these areas, with their apparent associations with ice—such as having origins at locations that are particularly heavily covered with ice-associated deposits—melting of ice may be implicated as the source of water for the features, as is suggested for valleys investigated by Fassett et al. (2010). It is possible that these features formed under different climate conditions than the valleys that drain into the pit and the alluvial systems on the crater interiors because these features do not appear to be from ice-melt. They generally have numerous tributaries and originate from locations within their crater that is not abnormally rich in ice-deposits. It may be that these external valleys formed during a time when the interior pit valley and alluvial valley systems were not active, either before or after these valley systems formed, or during a time when the valleys were inactive.

Though many of the craters exhibit features characteristic of ice on Mars (e.g., in craters 1 and 3), they are often in the form of mantling deposits that cover large areas of the craters. This observation suggests that at least the most recent ice-rich deposits post-date the formation of the pit valleys and alluvial systems and are thus unrelated to their formation. This stratigraphy is consistent with the interpretation that ice-rich mantling deposits are geologically young (less than a few million years) (e.g., Mustard et al., 2001; Head et al., 2003). Note that there are a few valley features, even inside the craters, that may be associated with ice-rich features, but they are small and disconnected from the older valleys (Figure 31). For this reason, they are not likely to be related to the more extensive valleys flowing into the central pits and associated with alluvial fans. Additionally, these features may be of the same age as ice-related valleys located exterior to the crater.

Some external valleys are not as clearly associated with ice-rich features. There are valleys on the crater rim that flow toward the crater exterior instead of its interior (Figure 21), similar to valleys that flow into the craters from depressed areas that are interpreted as areas that likely ponded. In crater 5, there are valleys that originate from terraces and other regions of low-slope along the rim of the crater. To the east of this area at the contact between two neighboring craters, a pair of valleys leads from a drainage divide into both neighboring craters (Figure 21).

## 5.2 Depositional Features

### 5.2.1 Alluvial Fans

The valleys that flow into the central pit of crater 5 are superposed by the toes of alluvial fans near the crater's rim (Figure 12). This suggests that the process of forming the alluvial fans continued after the valleys that debouch into the central pit ceased activity. On Earth, alluvial features generally form in conditions different from those of fluvial valley systems, because they have different flux requirements. For this reason, these systems generally do not coexist on Earth. If this pattern carries over to Mars, the superposition of these features may suggest that the environment in the region transitioned to more arid conditions over time, where alluvial fan formation was favored over more intense fluvial activity. In this scenario, the tributary systems that fed the late-stage alluvial fans may have previously been utilized as the tributaries of the fluvial systems on the crater floor. If this is the case, then the pathway for connecting the crater rim to the fluvial valley systems on the floor (in the form of tributaries) is now buried. It is unclear if this scenario applies to craters other than crater 5. For example, alluvial distributaries in crater 4 appear to clearly connect to the main pit valley within the crater.

Additionally, superposition of the alluvial fans over the fluvial valleys may suggest that the climate in the area changed relatively gradually from being capable of supporting liquid water flow to not having this capacity, from a wetter

climate to a more arid one. However, it is difficult to constrain the time over which alluvial activity continued after the pit valleys stopped forming. Therefore, it is currently unknown whether flux conditions changed gradually or rapidly, or if there was a prolonged time interval between the end of pit valley activity and alluvial fan formation.

Finally, it is important to note that this pattern may have occurred more than once, with the oldest generation of valley activity that fed the central pit having occurred and been superimposed by a younger alluvial fan, followed by another period of fluvial activity that eroded much of those fans (with this pattern repeating). This possibility is supported by the presence of eroded depositional features in the southwestern part of the floor of crater 5 as well as in a northern inverted fan in crater 4 (Figure 29).

The presence of the small (<100 m) valley cutting through a small crater superposed on alluvial fans in crater 5 is an important feature for the understanding of these systems. The valley extends towards the toes of its host alluvial fan, but diminishes in size with progression down-slope (Figure 13). It is possible that the valley may have lost water to the alluvial fan through infiltration during flow. The alluvial fan may have acted as a connection to the pre-existing valleys and allowed them to potentially form small young channels on their floors. This may be a means of formation of the small channels (<100 m in width) in crater 5's multi-generational valley system (Figure 22). This scenario does not

contradict the theory of a transitional or repeated climate. The small (< 100 m width) pit valleys in this instance would not be formed from as great a flux as the older valleys had done, as this would greatly erode the alluvial fans. This low flux requirement fits well within a climate change scenario where the flux is diminishing through time.

Another scenario is that the small interior channel within the valley feeding the pit in crater 5 is a result of diminishing flux towards the end of activity in the larger valley. In this case, the alluvial fans may have started forming while the pit valley systems were still active and simply continued after the pit valleys ceased flowing. This would also fit in with the repeated conditions theory where flux levels were conducive for one type of flow at different times, in which case this scenario would be towards the end of such a sequence.

Finally, the idea of transient climate excursions during this time may support the hypothesis of Segura et al. (2002) that impact induced rain-out was a source of water to these craters.

These scenarios derived for the variation in climatic conditions in crater 5, however, may not be similar to those of the other craters, although climate variations may have occurred there as well. The lack of superposition relations for features in many of the other craters makes this determination difficult, however.

Additionally, northern alluvial fans in crater 4 contain inverted and non-inverted channels that flow towards the northern pit valley. In this crater, there

was no evidence to suggest the age relationships (separation between fluvial and alluvial activity) seen within crater 5. This does not negate the analysis of crater 5, but instead demonstrates the likely variability between the craters. It is likely that they experienced varying climatic conditions at different times and intervals. The presence of alluvial fans draining into a valley that debouches into a central pit suggests that alluvial fans and fluvial activity coexisted in crater 4. Indeed, some of the alluvial fan features appear to have been cut by valleys that are significantly wider than the distributaries visible on adjacent alluvial fans (Figure 29). This suggests that in crater 4, the high flux valleys may have formed after the alluvial fans.

### 5.2.2 Pit Fans

Because the central pits have valleys that feed them, they may have once hosted lakes. If this is the case, the pit fan features are likely delta deposits formed when the pit valley systems drained into the pit lakes.

Pit fans are present in four of the five craters investigated. The crater that does not contain pit fans is crater 3. The lack of pit fans in that crater is potentially due to the relatively shallow depth of its central pit, which is ~135 m, less than half of the depth of the other 4 pits investigated (Table 2). This relatively shallow pit could have prevented the formation of a pit fan, with sediment instead being deposited by the pit valleys more evenly across the pit floor.

There are two pit fans in crater 4 that have distinctive morphological characteristics. The southern pit fan is almost perfectly fan-shaped and has a scarp at its toe (Figure 30) interpreted to have formed through erosion due to its irregular and crisp nature. The northeastern fan has a relatively gentle slope of approximately  $2^\circ$  (the southern fan had too limited MOLA data to calculate its slope) and extends across almost half of the pit floor. It has irregularities (areas where sediment appear to have been removed) along its edges, particularly the northern side, that are also attributed to erosion. This difference in morphology between the fans may be due to the direction of winds within the crater, or may reflect a significant difference in the fans' histories. If the latter is true, then it is possible that the fans formed and/or started eroding at different times and/or under different conditions (e.g., in obliquity cycles).

For example, if the southern valley network that feeds the pit was active before the northeastern valley system, then the southern fan may have formed first. In this case, either precipitation as rain or snow was preferentially deposited in the southern half of the crater, or melting of ice was favored in the southern half of the crater. Plausible physical conditions can lead to a preference for delivery of water from the equator-facing crater rim (the southern rim) to the pole-facing crater rim (the northern rim), because slope orientation has a strong influence on where precipitation and/or melting might occur inside craters (e.g., Costard et al., 2002).

In this scenario, the southern fan would have already existed by the time the northern fan formed, possibly with more limited activity in the southern valleys due to a change in conditions that led to preferential flow from the south originally. It is possible that there was a time of relatively little influx of water to the central pit between the formation of the two fans, in which case the southern fan could have started to undergo wind-induced erosion. Alternatively, after the southern fan formed, the northern valley's flow into the pit, potentially a lake at this time, could have caused the southern pit fan to undergo erosion at its toe. The upper areas of the fan may have been above water level and been relatively safe from this form of erosion while the northern fan began to form. At some later time, when the northern valley ceased being active (and the pit was no longer a lake), the northern fan would have then started to undergo its own sequence of erosion leading to its current form.

Another explanation for the morphological differences between the two fans is that the northern delta was formed through the deposition of smaller grain-sized sediment than the southern fan, allowing for particles to be transported farther into the pit. However, this theory seems unlikely because the grain sizes within the drainage basins for both valley systems should be the same, and this hypothesis is untestable with currently available remote sensing techniques. Finally, there are barely visible linear features (Figure 9) in the western and eastern regions of the crater that may be highly eroded remnants of valleys that used to flow into the pit. If these features are fluvial in nature, then the eastern

example may have contributed to part of the northern pit fan. This may help to explain the vast expanse of the northern fan, aside from the simple observation that the valley that drains the northern half of the crater is larger than the valley leading to the southern fan.

Based on MOLA data, the northern pit valley in crater 5 was not a source valley contributing water to the central pit, but was instead an outlet, draining water from the central pit into a northern floor depression (Figure 26).

Additionally, the results of flux calculations to determine the likelihood of the pit flooding at some time during its history suggest that the possibility of the pit of crater 5 flooding during some period in its history is reasonable (Tables 5 through 12). These results strongly support the hypothesis that the pit of crater 5 was a lake for some duration of time in Mars' past. This suggests that the fan-shaped deposits within the pit are indeed delta features.

### 5.3 Timing of Valley Formation (Relative to Crater Emplacement)

The timing of the formation of the valley systems relative to crater emplacement is essential to understanding the formational processes of the valley systems and their relationship to their central pits.

A central pit is formed during crater emplacement because it is a characteristic component of the crater itself. Evidence in this study suggests that the valleys were not formed soon after the impact. For example, in crater 5 there is a small crater (<800 m diameter) that is cut by a small valley (<100 m width). The small

crater is interpreted to be relatively young, and a significant amount of time is likely to have passed between the formation of the broader pit crater and this superposed impact structure. This would suggest that the small valley located atop alluvial fans is relatively young as well. This would require that valley formation occurred at a time significantly later than crater emplacement, and therefore pit formation. This, coupled with several lines of evidence for multi-generational valleys (Figures 22 and 23), suggests that the valley formation conditions were present (at least intermittently) for a significant amount of time: from at least as early as the oldest pit valley system, to the time of the valley that cut the <800 m diameter crater. The climatic conditions and flux necessary for the formation of these valleys may not have been present consistently during this entire time. Indeed, the wide range in valley widths suggests that flux was quite variable. Additionally, there is nothing to say that the valleys were continuously active. In fact, they could have been present for relatively limited amounts of time: long enough to form their winding natures and extensive tributaries, but not as long at the time interval between crater emplacement and the cessation of flow in the valley that cuts the small crater.

It is not clear how long after crater formation the valley activity was initiated, though the conditions that enabled erosion of the valleys significantly post-dated crater formation (possibly in several recurrent periods).

#### 5.4 Valley Formation and its Relation to Central Pit Formation

The conditions that allowed for the formation of the valley systems may have been the same as those that allowed for the formation of the central pits, though not forming concurrently. The pit would have been formed before the valley networks because central pits form during crater emplacement and the valleys clearly postdate the craters due to super-position.

The presence of diagnostic erosional features (the valley systems), depositional features (alluvial fans and possible delta features), and the evidence for paleo-lakes in the central pits and along the rims of the craters all imply that water was important for the formation of features within the pit craters.

An alternative hypothesis is that these features are not related to meteoric water, and are instead related to impact melt, as suggested by Jones et al. (2011) and Morris et al. (2010). In this scenario, the valleys and pits could have formed at approximately the same time during crater emplacement. Multiple lines of evidence suggest this scenario is unlikely, however. The presence of the small (<100 m wide) valley cutting through the young crater (base on its diameter of < 800 m) within crater 5 requires that valley activity must have occurred significantly later than the emplacement of the crater and central pit formation. Because impact melts are restricted to the time immediately after (and during) impact, these channels cannot be from impact melt flows. Additional evidence that marks these features as liquid water formed valley networks is the

depositional fan features present at the contact between the pit valleys and their pits. These do not resemble melt flow features in that they are not lobate at their margins (Mouginis-Mark et al., 2007).

These factors require that the valley systems be unrelated to central pit formation, at least beyond their deposition of sediment within the pits. The formation of the central pit, however, did have an effect on the valley systems and their related features, providing a location for drainage and helping to control the nature of the associated depositional features.

One of the hypotheses for central pit formation is the devolatilization of subsurface volatiles during crater emplacement. If this is required for pit formation, then subsurface ice or water in the target material would have been present during the time of crater emplacement (Wood et al., 1978; Senft and Stewart, 2009). As such, it is possible that the conditions allowing for the formation of the valleys may have been present prior to and during pit crater formation. In this scenario, local wet conditions would only need to persist or recur in order to form the valley networks seen on the pit crater interiors.

Another scenario proposed for pit formation by Croft (1981) invokes drainage of melt and brecciated material around relatively competent uplifted rocks through fractures formed during impact, and does not have the same requirement for water being present during formation. Despite this, a drainage scenario does not negate the possibility of the region being water-rich during impact. This

hypothesis is potentially supported by the presence of some linear valley features in crater 4 (Figure 25) that could potentially correspond to fault controls acting on valley formation.

An alternative method for the formation of linear valley features is preferential erosion from a knick-point in the pit wall that would cause the erosion to extend linearly backwards away from the crater (Foster and Kelsey, 2012). In this case, no faulting would be necessary in the investigated craters to lead to rectilinear valleys.

## 5.5 Pit Lakes

### 5.5.1 Valley and Channel Flux Implications

The vast differences among the inferred valley and channel fluxes provide a good range for the fluxes of the valley networks under peak conditions. When less highly active, the valleys/channels would have had less water moving through them, perhaps fluxes insufficient to erode bedrock. The smaller channels may have formed during reduced flux periods, although it is unlikely that any of the measurements denote the lowest fluxes through the systems.

The difference between valley and channel fluxes when determining the implications on pit filling are approximately one order of magnitude different. However, even allowing for this, the water drained into the central pits is not negligible. For example, the lowest percent of the host pit filled by an individual

channel in one day is 0.55%, but this still represents  $56.7 \times 10^6 \text{ m}^3$  of water. These fluxes are likely to overwhelm any plausible loss mechanisms from the pit (either to infiltration or evaporation). Because a pit lake was once present within crater 5 and there are delta-like features in three of the other craters, that ponding must have occurred within a number of the craters. Even with low flow, or flow through only a single channel, a shallow lake could still have formed, as long as the influx was sufficient to overcome losses to groundwater or evaporation. Additionally, in a number of the craters, more than one valley is likely to have been active at a time. For example, crater 5 has valleys that are in close proximity and are likely to have been similarly affected by changes in obliquity and water supply to their shared regions of the crater.

### 5.5.2 Implications for Chemistry

The sinuous nature of the largest valley systems suggests that they were active for a significant amount of time. It is generally difficult to form deep, sinuous valleys on short time scales, as growth of meanders typically evolve over decades (Parker and Andrews, 1986). A long duration of flow would imply a consistent presence of a pit lake, at least when fluxes were high enough. If it was consistently present, a deep lake could have developed, leading to aqueous alteration from the combined presence of water and the influx of sediment from the valleys draining into it. For this reason, this topic of investigation will be important for future study. The central pit in crater 3 may represent either a crater

that was too shallow to form distinct fans, and so deposited its sediment relatively evenly across its floor, or a crater that has undergone more extensive filling by fluvial or aeolian material than in the other craters.

Morphological results from this investigation strongly suggest that the pit of crater 5 was a paleo-lake during some sub-set of martian history. The pit is found to have a valley that drains it through a breach in its northern rim. This valley drains into the northern floor area of the crater (Figure 26). The gradient of topography of crater floor and pit (Figure 27) suggests that the southern region of the crater floor was at least partially flooded during this time. This introduces the possibility that both the northern and southern floors of the crater may have aqueously altered minerals provided the areas were flooded for a sufficient duration of time.

Crater 2 may have also flooded during its history. The southeastern region of the crater floor is relatively topographically depressed compared to the area around it and appears to have interacted with outflow from the central pit (Figure 28). If this area were flooded for a sufficient time interval, it may have undergone aqueous alteration as well.

## 6. CONCLUSIONS

This study has provided new insight into the processes and conditions within central pit craters that contain valley networks. A few of the major results are highlighted below.

The case for precipitation (either as snow or rain) as the main source of water to the investigated central pit crater valley systems is strongly supported by our findings. In particular, the observation of topographic depressions and flat terrain that form the upper portion of the watersheds of a number of internal valley systems provides compelling evidence. Additionally, hypotheses for valley formation from groundwater alone are unlikely to be consistent with headwaters at varying elevations within the craters and high on the crater rim. Although features potentially related to the melting of ground-ice were identified, it could not be a viable source for the investigated fluvial and alluvial systems. Although ice-mantling was present within the craters, the investigated valleys did not originate from them, but were instead only covered by them (Figure 16).

The observations that support a recurring and/or transitional climate are also important results of this investigation. These findings have implications for the post-Noachian climate, at least regionally, in that they suggest that water was

stable for either relatively short periods of time (yet long enough to form valley systems with extensive tributaries) but was recurrent, or that water was consistently present but in an evolving and diminishing capacity. There may have been a trigger that repeated, causing valley-forming conditions in the area to also re-occur, or that allowed for sustained valley formation for a significant amount of time: long enough to form the observed sedimentary features and extensively erode the craters, at least locally. This trigger and the exact nature of the conditions (temperature, atmospheric density, etc.) are not yet known. Still, these results suggest that post-Noachian water-valley features were not limited to simple cataclysmic flow events. Instead, they were significant systems that bear further investigation in order to explore the extent of their place in the history of water on Mars.

Investigation into the sedimentary fans in these systems has led to insights into the history of the individual craters. In crater 5, alluvial fans helped to determine the history of water within the crater and derive timelines of formation to explain these findings. These observations are important in their implications for the presence of liquid flowing water on Mars during the post-Noachian.

Additionally, key relationships exist between valleys and their associated sedimentary fans in crater 5. In particular, clear age relationships and observations suggest that depressed areas of the crater floor may have once been paleo-lakes. This helps to create a more complete picture of the crater system, and is consistent

with the environment within the crater having changed greatly over time, from wet conditions to the dry conditions seen today. Many characteristics of the sedimentary fans, such as their shape, topography, and setting, demonstrate that the valleys themselves were formed through erosion by liquid water instead of by impact melt.

Finally, the relationship of the initial formation of the pit crater to later valley development is an intriguing topic described in this study, although the importance of this relationship remains unknown. Further characterization of these systems and their relationship to the as yet unknown process for pit formation remains a major point of interest. What is clear is that valley formation occurred at a time significantly post-dating the emplacement of the host crater and central pit. Observations in this investigation also point towards a significant time duration for the formation of the valley systems. Valley activity appears to have occurred post crater emplacement and before the most recent ice mantling (for all craters), and continuing after the formation of the small (<800 m diameter) crater (for crater 5). The separation of valley activity from crater formation in crater 5 is supported by the existence of a small (<800 m diameter) crater that is located atop the eastern alluvial fans of the crater that is flooded and then breached by a small (<100 m wide) valley. The alluvial fans of crater 5 (assuming the scenario of a gradual change in climate) appear to mark the end of pit valley formation, and the initiation of alluvial systems that are relatively young. Additionally, the post-emplacement modification of the central pits, for example, by fan deposition, is

clearly significant. Though the pits were structurally formed during crater emplacement, they are by no means finished developing by the time valley formation is initiated, as their floors are modified by the valleys they drain.

This investigation has helped characterize the valleys associated with pit craters. However, specific questions remain, including: (1) Why are internal valley systems not more common in pit craters? (2) What are the necessary conditions for the pits (and their valleys) to form? (3) What is the mineralogy of the fans and what sort of aqueous alteration took place, if any? (4) How long did it take for fans to form? (5) Did the internal features form during the Hesperian or Amazonian (or both)? The answers to these questions will build upon this study and help further our knowledge of both these systems and the history of water on Mars.

To this end, further research will investigate valley hydrology, the relation between the valleys and their pits during formation, and the evolution of the entire systems with time. These additional analyses will address these questions by further examination of the sedimentary fans, crater counting, mapping of key stratigraphic relationships, and assessment of spectroscopic information of the craters, valleys, and fans.

## 7. FIGURES

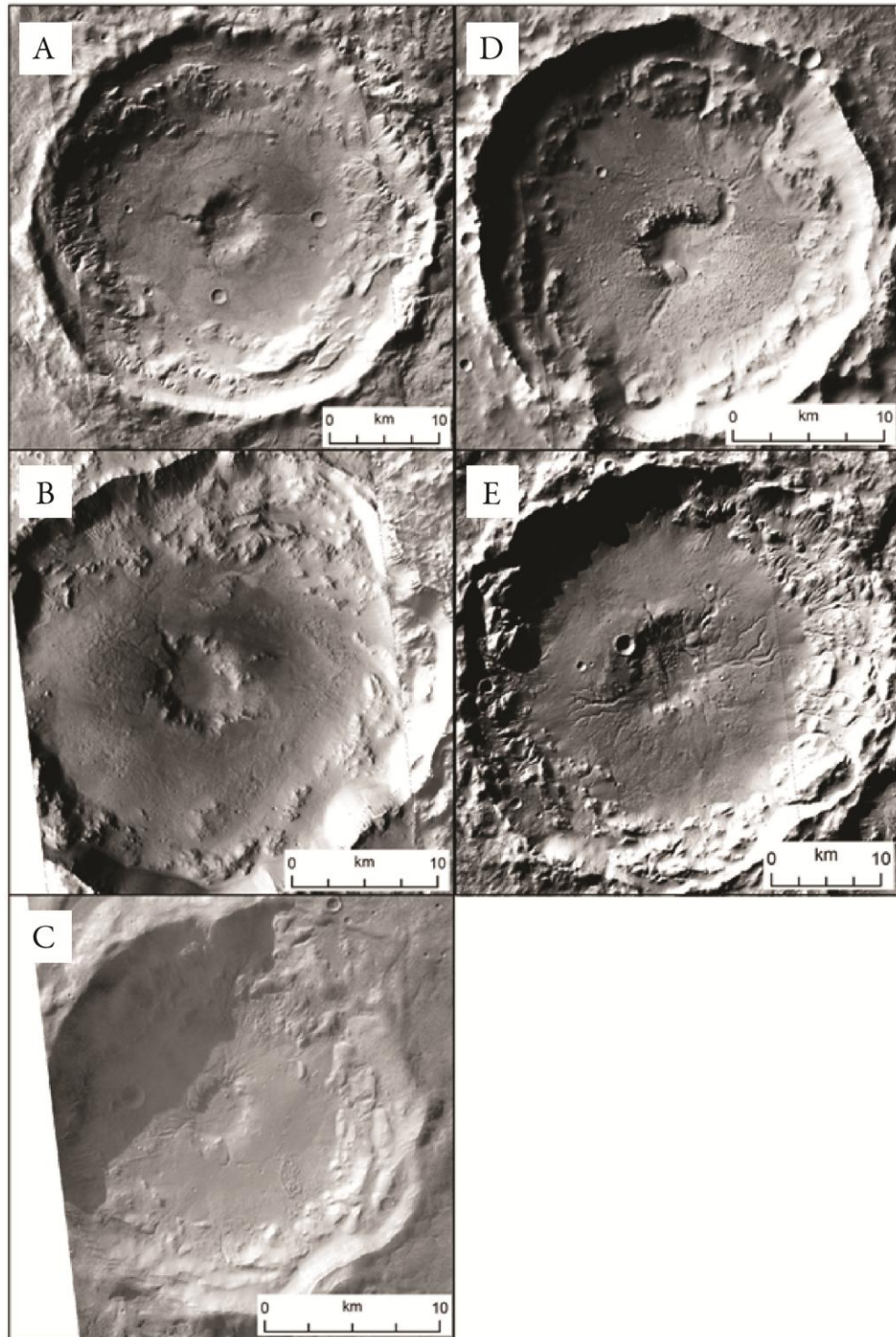


Figure 1: Image of each of the five craters investigated, showing the central pits and the valleys that drain into them: (A) crater 1; (B) crater 2; (C) crater 3; (D) crater 4; (E) crater 5.

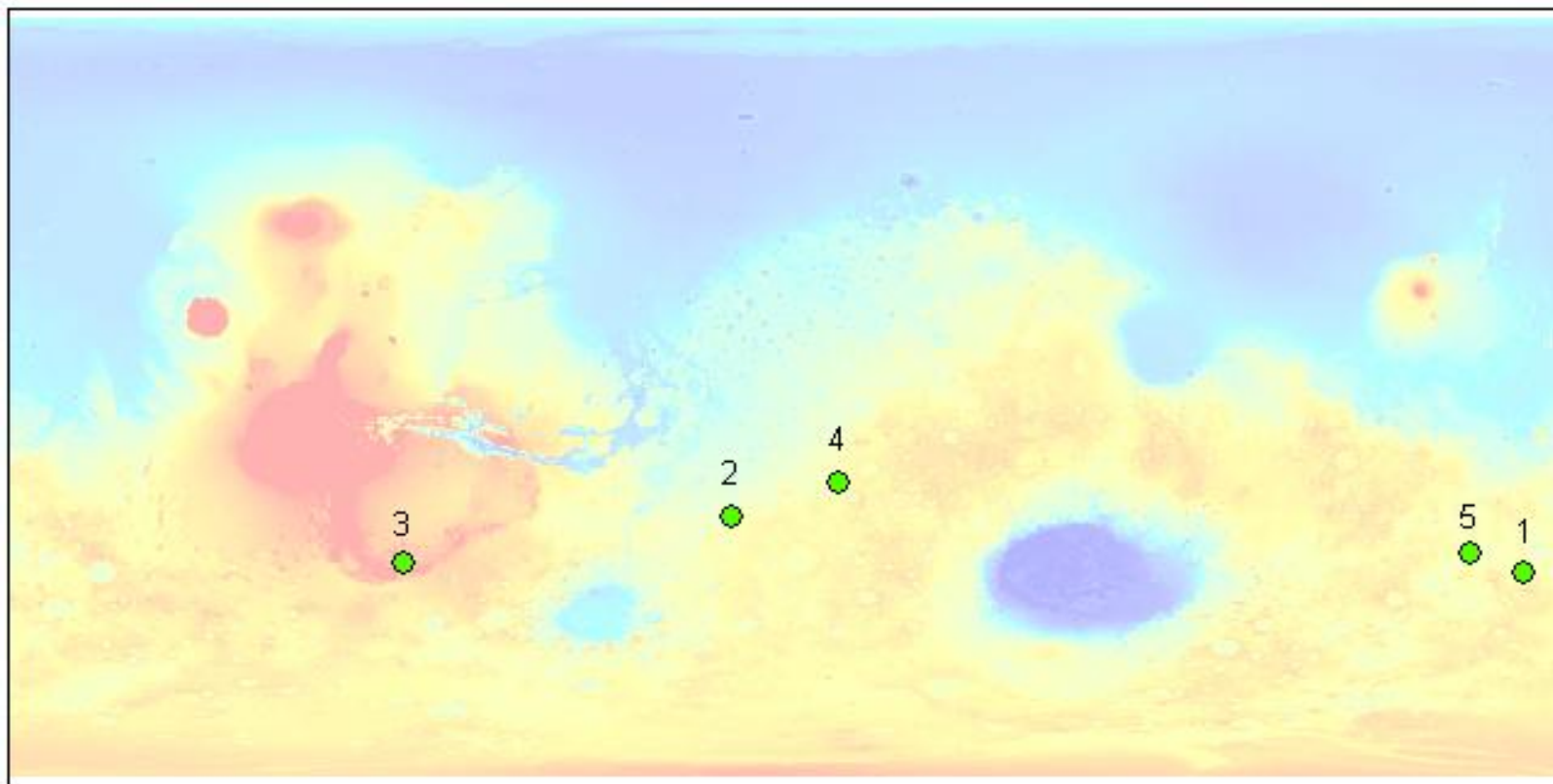


Figure2: Map of the locations of each investigated crater. Crater numbers are arbitrary.

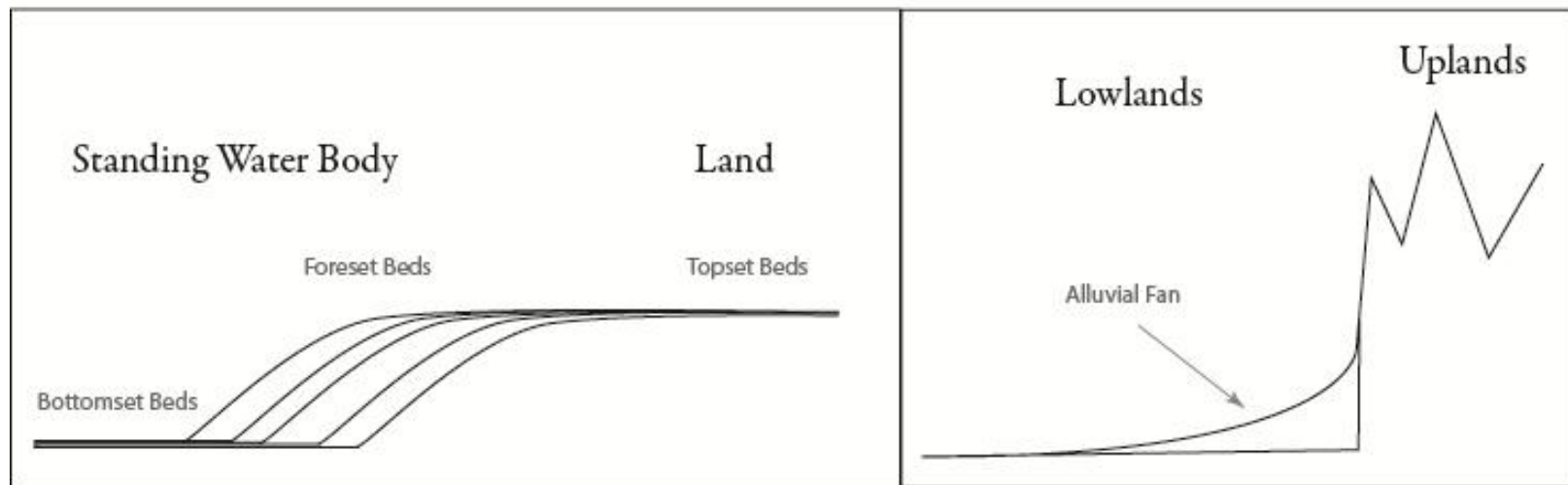


Figure 3: Cross-section of delta bedding structures (left) and alluvial fan (right). The apex of the fans in both images are to the right. Note that the thickness at the apex of the alluvial fan is exaggerated (uplands-lowland transition appears to form a right angle). (Images are not intended to be to scale.)

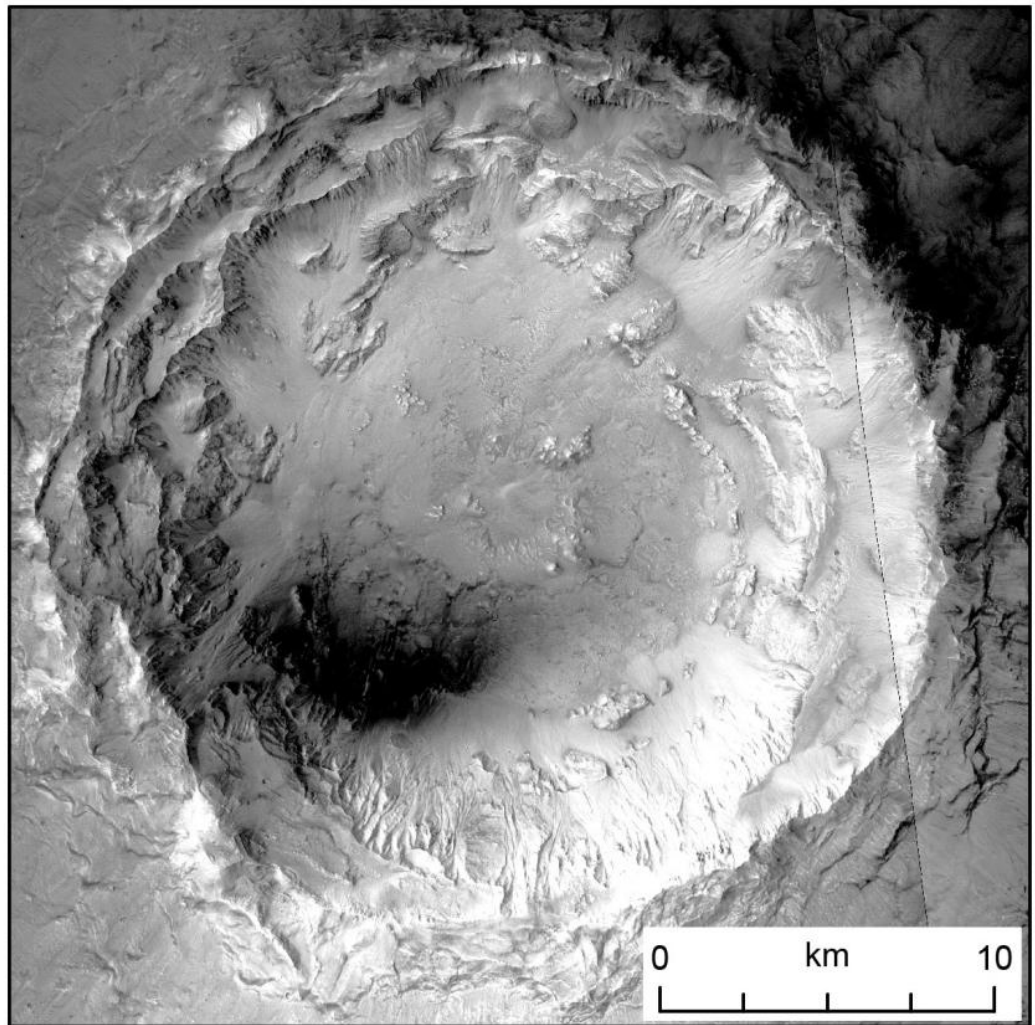


Figure 4: Example of a central floor pit crater found on Mars. Diameter = ~3.5 km. (CTX image: P14\_006538\_1421\_XN\_37S203W.tif)

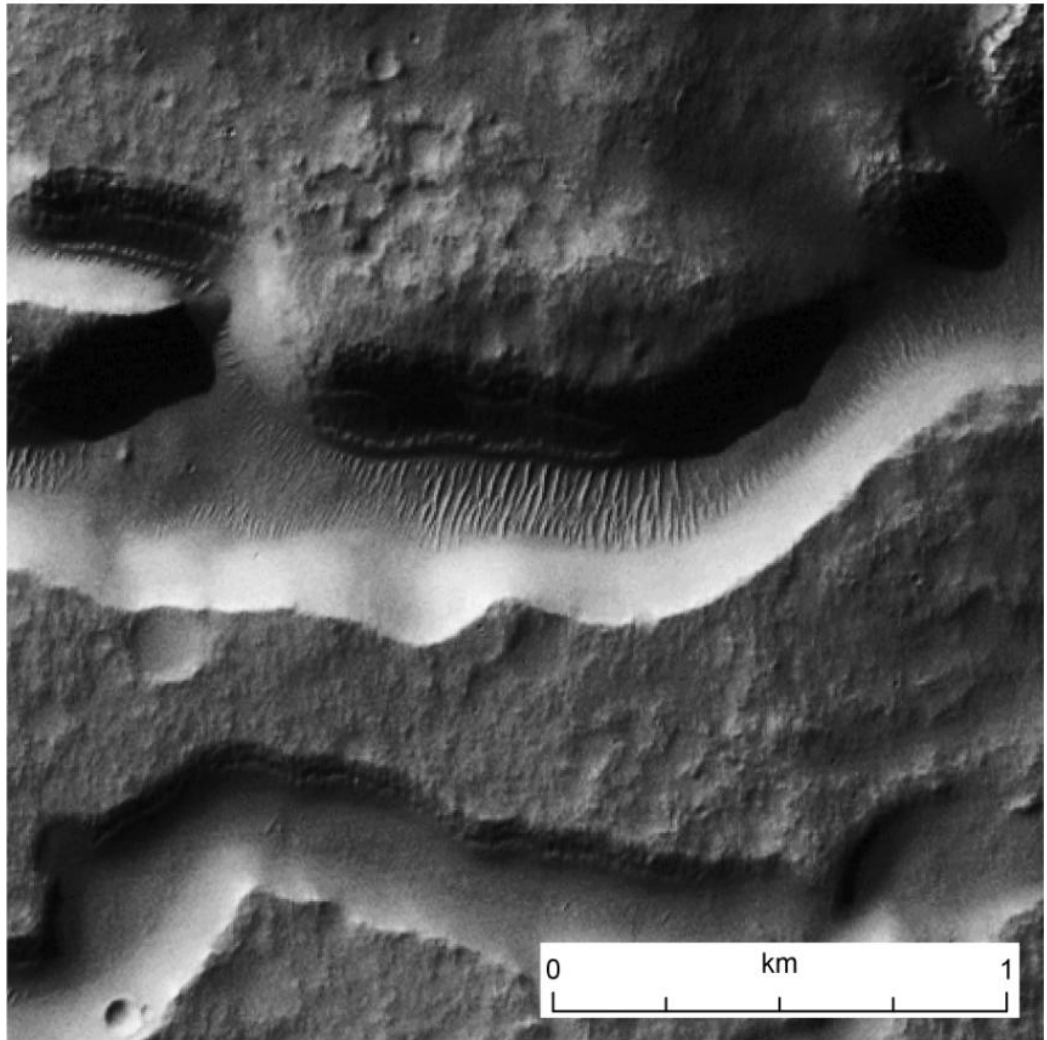


Figure 5: Example of the section of a valley floor and the aeolian deposits located on the floor. Mantling material is also visible on the walls of these craters as well as the crater floor. (This valley is located in crater 5.)

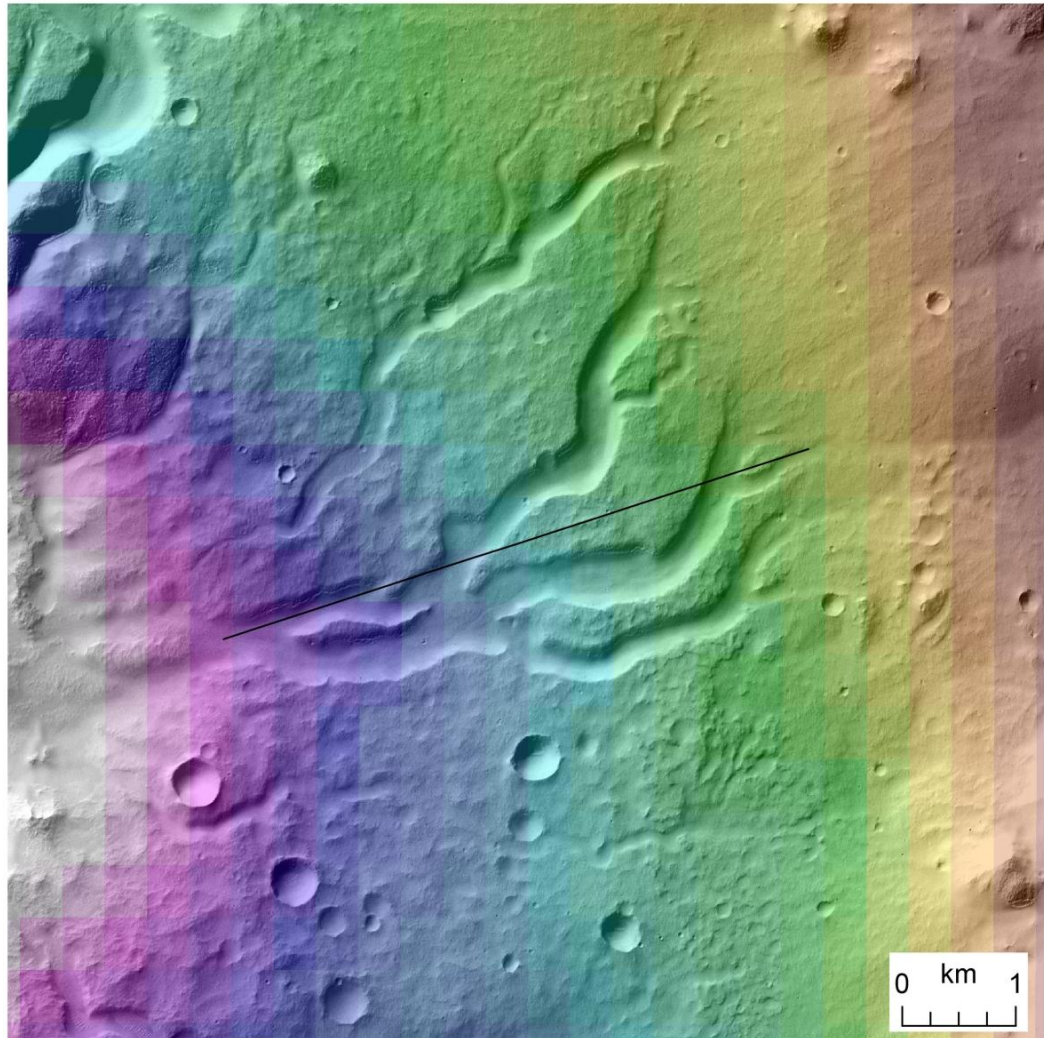


Figure 6: Image of the line of investigation that was drawn from the highest elevation of the visible valleys to the contact between the valleys and the pit they drain into. (DTM overlaid with highest elevation in red and lowest elevation in white.)

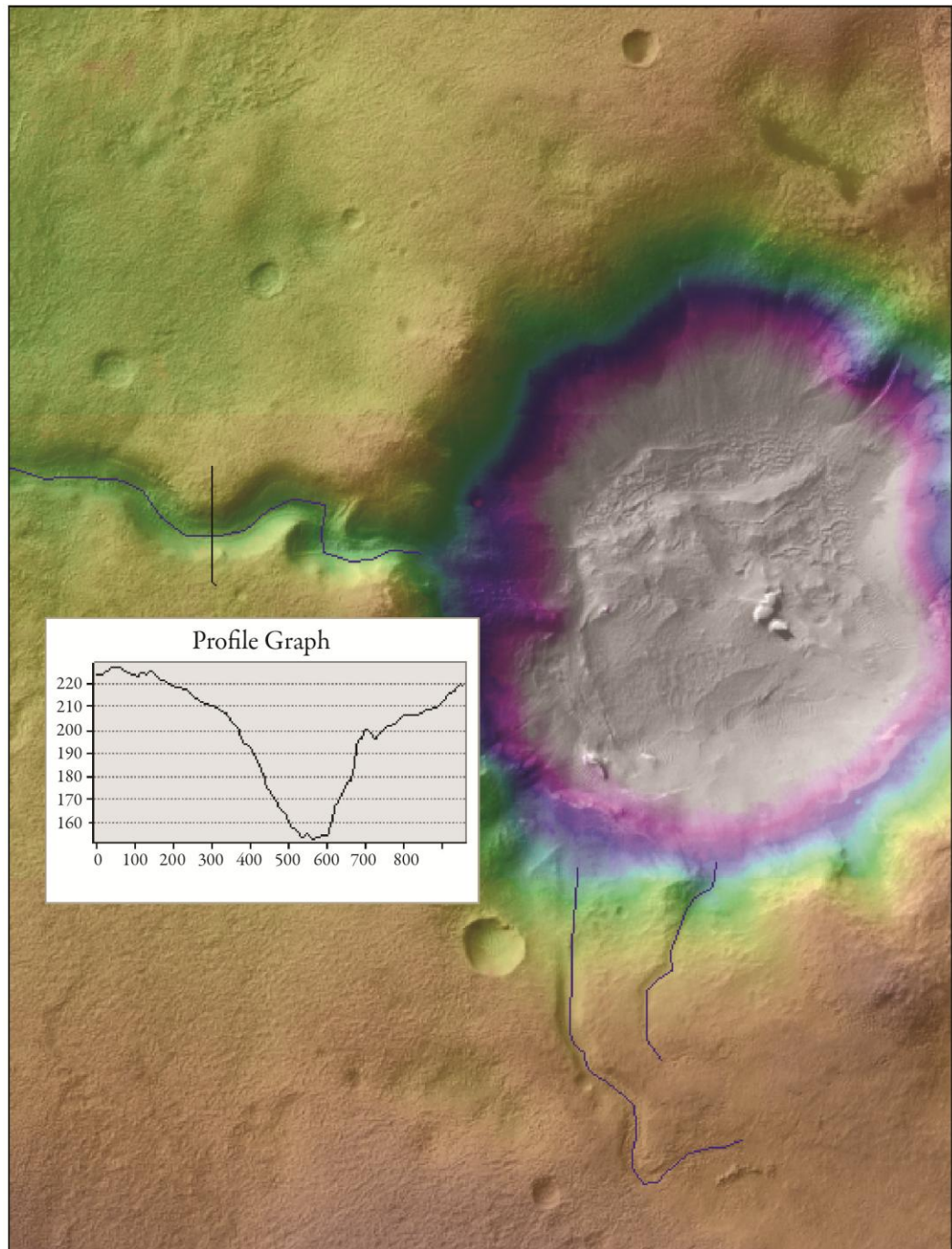


Figure 7: Example of a V-shaped cross-section (with fill) (axes are in meters) of the western valley in crater 1. Note that the profile graph is vertically exaggerated. (DTM overlaid with highest elevation in red and lowest elevation in white.)

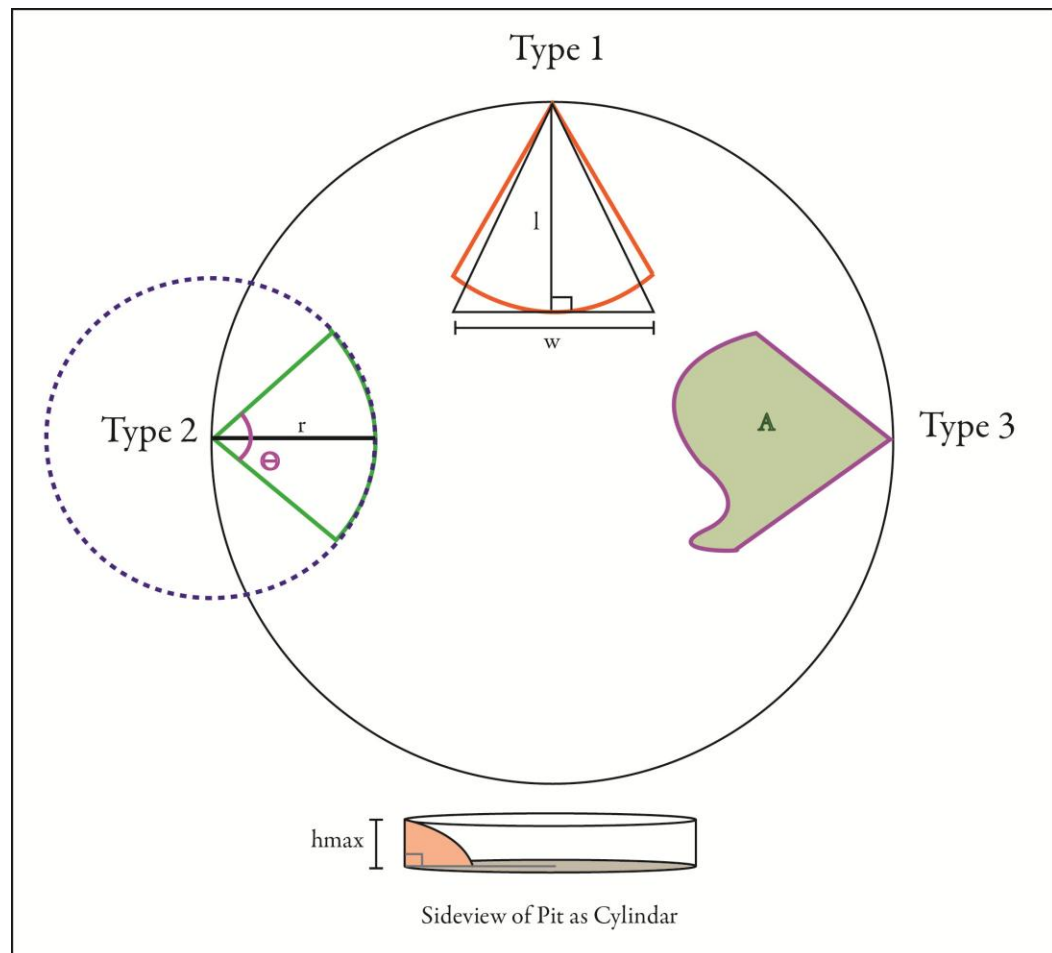


Figure 8: Diagram of the definitions of the variables and the assumptions taken for each of the pit fan volume measurement methods. The large circle to which all the different pit fan models connect at their apex is representative of the rim of the central pit. The bottom-most diagram depicts the assumptions made of the pit structure in order to make the pit volume calculations: cylindrical with right angles at top and bottom.

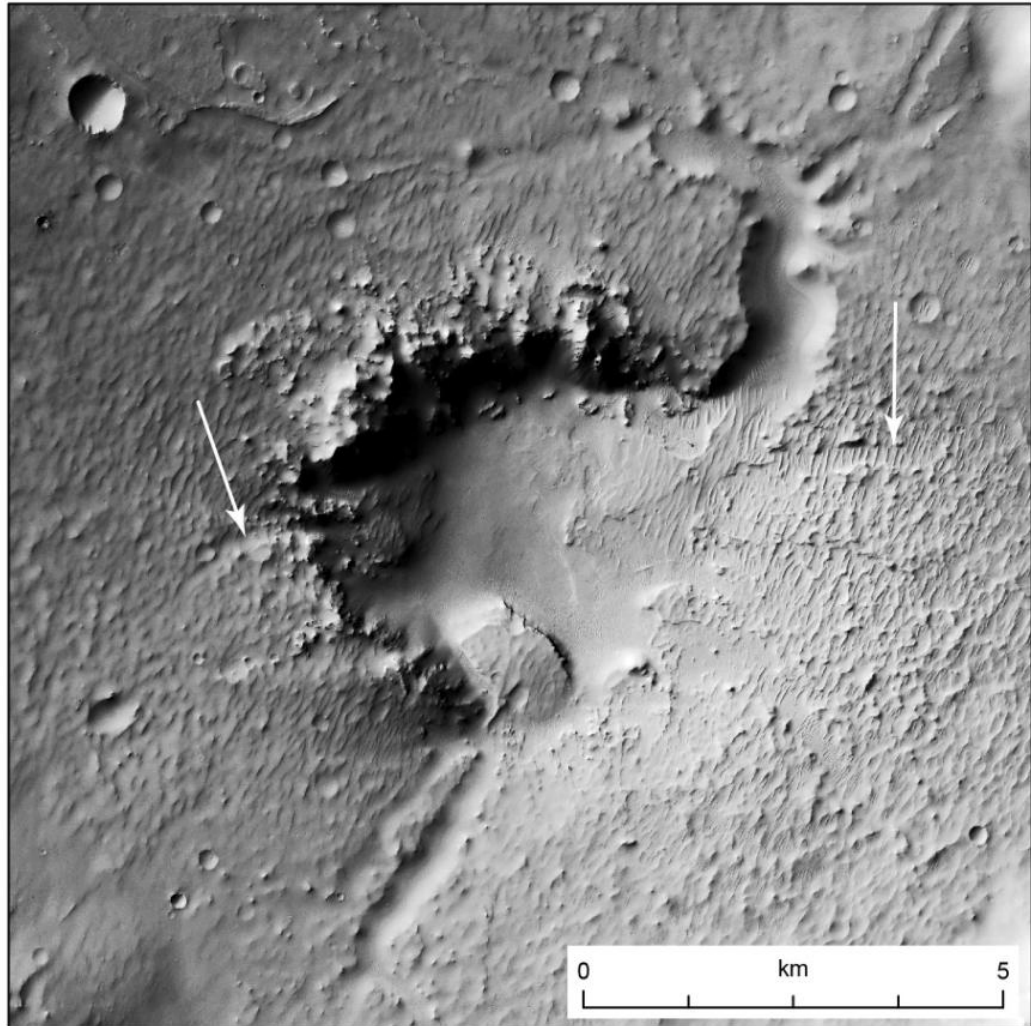


Figure 9: Image of the pit region of crater 4. The arrows point to the features that appear to be highly eroded valleys.

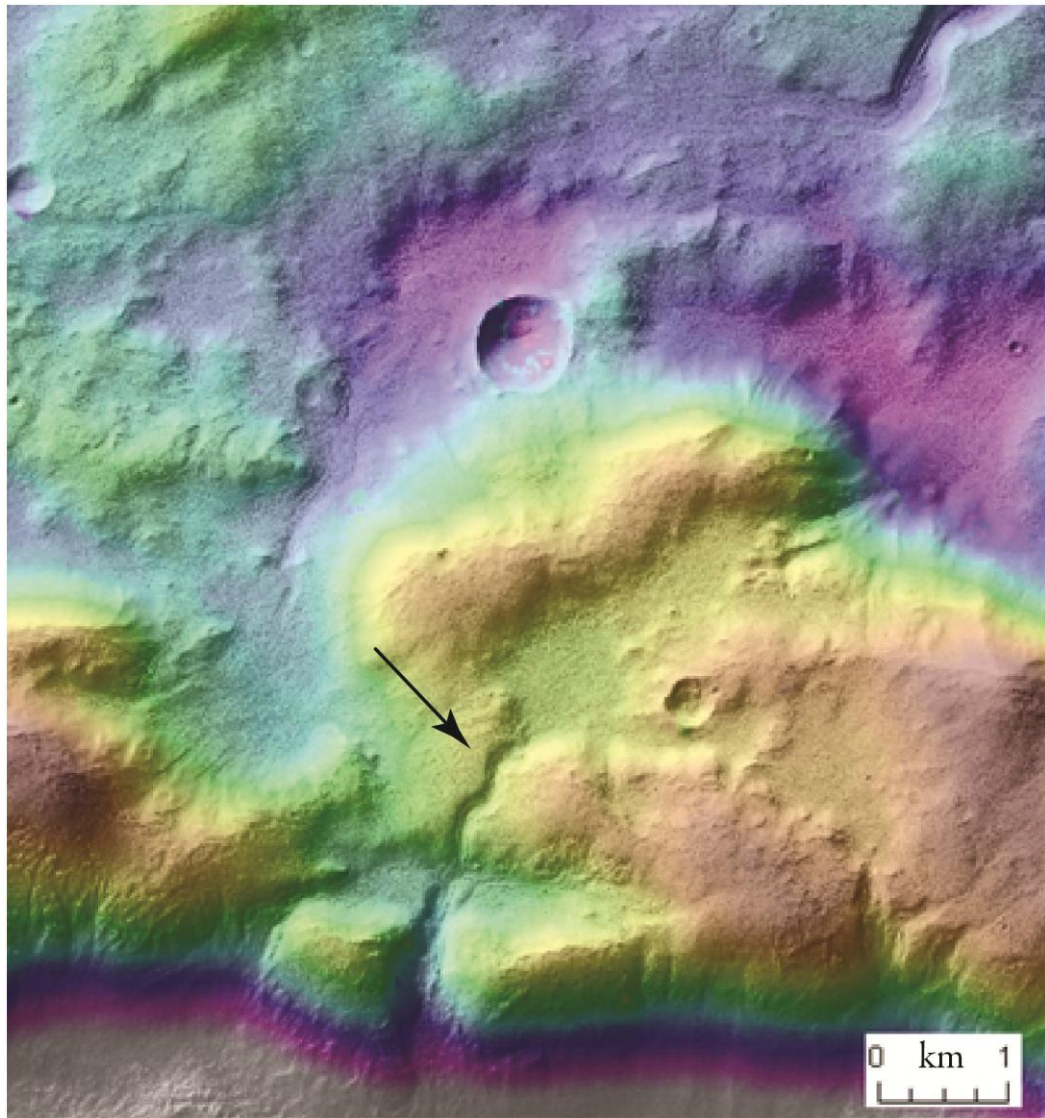


Figure 10: Depression on the northern rim of crater 1. Arrow points to valley draining the southern edge of the depression lake. (DTM overlaid with highest elevation in red and lowest elevation in white.)

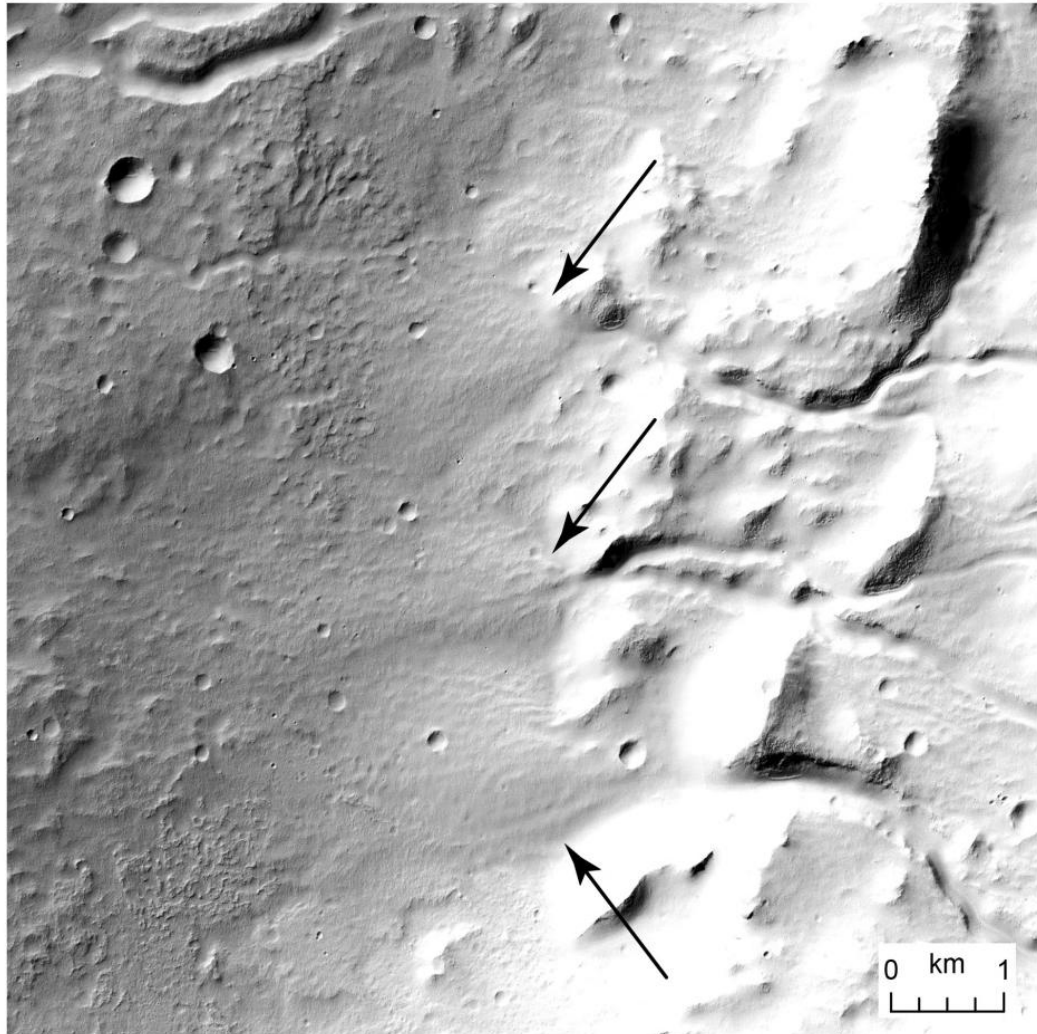


Figure 11: Image of three alluvial fans in the eastern floor of crater 5. The black arrows point to the individual fans.

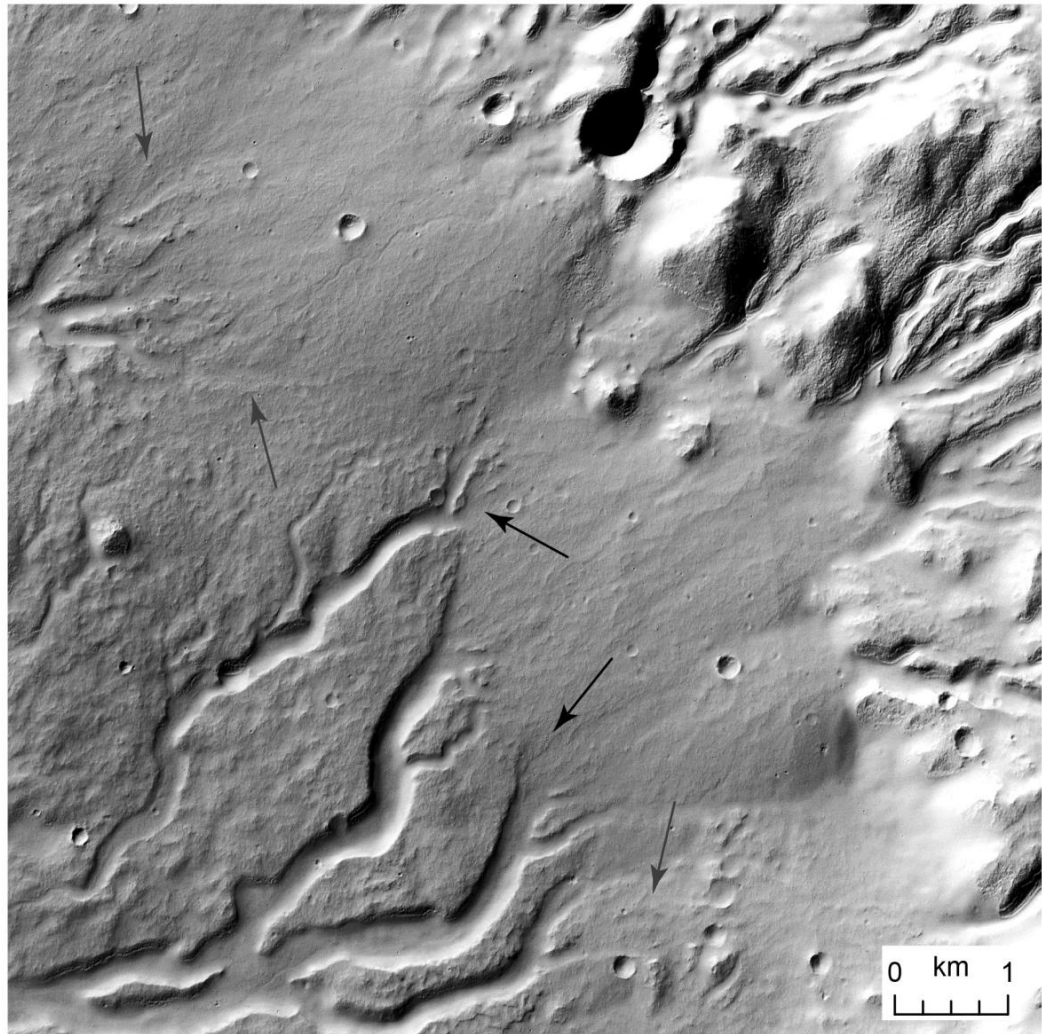


Figure 12: Alluvial fans in the eastern region of crater 5. The toes of the alluvial fans superpose the visible headwaters of the pit valley systems in the area. This causes the headwaters to appear abrupt in some areas (black arrows) and gradual in others (grey arrows).

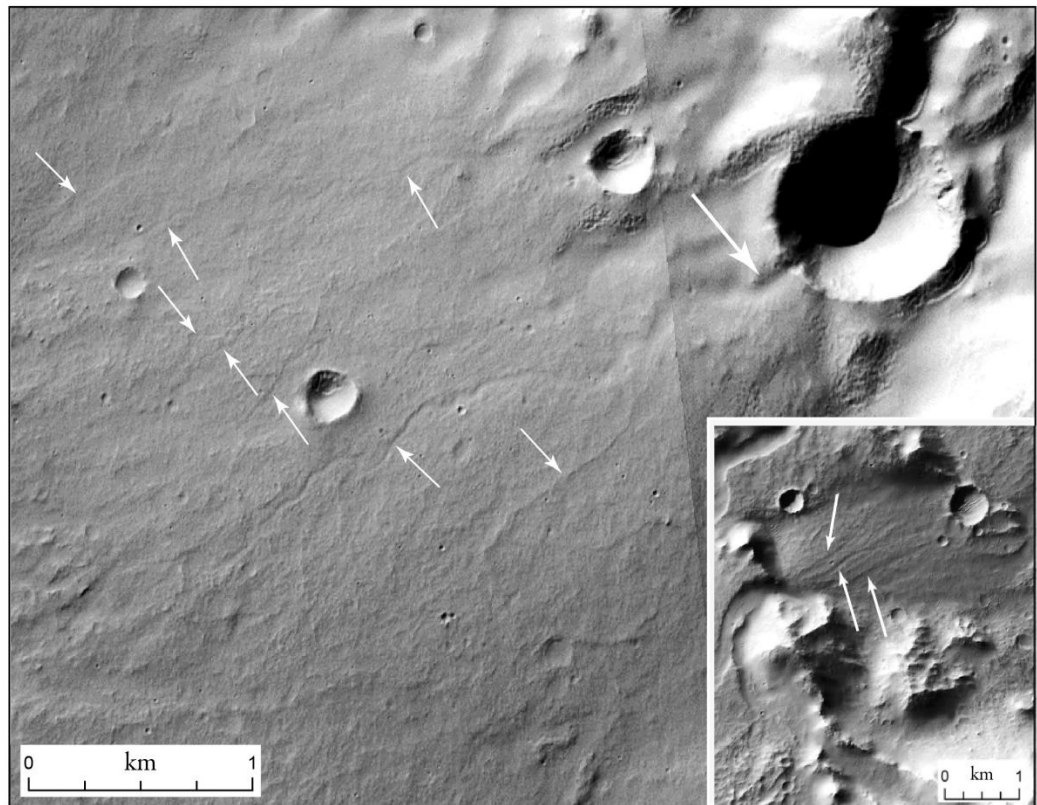


Figure 13: Image of alluvial fan distributaries (small white arrows) on a bajada system on the eastern region of crater 5. There is a small valley (large white arrow) that cuts through a small crater, and diminishes in width as it flows down to a smaller white arrow. (Inset) Image of alluvial fan with distributary channels in the southwestern region of crater 5. Arrows point to the distributary channels in both images. All channels are < 100 m wide.

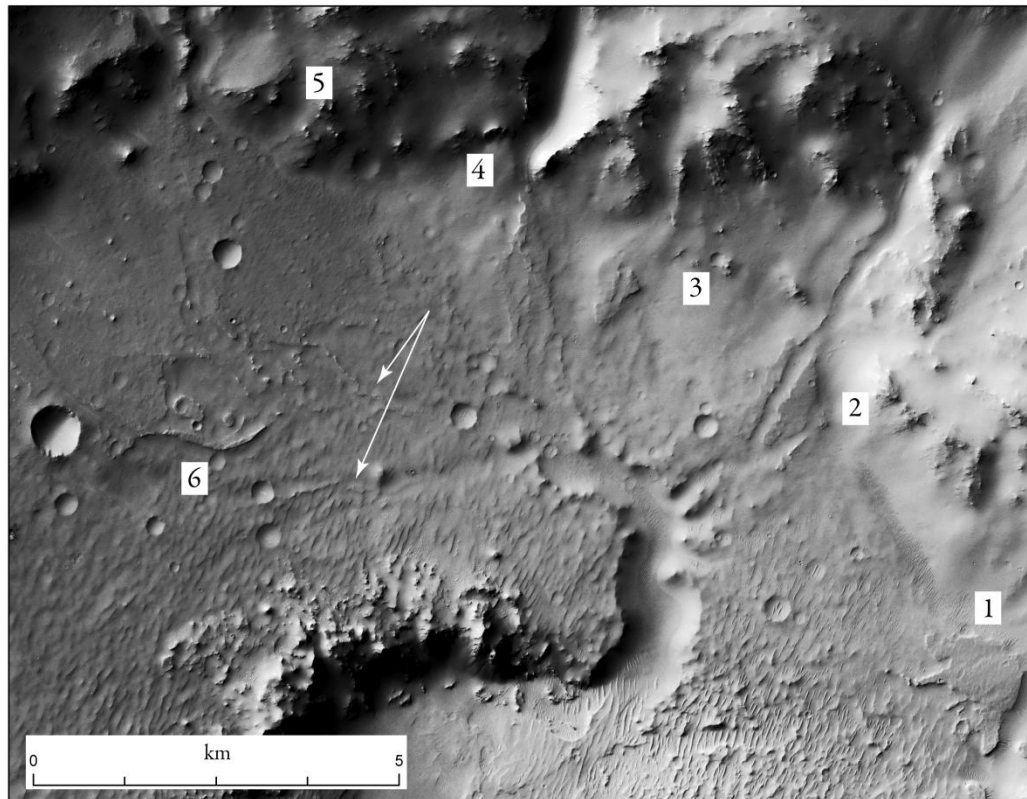


Figure 14: [North is up in the figure.] An inverted alluvial fan (1) that still retains its fan-shape. Alluvial fan (2) that exhibits a valley running through it and towards the trunk of the pit valley as does (3). This is possibly due to a higher flux moving through the systems and eroding the fans. Depositional feature (4) that is very highly eroded, but appears to contain a small channel running positive feature in its tributary. The feature marked by (5) is just SW of the marker and is an alluvial fan that has preserved channels (white arrows) flowing E towards the northern pit valley. A curved form (6) interpreted as being either a paleo-channel that was curving along contour due to some unknown control, or a particularly well-preserved area of the toe of the alluvial fan marked by (5).

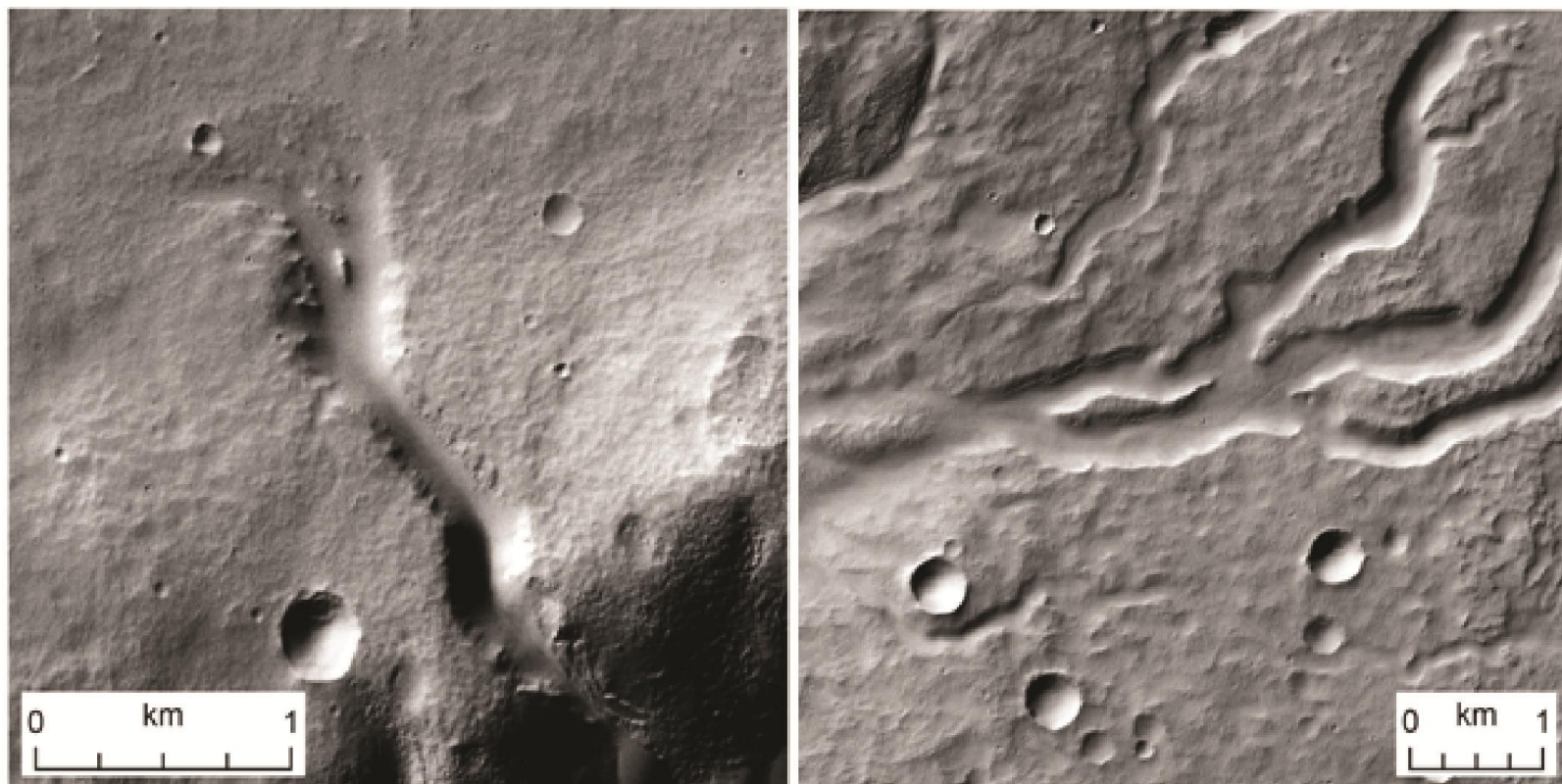


Figure 15: Two images of streamlined islands interpreted as being due to water flow through the valleys in crater 5. (Left) Island formed in the valley that breaches the northern rim of the crater. (Right) Long island formed due to the joining of the northernmost valley with the southern valley systems just upstream of the island.

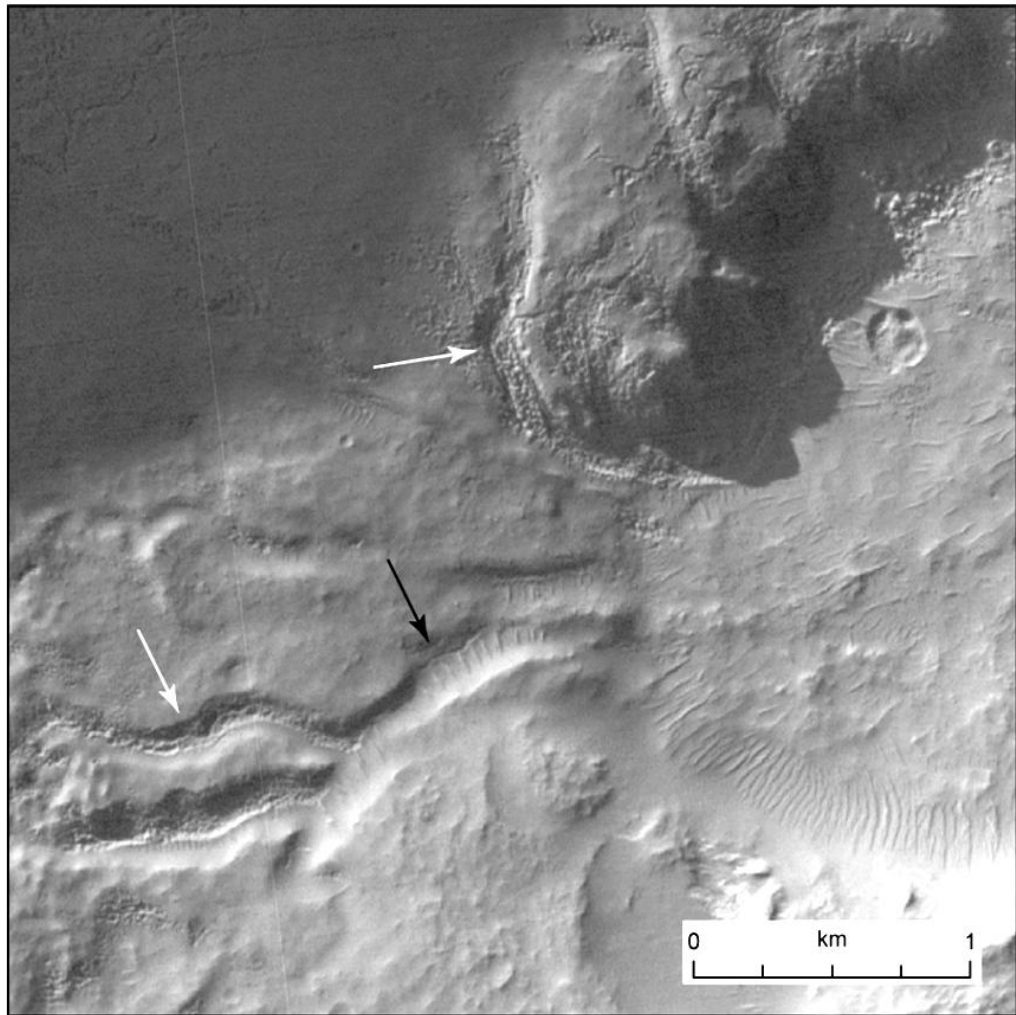


Figure 16: Valleys in crater 3 that are obscured by ice. White arrows point to heavier mantling of valleys, while the black arrow points to areas that are minimally mantled.

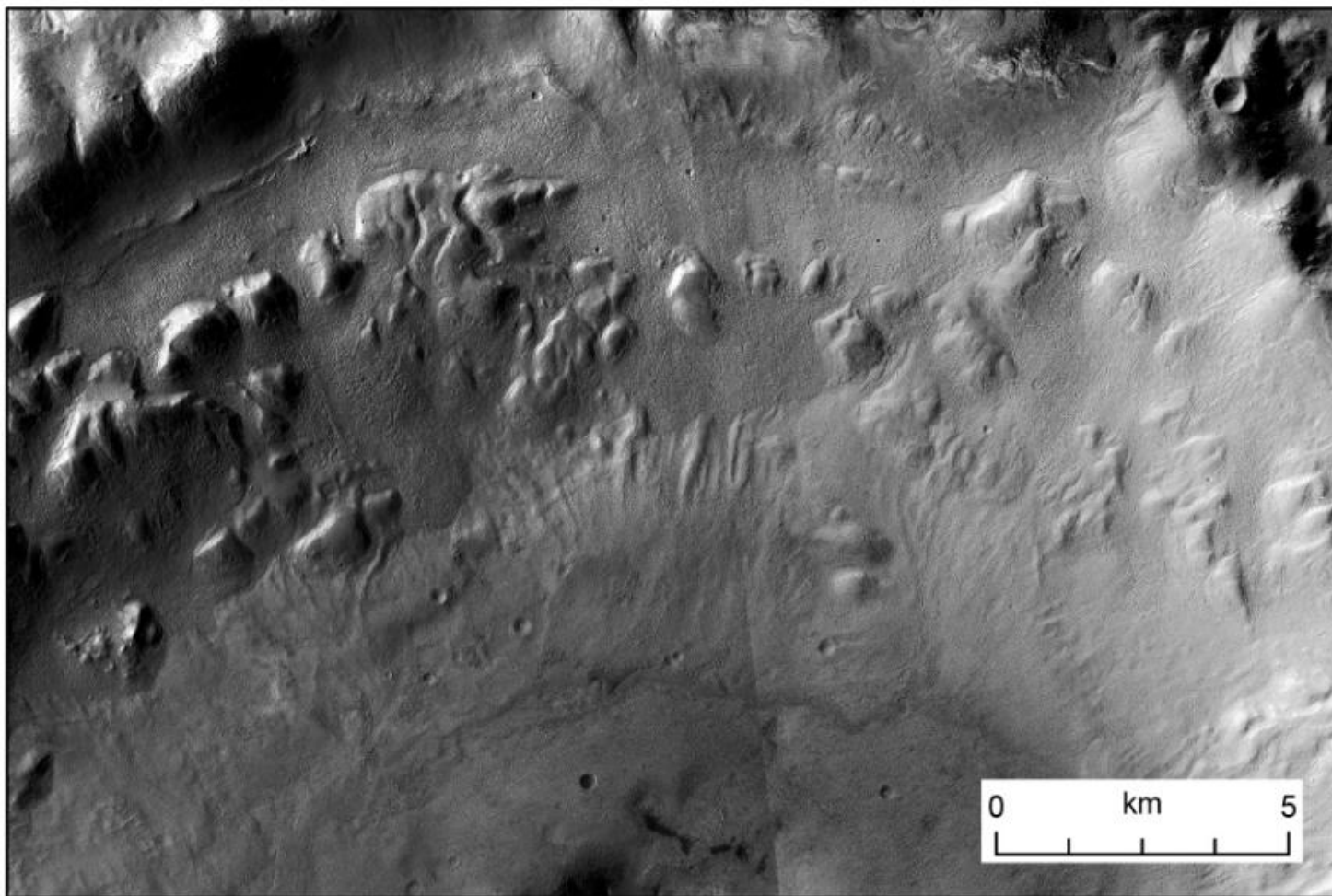


Figure 17: The northern wall of crater 1 showing the large degree of ice-related coverage in the area.

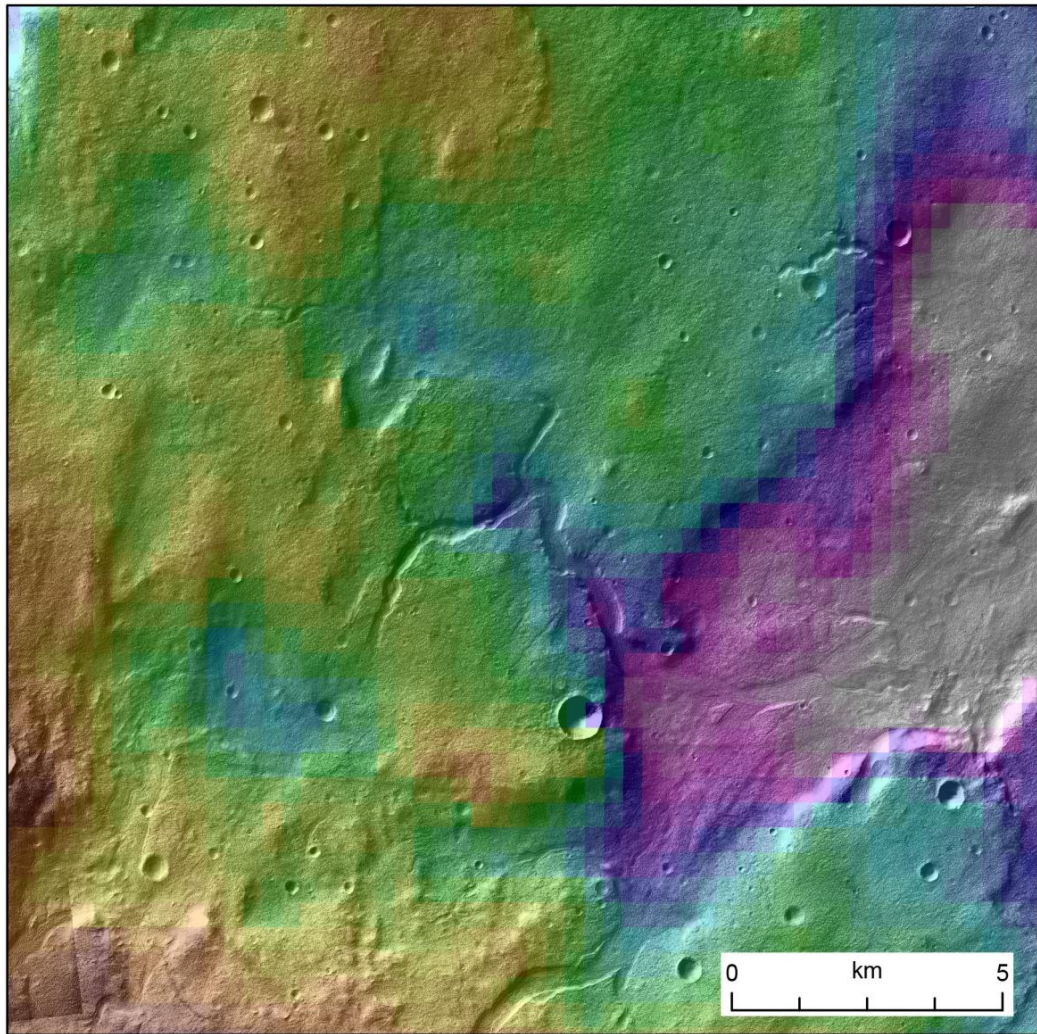


Figure 18: (In NE ejecta blanket region of crater 1.) Image of external valley system northeast of crater 1. MOLA DTM is overlaid atop CTX mosaic: white marks the lowest elevation within the image; red denotes the highest. The valleys are seen connecting depressed areas in green and blue (possible paleo-lakes), and draining the area into the large low in white.

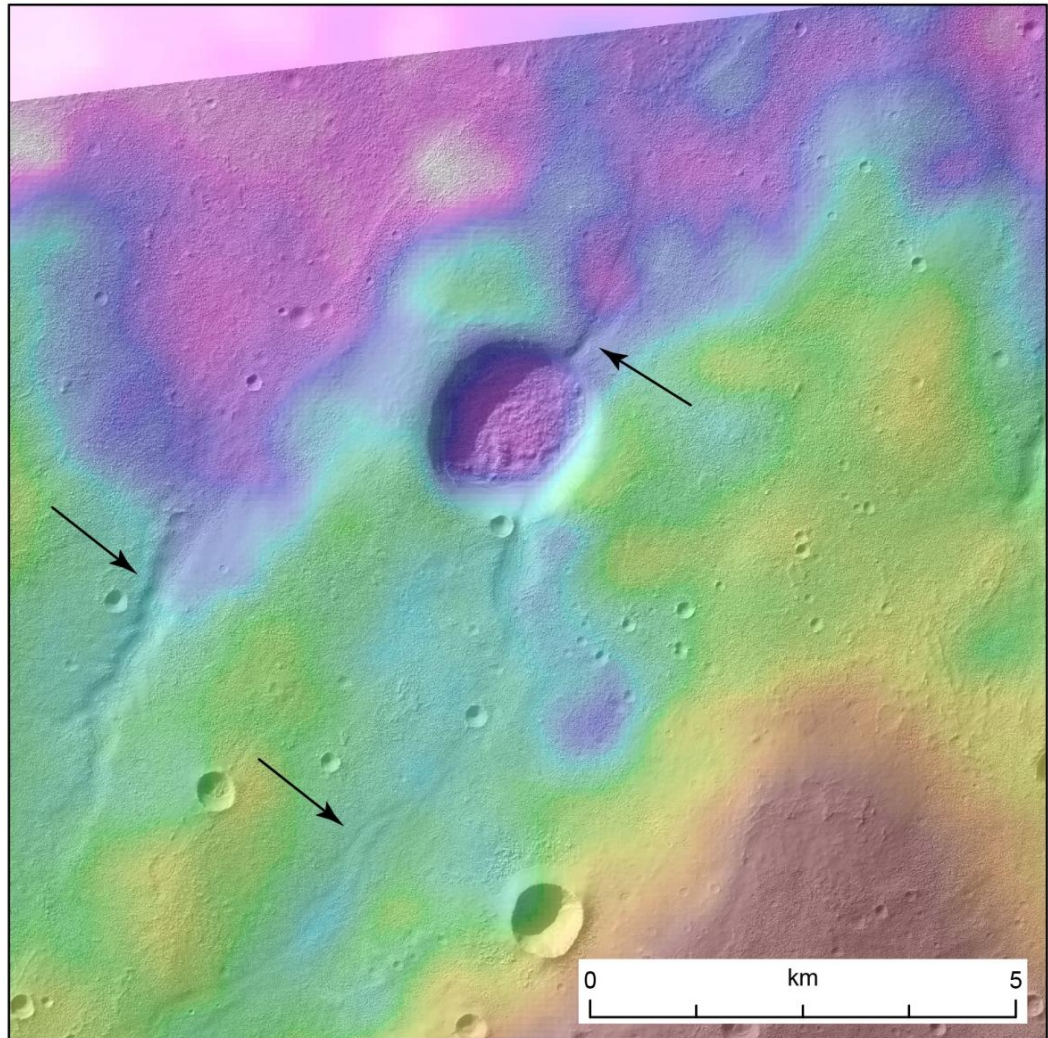


Figure 19: Image of a valley located near crater 3 that drains into a crater. The crater (a possible paleo-lake) is then breached on its northern side. (HRSC DTM with highest elevation in red and lowest elevation in white.) Black arrows point out valley features in this image.

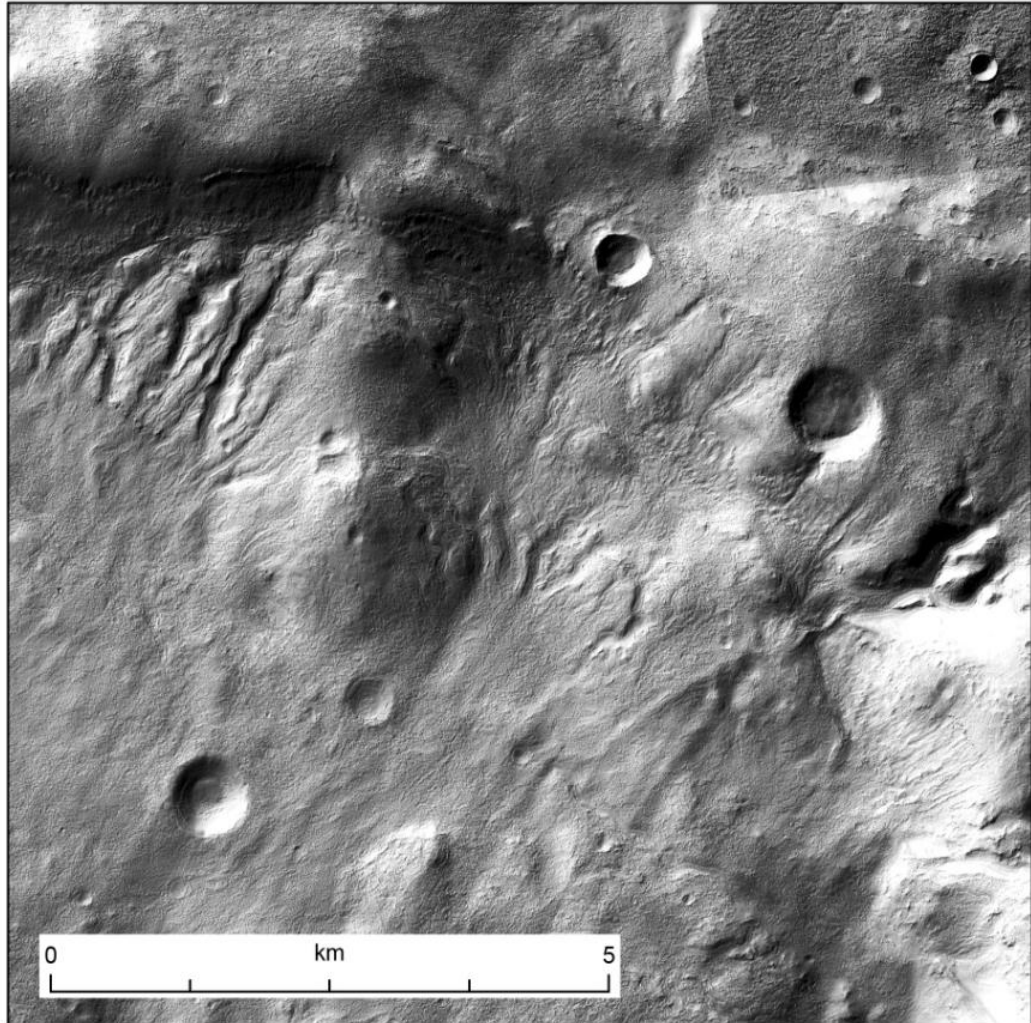


Figure 20: Image of valleys west of crater 1 that appear related to ice-rich mantling, particularly at a number of their origins.

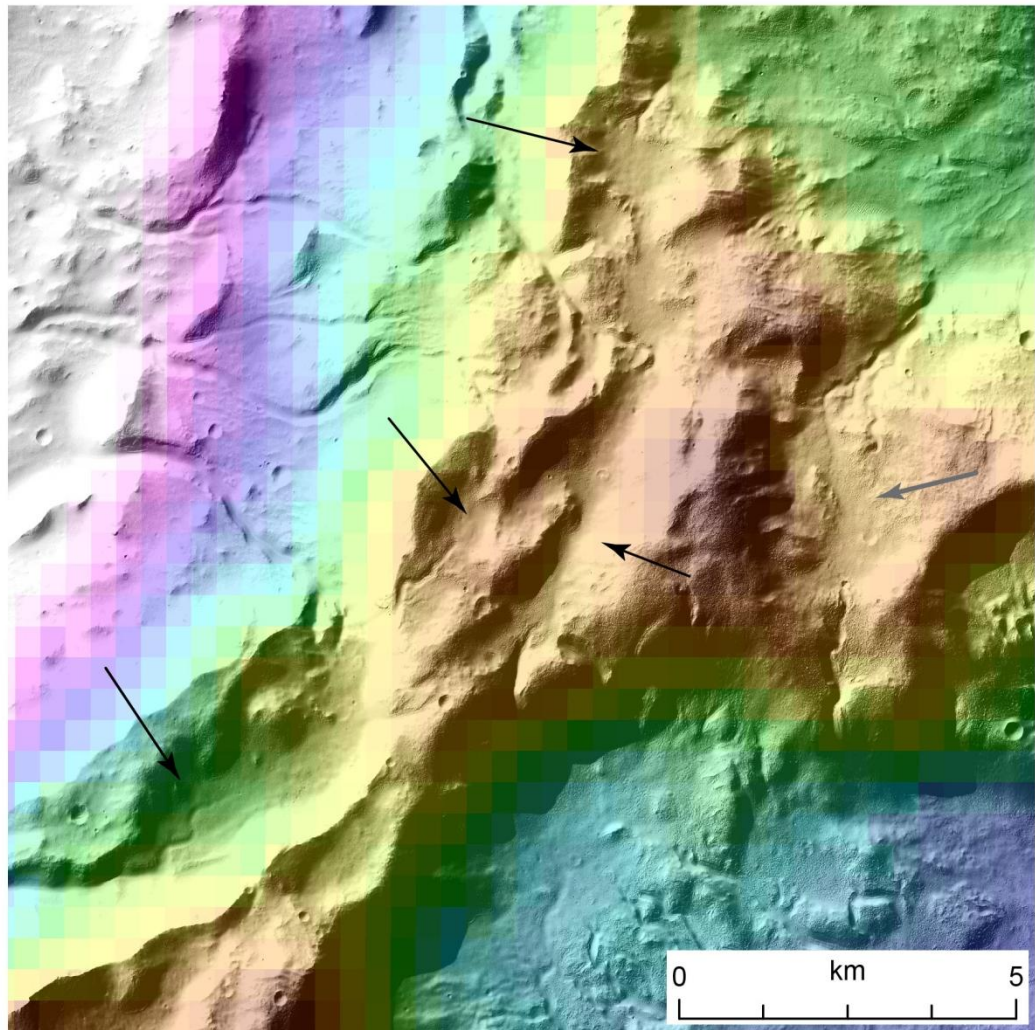


Figure 21: Relatively flat areas on the eastern rim of crater 5 that contain the headwaters of valleys: black arrows. Similar feature, but located at the shared rim of two neighboring craters to crater 5: grey arrow. Note that the features marked by black arrows do not have raised rims and so are not interpreted as paleo-lake features. (DTM overlaid with highest elevation in red and lowest elevation in white.)

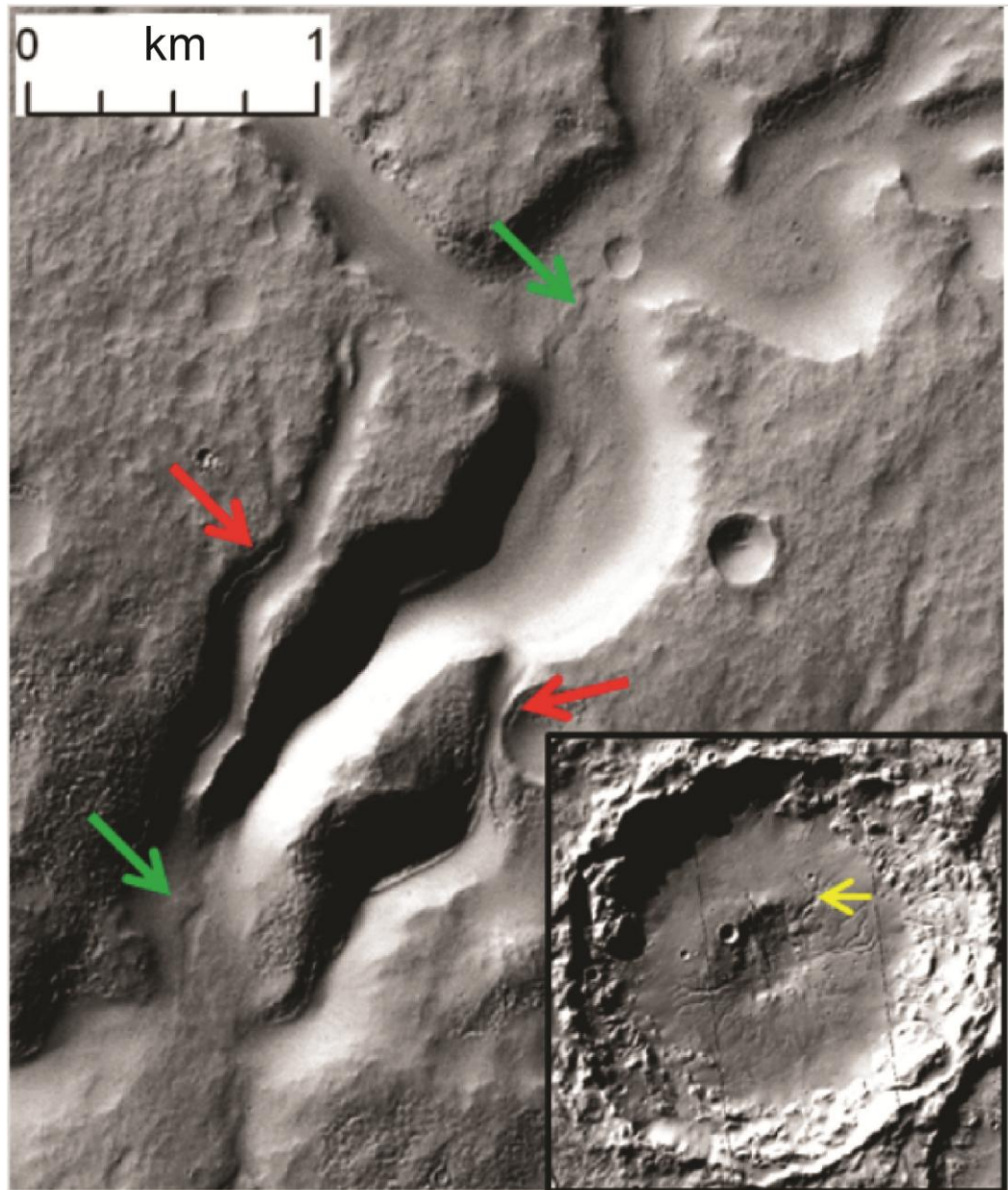


Figure 22: Multi-generational valley system in crater 5. The oldest two valleys are marked by red arrows; the intermediate-aged valley is the valley that hosts the younger two valley features that are marked by green arrows (<100 m in width). (Inset) Full image of crater 5: yellow arrow denotes location of multi-generational system.

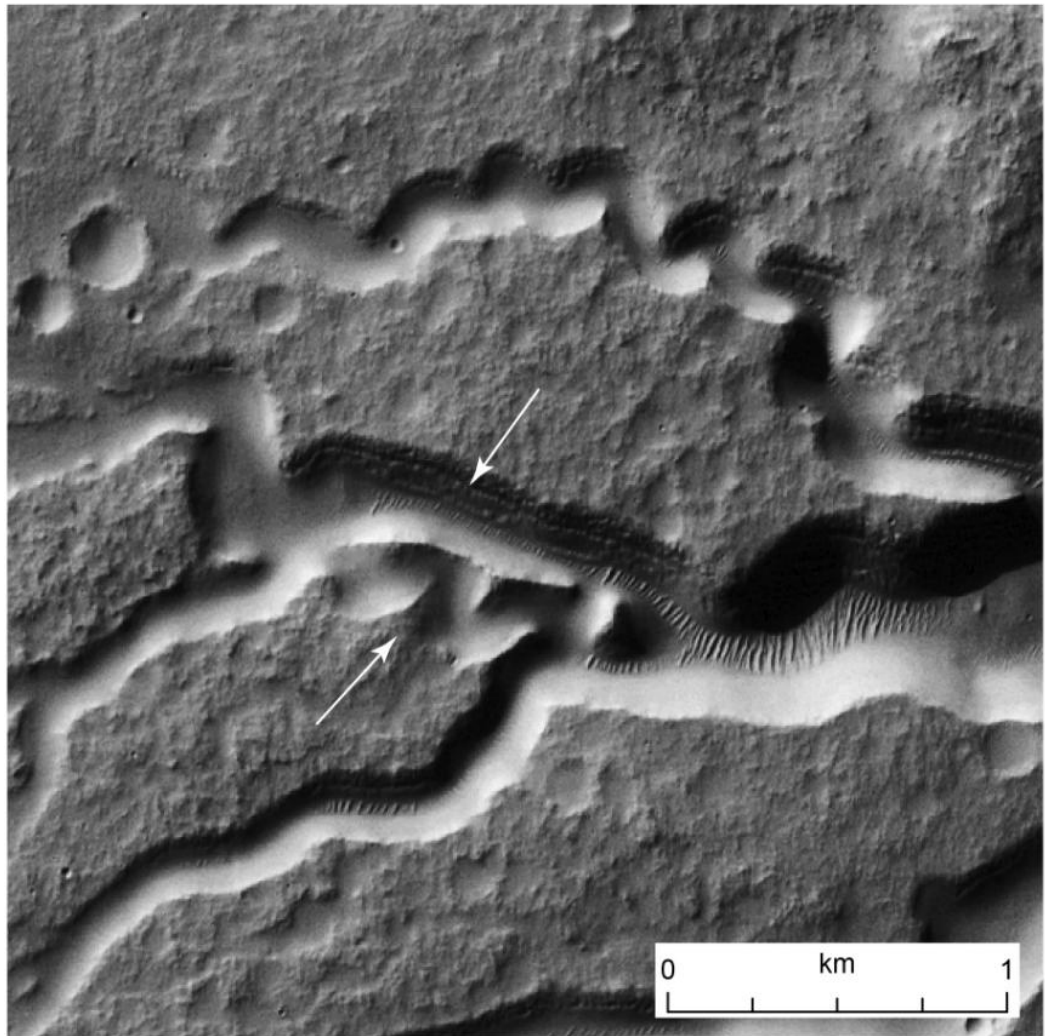


Figure 23: Multi-generational tributary system in the western region of crater 5: valleys are pointed out by white arrow. The lower channel is the older system that has been abandoned in favor of the other younger path. This is evident as the preferred path has incised deeper into the floor.

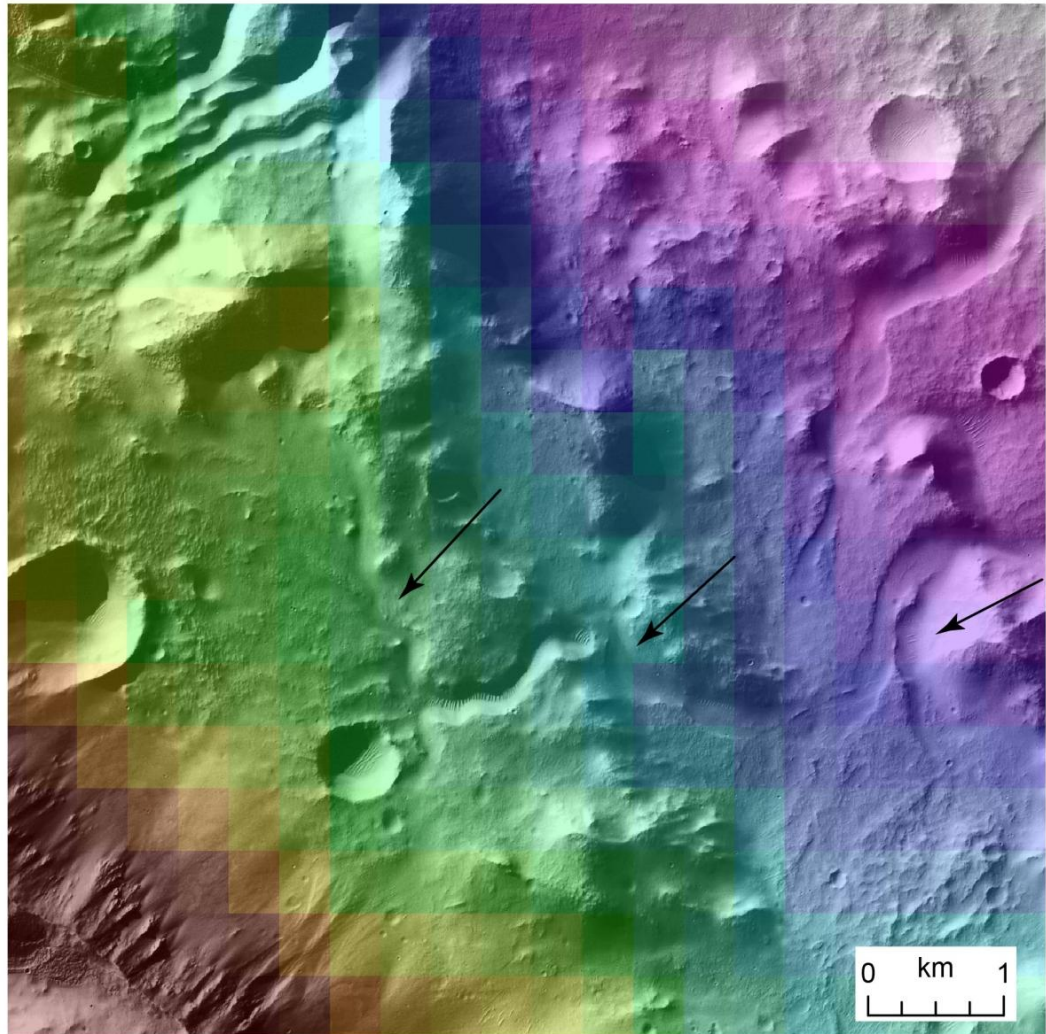


Figure 24: Valleys being forced to flow perpendicular to the radius of the crater by the presence of terrace walls (black arrows). Once each wall is cleared, the valley recommences flowing approximately parallel to the radius of the crater. The downhill direction is towards the upper right of the image.

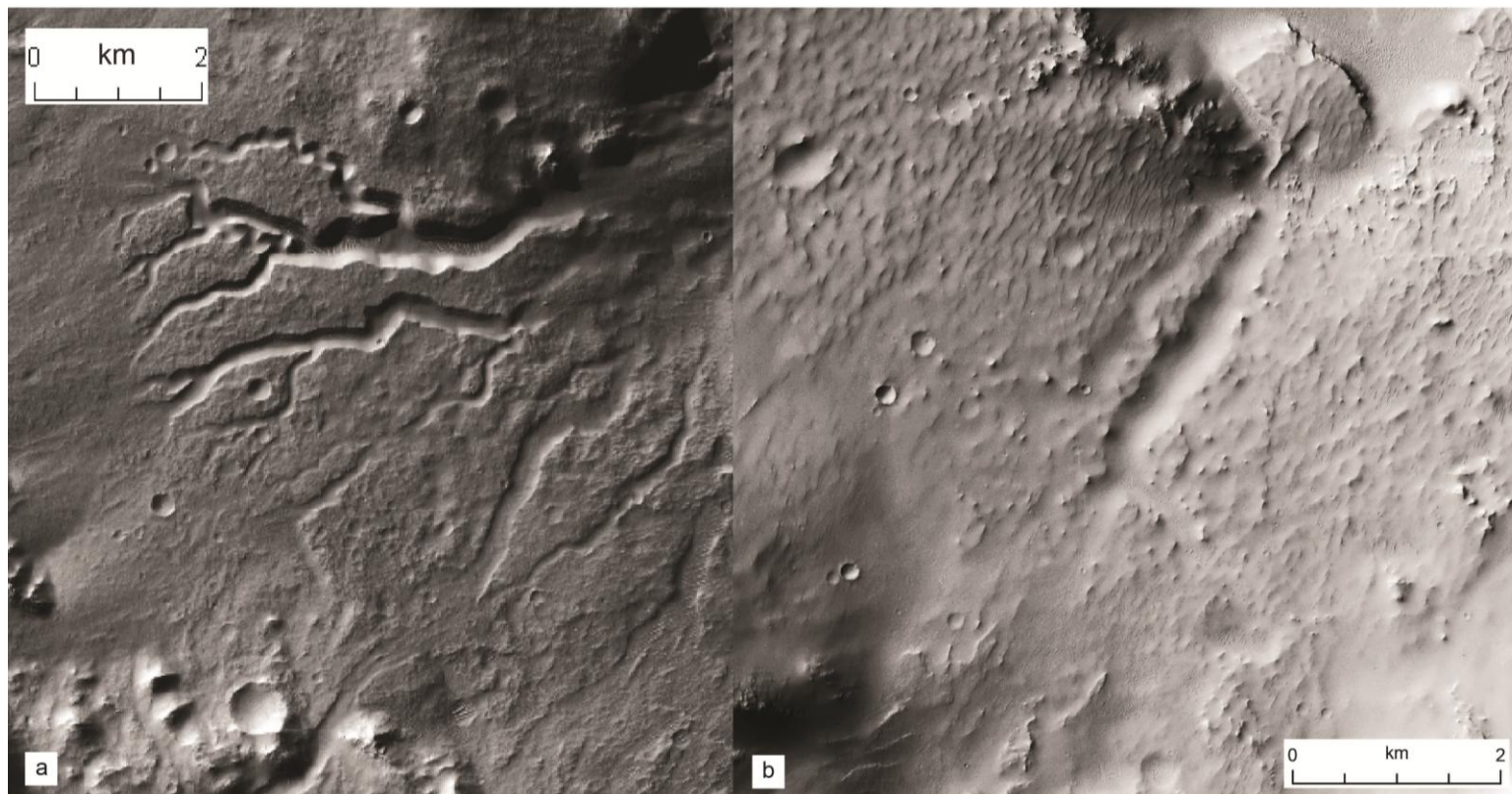


Figure 25: (a) Dendritic drainage pattern present in pit valley systems in crater 5. (b) Highly linear valley features present in crater 4.

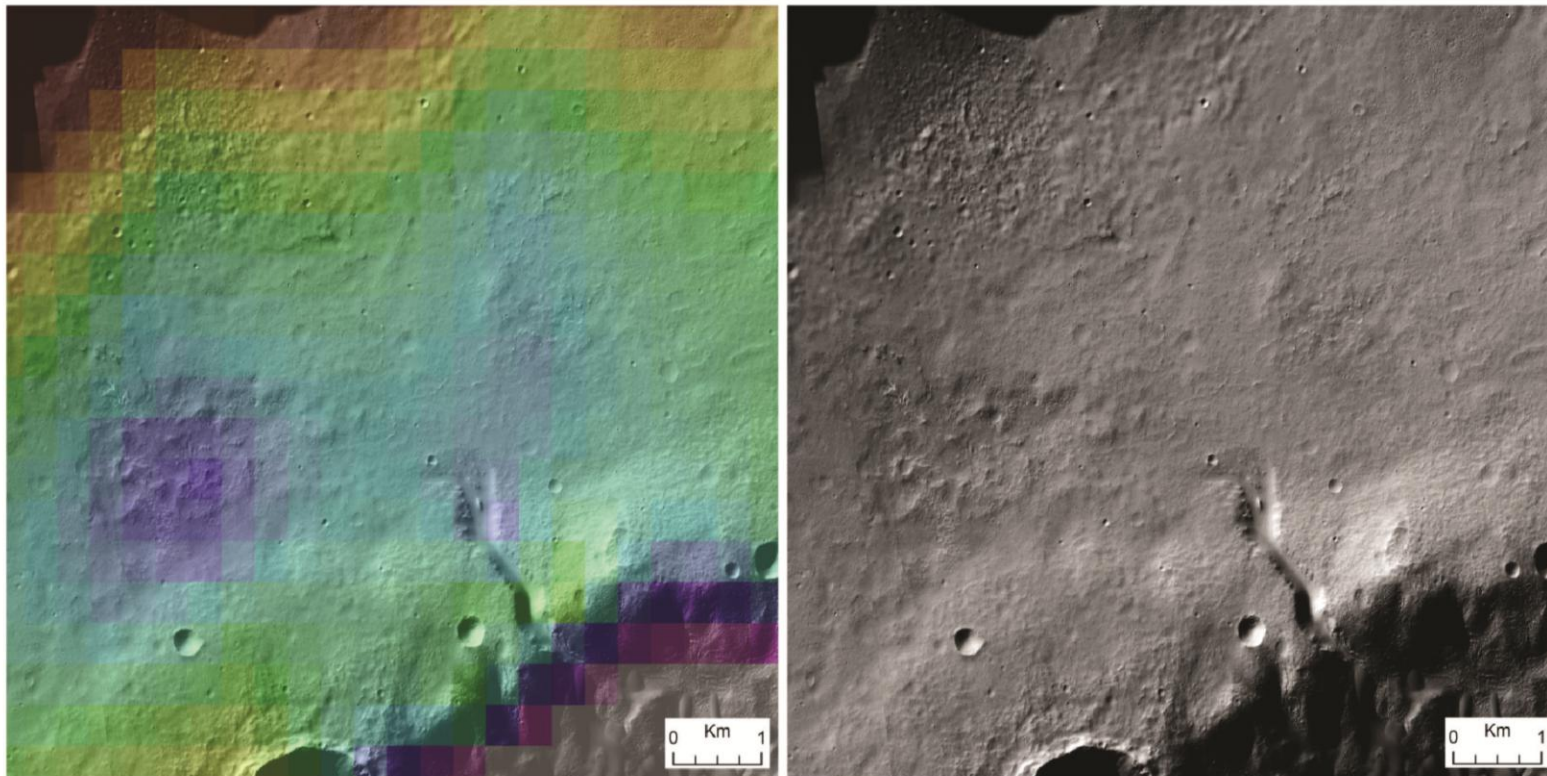


Figure 26: Northern floor of crater 5. (Left) DTM draped over the northern floor of crater 5. The highest topography is marked in red; the lowest topography is in white. (Right) Northern floor of crater 5 without DTM. In both images there is a valley flowing out of the central pit and onto the surrounding crater floor. Note that the depressed areas on the crater floor, marked in blue in the elevation map, have a different texture than the surrounding area.

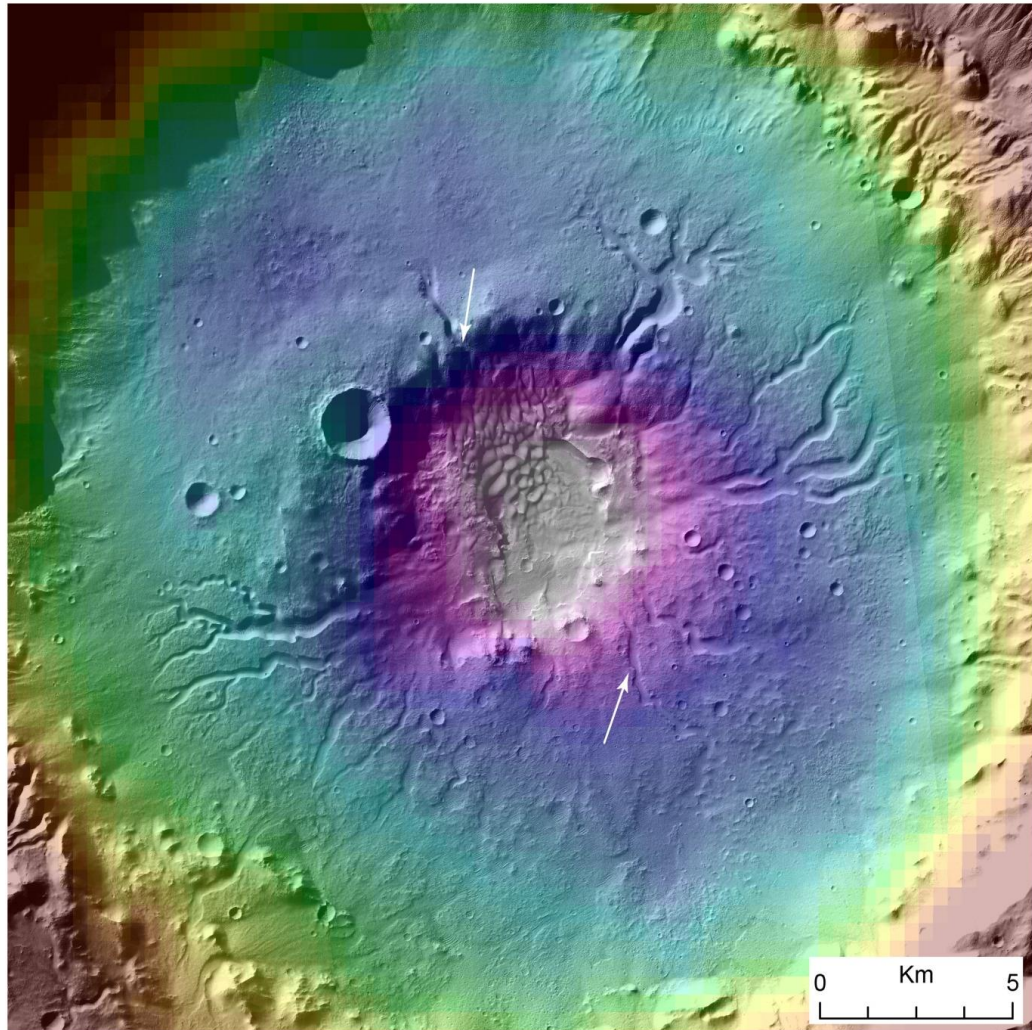


Figure 27: Full map of crater 5 showing the level of the interpreted lake surface. The topography of the image is such that the highest elevations are colored in red and the lowest elevation is in white. The upper white arrow points to the level of the breach at the northern rim. The lower white arrow points to a valley at the southern rim of the pit that is lower in elevation than the level of the pit lake at breach.

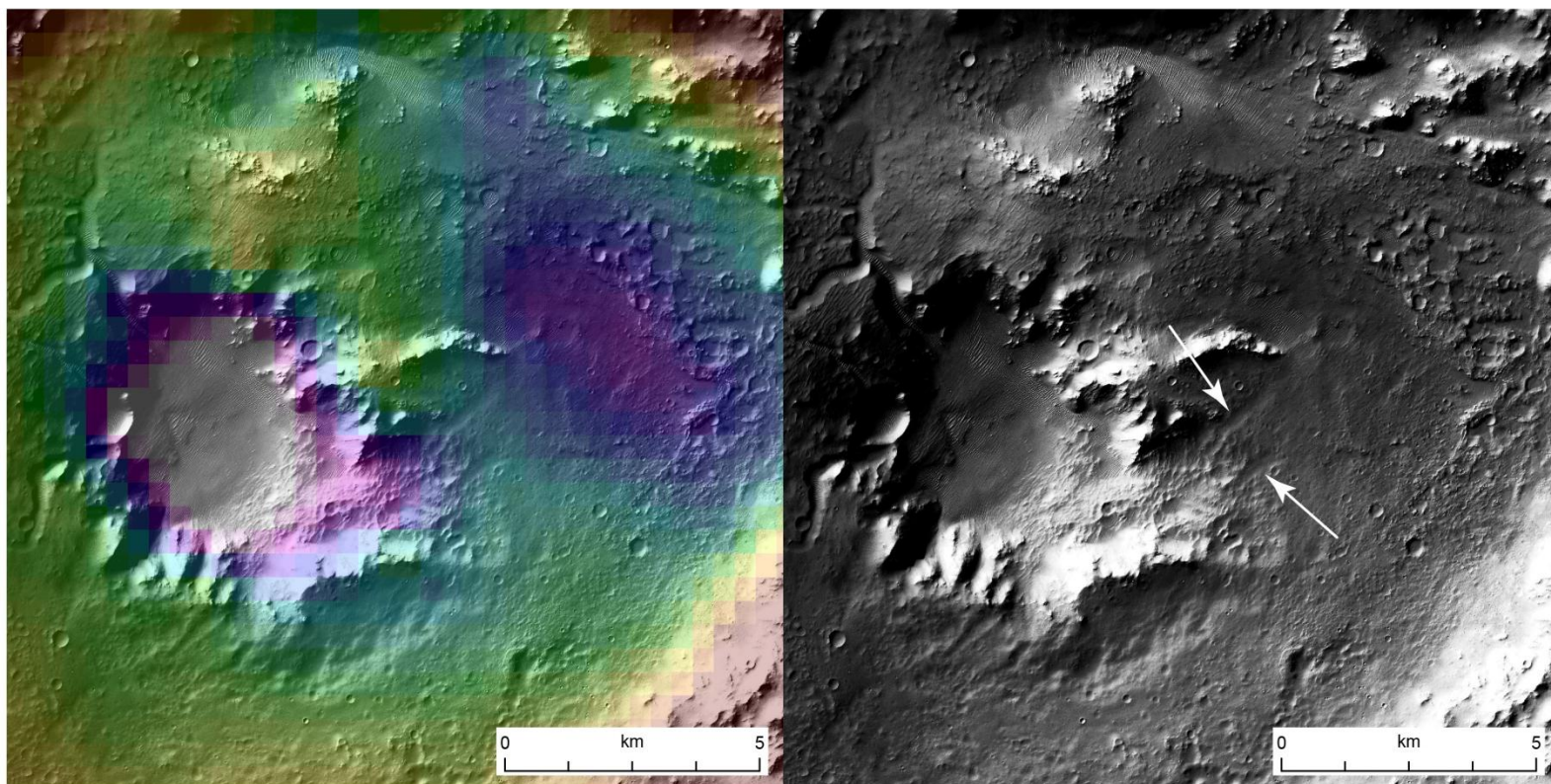


Figure 28: (Left) Image of crater 2 with a MOLA DTM overlay to display the relatively depressed southeastern floor. The highest elevation is red and the lowest is white. (Right) Image of crater 2 without DTM coverage. White arrows point to valley features.

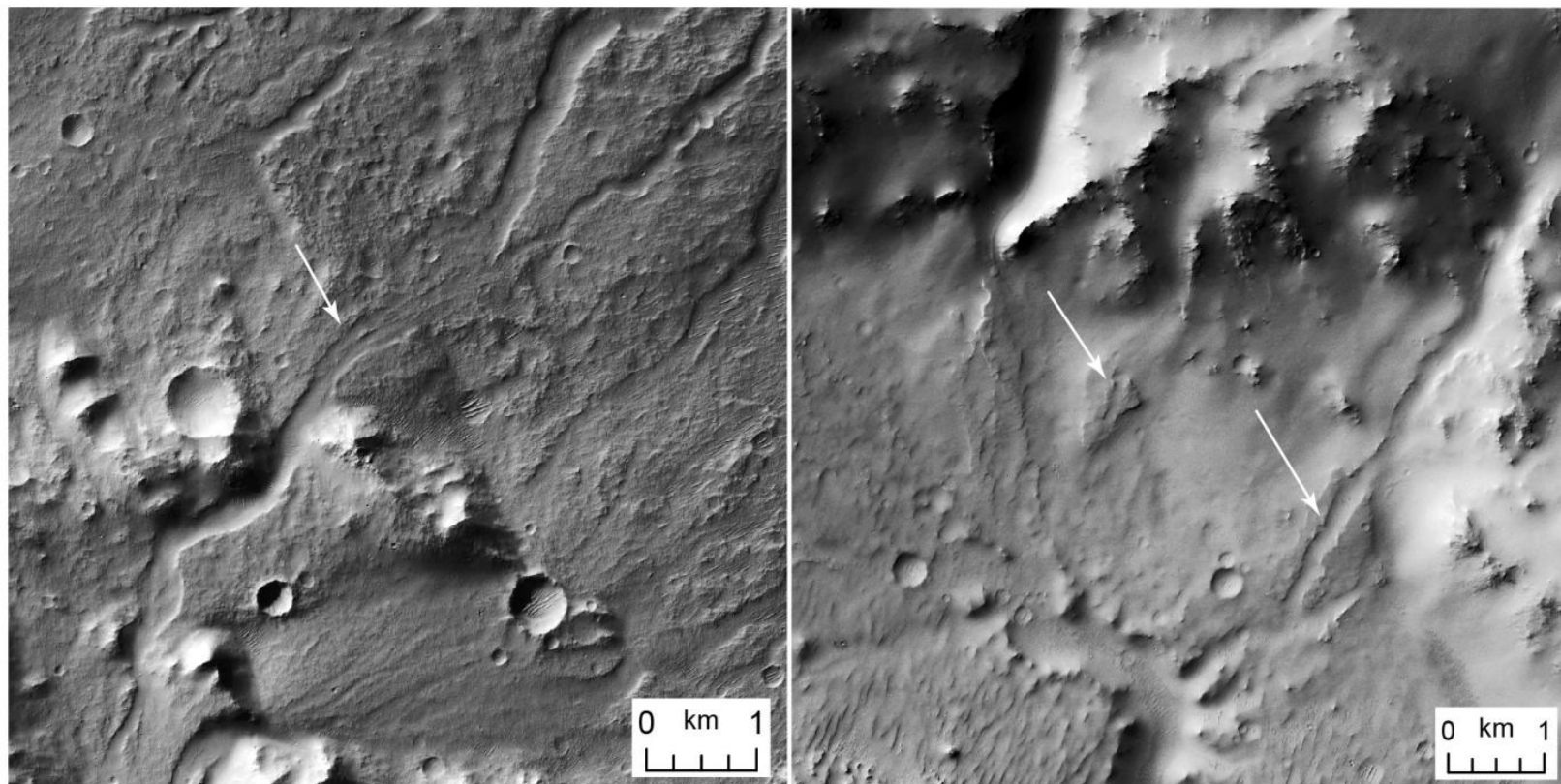


Figure 29: White arrows point to valley channels within the alluvial fans that may be due to higher fluxes moving through their parent channels. (Left) Alluvial fans in the southwestern region of crater 5. (Right) Alluvial fans in the northern half of crater 4.

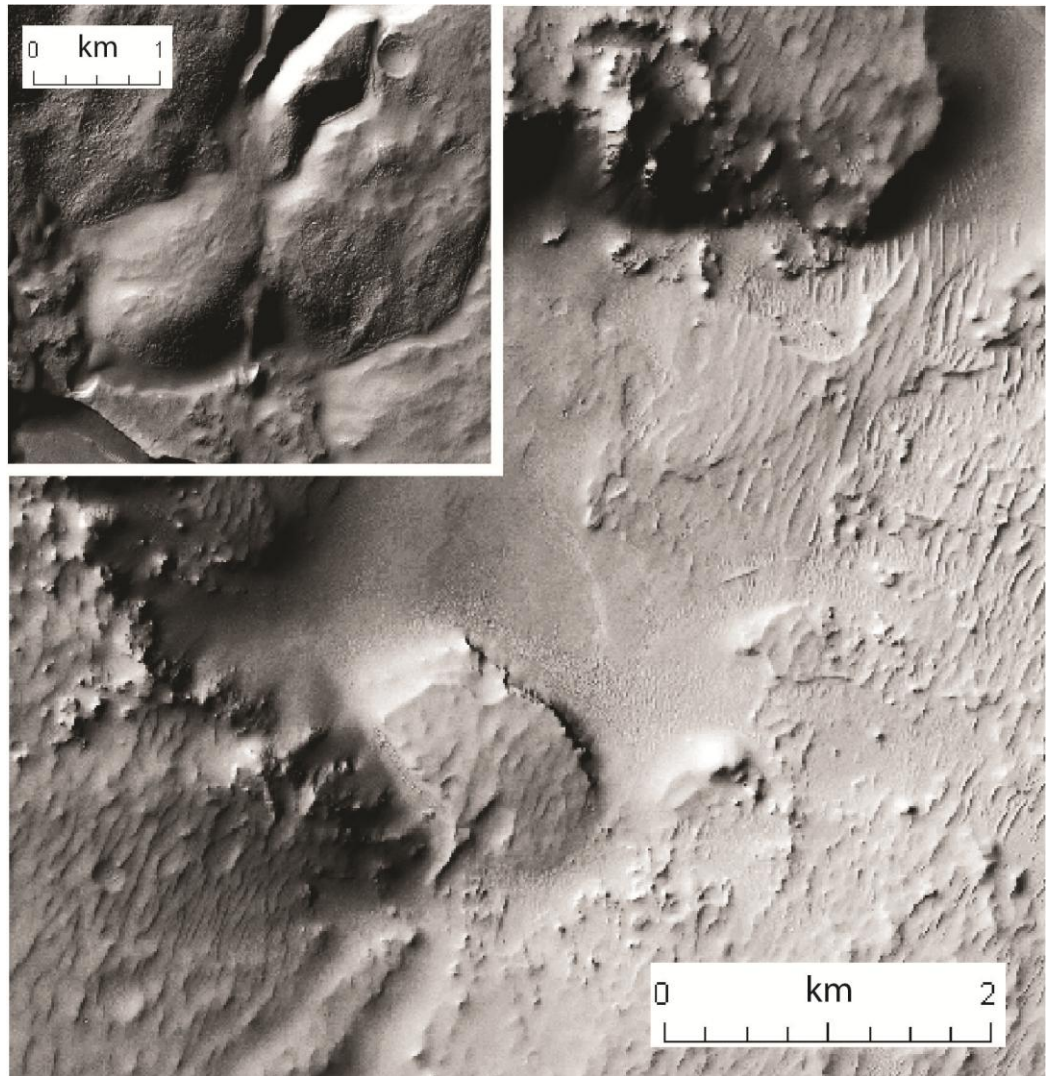


Figure 30: Pit fans located at the termini of the valleys that debouch into crater 4. Note the difference in form between the two fans. (Inset) Pit fan located at the terminus of the multi-generation valley system in crater 5.

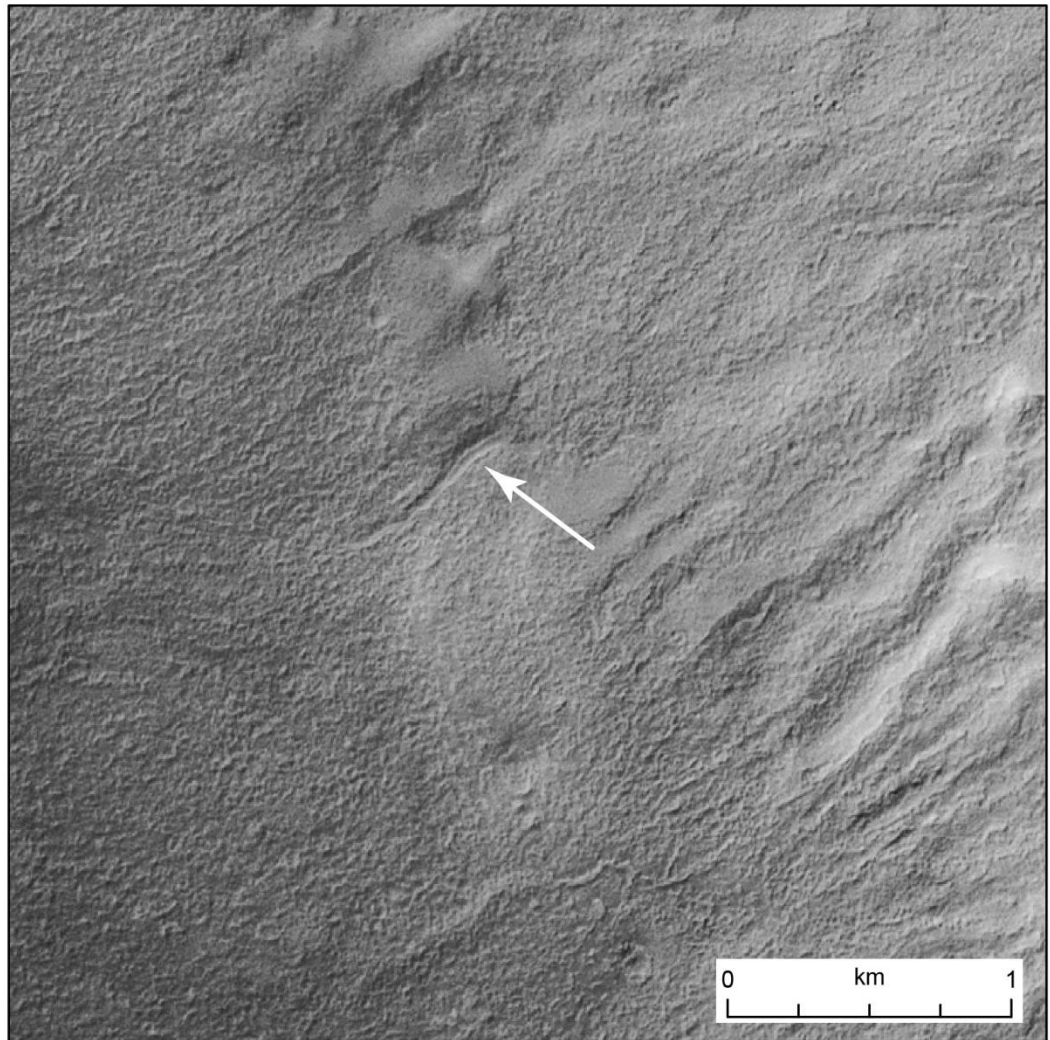


Figure 31: Valley (indicated by white arrow) located within crater 1 that appears associated with ice features.

## 8. TABLES

**Table 1: General Valley Results**

Crater #	CTX Image	Sources of Error	Valley Network	Valley Length (m)	Valley Width (m)	Valley Depth (m)	Channel Widths (m)	Channel Depth (m)	Water-shed Area (m <sup>2</sup> )	Slope	(Rect.) Valley Vol. (m <sup>3</sup> )	(Tri.) Valley Vol. (m <sup>3</sup> )
1	P05_002819_1385_XN_41S189W		W	6140	400	40	120	12	23.86x10 <sup>6</sup>	0.013	9.82x10 <sup>7</sup>	49.12x10 <sup>6</sup>
1	P05_002819_1385_XN_41S189W		E	6040	250	25	80	8	15.45x10 <sup>6</sup>	0.035	3.78x10 <sup>7</sup>	18.88x10 <sup>6</sup>
1	P05_002819_1385_XN_41S189W		S1 (right)	1830	140	14	40	4	15.28x10 <sup>5</sup>	0.153	3.59x10 <sup>6</sup>	17.93x10 <sup>5</sup>
1	P05_002819_1385_XN_41S189W		S2 (left)	3690	200	20	60	6	10.73x10 <sup>7</sup>	0.062	1.48x10 <sup>7</sup>	73.80x10 <sup>5</sup>
2	P05_003063_1523_XI_27S012W		W1 (top)	11440	450	45	180	18	14.02x10 <sup>7</sup>	0.026	2.32x10 <sup>8</sup>	11.58x10 <sup>7</sup>
2	P05_003063_1523_XI_27S012W	valley impacted	W2 (mid.)	2730	220	22	100	10	27.76x10 <sup>6</sup>	0.040	1.32x10 <sup>7</sup>	66.07x10 <sup>5</sup>
2	P05_003063_1523_XI_27S012W	valley impacted	W3 (bottom)	5670	300	30	160	16	11.62x10 <sup>7</sup>	0.011	5.10x10 <sup>7</sup>	25.52x10 <sup>6</sup>
3	B20_017412_1407_XN_39S088W	ice-rich area	N Right	10230	150	15	70	7	24.58x10 <sup>6</sup>	0.027	2.30x10 <sup>7</sup>	11.51x10 <sup>6</sup>
3	B20_017412_1407_XN_39S088W		N Middle	2499	100	10	50	5	N/A	0.064	2.50x10 <sup>6</sup>	12.50x10 <sup>5</sup>
3	B20_017412_1407_XN_39S088W		N Left	4327	100	10	50	5	85.97x10 <sup>6</sup>	0.037	4.33x10 <sup>6</sup>	21.64x10 <sup>5</sup>
3	B20_017412_1407_XN_39S088W	heavily mantled; shadow	NW	1409	95	9.5	20	2	25.17x10 <sup>6</sup>	0.071	1.27x10 <sup>6</sup>	63.58x10 <sup>4</sup>
3	B20_017412_1407_XN_39S088W		W Down	3733	200	20	80	8	42.29x10 <sup>6</sup>	0.038	1.49x10 <sup>7</sup>	74.66x10 <sup>5</sup>
3	B20_017412_1407_XN_39S088W		W Middle	2579	170	17	70	7	32.74x10 <sup>6</sup>	0.062	7.45x10 <sup>6</sup>	37.27x10 <sup>5</sup>
3	B20_017412_1407_XN_39S088W	heavily mantled; shadow	W Upper (longer)	1922	150	15	~80	8	19.97x10 <sup>6</sup>	0.073	4.32x10 <sup>6</sup>	21.62x10 <sup>5</sup>

3	B20_017412_1407_ XN_39S088W		S	8780	200	20	60	6	14.52x10 <sup>7</sup>	0.018	3.51x10 <sup>7</sup>	17.56x10 <sup>6</sup>
4	B21_017751_1609_ XN_19S347W		NE	15816	780	78	200	20	20.06x10 <sup>7</sup>	0.051	9.62x10 <sup>8</sup>	48.11x10 <sup>7</sup>
4	B21_017751_1609_ XN_19S347W	highly eroded	SW (TOP)	2854	230	23	80	8	21.82x10 <sup>6</sup>	0.091	1.51x10 <sup>7</sup>	75.49x10 <sup>5</sup>
4	B21_017751_1609_ XN_19S347W		SW (BOT- TOM)	4348	420	42	150	15	53.54x10 <sup>6</sup>	0.063	7.67x10 <sup>7</sup>	38.35x10 <sup>6</sup>
4	B21_017751_1609_ XN_19S347W	highly eroded	W	1726	200	20	66	6.6	35.91x10 <sup>6</sup>	0.070	6.90x10 <sup>6</sup>	34.52x10 <sup>5</sup>
4	B21_017751_1609_ XN_19S347W	highly eroded	E	1752	280	28	200	20	38.91x10 <sup>6</sup>	0.080	1.37x10 <sup>7</sup>	68.68x10 <sup>5</sup>
5	B10_013658_1434_ XI_36S202W		SW UPPER- MOST	17544	400	40	180	18	56.41x10 <sup>6</sup>	0.019	2.81x10 <sup>8</sup>	14.04x10 <sup>7</sup>
5	B10_013658_1434_ XI_36S202W		SW 2nd	20360	260	26	40	4	52.19x10 <sup>6</sup>	0.017	1.38x10 <sup>8</sup>	68.82x10 <sup>6</sup>
5	B10_013658_1434_ XI_36S202W		SW 3rd	5720	260	26	90	9	42.41x10 <sup>6</sup>	0.044	3.87x10 <sup>7</sup>	19.33x10 <sup>6</sup>
5	B10_013658_1434_ XI_36S202W		SW 4th	4882	190	19	50	5	42.41x10 <sup>6</sup>	0.051	1.76x10 <sup>7</sup>	88.12x10 <sup>5</sup>
5	B10_013658_1434_ XI_36S202W		NE UPPER- MOST	14950	400	40	200	20	11.83x10 <sup>7</sup>	0.013	2.39x10 <sup>8</sup>	11.96x10 <sup>7</sup>
5	B10_013658_1434_ XI_36S202W		NE 2nd	6708	120	12	50	5	76.15x10 <sup>5</sup>	0.043	9.66x10 <sup>6</sup>	48.30x10 <sup>5</sup>
5	B10_013658_1434_ XI_36S202W		NE 3rd	10620	260	26	150	15	16.94x10 <sup>6</sup>	0.036	7.18x10 <sup>7</sup>	35.90x10 <sup>6</sup>
5	B10_013658_1434_ XI_36S202W		NE 4th + 5th	21451	400	40	250	25	10.41x10 <sup>7</sup>	0.017	3.43x10 <sup>8</sup>	17.16x10 <sup>7</sup>
5	B10_013658_1434_ XI_36S202W		NE 6th	7452	160	16	60	6	20.31x10 <sup>6</sup>	0.048	1.91x10 <sup>7</sup>	95.39x10 <sup>5</sup>
5	B10_013658_1434_ XI_36S202W		SE UPPER	4679	300	30	90	9	69.42x10 <sup>6</sup>	0.046	4.21x10 <sup>7</sup>	21.06x10 <sup>6</sup>

5	B10_013658_1434_XI_36S202W		SE LOW-ER	6621	200	20	70	7	$16.75 \times 10^7$	0.045	$2.65 \times 10^7$	$13.24 \times 10^6$
5	B10_013658_1434_XI_36S202W		S	1997	170	17	60	6	$82.23 \times 10^6$	0.125	$5.77 \times 10^6$	$28.86 \times 10^5$
5	B10_013658_1434_XI_36S202W		North-ern Breach Valley	3652	280	28	80	8	N/A	0.011	$2.86 \times 10^7$	$14.31 \times 10^6$

**Table 2: Pit Data**

Crater #	Fan ID	Pit Depth (m)	Pit Vol. (m <sup>3</sup> )	Avg. Fan Slope (°)	Pit Fan Area (m <sup>2</sup> ) "A"	Fan Length (m) "l" or "r"	Max. Thickness "h <sub>max</sub> " (m)	Max Fan Width (m) "w"	Angle Width of Fan "θ"	Type 1: Fan Vol. (m <sup>3</sup> )	Type 2: Fan Vol. (m <sup>3</sup> )	Type 3: Fan Vol. (m <sup>3</sup> )
1	west	465	$35.84 \times 10^8$	10.69	$1.10 \times 10^6$	1218.44	230.04	1410	100.39	$19.76 \times 10^7$	$29.92 \times 10^7$	$25.38 \times 10^7$
1	east	465	$35.84 \times 10^8$	--	$6.22 \times 10^5$	--	--	--	--	--	--	--
2	upper nw	416.2	$46.41 \times 10^8$	--	$3.01 \times 10^6$	--	--	--	--	--	--	--
2	lower nw (with crater)	416.2	$46.41 \times 10^8$	--	$2.21 \times 10^6$	--	--	--	--	--	--	--
3	N/A	135.6	$33.46 \times 10^7$	N/A	N/A	N/A	N/A	N/A	N/A	N/A	N/A	N/A
4	south	317.4	$15.28 \times 10^8$	--	$1.50 \times 10^6$	--	--	--	--	--	--	--
4	North-east	317.4	$15.28 \times 10^8$	2.08	$4.33 \times 10^6$	2613.09	95	2580	61.93	$32.02 \times 10^7$	$35.06 \times 10^7$	$41.13 \times 10^7$
5	North-east	340	$10.30 \times 10^9$	5.25	$1.88 \times 10^6$	1850	170.04	1700	73.1	$26.74 \times 10^7$	$37.12 \times 10^7$	$31.96 \times 10^7$

Dashed cells refer to measurements that were not taken due to the fans not corresponding to MOLA Pedr data points.

**Table 3: Valley Fluxes**

Valley Network	Valley Flux: Type 1 (m <sup>3</sup> /s)	Valley Flux: Type 2 (Gravel) (m <sup>3</sup> /s)	Valley Flux: Type 2 (Sand) (m <sup>3</sup> /s)	Valley Flux - TYPE3 (m <sup>3</sup> /s)	Amount of liquid water (m/day) produced over the watershed (with flux of Type 3)
1W	17003	17930	21088	706	0.26
1E	19541	20636	24450	600	0.34
1S1 (rt. side)	21477	22713	27304	447	25.27
1S2 (left side)	15392	16276	19511	472	0.38
2W1 (top)	378989	390034	348946	2492	1.54
2W2 (mid.)	69726	73151	84673	1041	3.24
2W2 (bottom)	83610	87097	99471	1519	1.13
3N Right	20630	21771	25695	8015	28.17
3N Mid.	2759	2908	3651	213	--
3N Left	8191	8664	10480	398	0.40
3NW	9896	10467	12704	374	1.28
3W dn.	16710	19657	21011	548	1.12
3W Mid.	10603	11215	13566	398	1.05

3 W Upper	11505	12170	14720	398	1.72
3S	3151	3331	4091	303	0.18
4NE	122920	128497	147628	1276	0.55
4SW (top)	118405	124109	143364	1099	4.35
4SW (dn.)	430927	445190	503005	2158	3.48
4W	146980	153622	176436	1287	3.10
4E	76477	80376	93458	926	2.06
5SW uppermost	236652	244485	276235	2158	3.31
5SW 2nd	70968	74188	85233	1276	2.11
5SW 3rd	114173	119353	137123	1276	2.60
5SW 4th	53256	56019	65302	871	1.77
5NE Uppermost	195752	202231	228494	2158	1.58
5NE 2nd	14359	15180	18151	497	5.64
5 NE 3rd	103273	107959	124032	1276	6.51
5NE 4th+5th	223850	231260	261292	2158	1.79
5NE 6th	32672	34453	40521	706	3.00
5SE upper	170979	178108	203413	1519	1.89

5SE 2nd	57358	60282	70094	926	0.48
5S	63204	66595	78073	760	0.80
5 Northern Breach Val.	69560	72587	83133	1397	N/A

Crater number and network name is combined in this table to conserve space.

**Table 4: Channel Fluxes**

Val. Network	Channel Flux: Type 1 (m <sup>3</sup> /s)	Channel Flux: Type 2 (Gravel) (m <sup>3</sup> /s)	Channel Flux: Type 2 (Sand) (m <sup>3</sup> /s)	Channel Flux: Type 3 (m <sup>3</sup> /s)	Amt. Of liquid water produced over the watershed (m/day) (with flux of type 3)
1W	7895	8347	9980	497	0.18
1E	4394	4645	5705	303	0.17
1S1 (rt. side)	1433	473	616	130	7.35
1S2 (left side)	2715	2862	3594	213	0.17
2W1 (top)	32920	34657	40511	815	0.50
2W2 (mid.)	8517	9008	10896	398	1.24
2W2 (bottom)	15641	16493	19398	706	0.52
3N Right	2703	2854	3541	257	0.90

3N Mid.	1697	1782	2273	171	--
3N Left	1290	1355	1728	171	0.17
3NW	155	157	221	56	0.19
3W dn.	4578	4840	5945	303	0.62
3W Mid.	4096	4325	5366	257	0.68
3 W Upper	6346	6708	8239	303	1.31
3S	1463	1542	1936	213	0.13
4NE	61062	64175	74621	426	0.18
4SW (top)	7046	7448	9149	303	1.20
4SW (dn.)	31513	33255	39250	652	1.05
4W	3720	3926	4892	240	0.58
4E	76477	80376	93458	926	2.06
5SW uppermost	28141	29627	34630	815	1.25
5SW 2nd	482	504	656	130	0.215
5SW 3rd	6744	7133	8689	650	1.32
5SW 4th	1515	1591	2029	171	0.35
5NE Uppermost	30829	32400	37674	926	0.68

5NE 2nd	1391	1461	1863	171	1.94
5 NE 3rd	23821	25139	29670	652	3.33
5NE 4th+5th	63920	66880	76968	1216	1.01
5NE 6th	2389	2518	3162	213	0.91
5SE upper	6896	7293	8884	350	0.44
5SE 2nd	3490	3685	4571	257	0.13
5S	1243	1310	1646	213	0.22
5 Northern Breach Val.	2463	2604	3198	303	N/A

Crater number and network name is combined in this table to conserve space.

**Table 5: Valley Flux Type-1 Results**

Valley Network	Time required to fill pit with all valleys flowing (s)	Time required to fill pit with a single valley flowing (s)	Amt. Of water in pit in one earth day with all valleys flowing (m <sup>3</sup> )	Amt. Of water in pit in one earth day with one valley flowing (m <sup>3</sup> )	Amt of water in pit in 7 days with all valleys flowing (m <sup>3</sup> )	Amt. Of water in pit in 7 days with one valley flowing (m <sup>3</sup> )
1W	48822	210796	63.42x10 <sup>8</sup>	14.69x10 <sup>8</sup>	44.40x10 <sup>9</sup>	10.28x10 <sup>9</sup>
1E		183417		16.88x10 <sup>8</sup>		11.82x10 <sup>9</sup>
1S1 (rt. side)		166884		18.56x10 <sup>8</sup>		12.99x10 <sup>9</sup>
1S2 (left		232858		13.30x10 <sup>8</sup>		93.09x10 <sup>8</sup>

side)						
2W1 (top)	8718	12245	$45.99 \times 10^9$	$32.74 \times 10^9$	$32.20 \times 10^{10}$	$22.92 \times 10^{10}$
2W2 (mid.)		66555		$60.24 \times 10^8$		$42.17 \times 10^9$
2W2 (bottom)		55503		$72.24 \times 10^8$		$50.57 \times 10^9$
3N Right	4010	16220	$72.10 \times 10^8$	$17.82 \times 10^8$	$50.47 \times 10^9$	$12.48 \times 10^9$
3N Mid.		121279		$23.84 \times 10^7$		$16.69 \times 10^8$
3N Left		40851		$70.77 \times 10^7$		$49.54 \times 10^8$
3NW		33813		$85.50 \times 10^7$		$59.85 \times 10^8$
3W dn.		20024		$14.44 \times 10^8$		$10.11 \times 10^9$
3W Mid.		31558		$91.61 \times 10^7$		$64.13 \times 10^8$
3 W Upper		29084		$99.40 \times 10^7$		$69.58 \times 10^8$
3S		106191		$27.22 \times 10^7$		$19.06 \times 10^8$
4NE	1706	12433	$77.39 \times 10^9$	$10.62 \times 10^9$	$54.17 \times 10^{10}$	$74.34 \times 10^9$
4SW (top)		12907		$10.23 \times 10^9$		$71.61 \times 10^9$
4SW (dn.)		3546		$37.23 \times 10^9$		$26.06 \times 10^{10}$

4W		10397		$12.70 \times 10^9$		$88.89 \times 10^9$
4E		19983		$66.08 \times 10^8$		$46.25 \times 10^9$
5SW uppermost	7705	43513	$11.55 \times 10^{10}$	$20.45 \times 10^9$	$80.83 \times 10^{10}$	$14.31 \times 10^{10}$
5SW 2nd		145101		$61.32 \times 10^8$		$42.92 \times 10^9$
5SW 3rd		90192		$98.65 \times 10^8$		$69.05 \times 10^9$
5SW 4th		193359		$46.01 \times 10^8$		$32.21 \times 10^9$
5NE Uppermost		52605		$16.91 \times 10^9$		$11.84 \times 10^{10}$
5NE 2nd		717149		$12.41 \times 10^8$		$86.84 \times 10^8$
5 NE 3rd		99712		$89.23 \times 10^8$		$62.46 \times 10^9$
5NE 4th+5th		46002		$19.34 \times 10^9$		$13.54 \times 10^{10}$
5NE 6th		315179		$28.23 \times 10^8$		$19.76 \times 10^9$
5SE upper		60227		$14.77 \times 10^9$		$10.34 \times 10^{10}$
5SE 2nd		179531		$49.56 \times 10^8$		$34.69 \times 10^9$
5S		162925		$54.61 \times 10^8$		$38.23 \times 10^9$
5 Northern		148038		$60.10 \times 10^8$		$42.07 \times 10^9$

Breach Val.						
-------------	--	--	--	--	--	--

Crater number and network name is combined in this table to conserve space.

**Table 6: Valley Flux Type-2 Results (Gravel)**

Valley Network	Time required to fill pit with all valleys flowing (s)	Time required to fill pit with a single valley flowing (s)	Amt. Of water in pit in one earth day with all valleys flowing (m <sup>3</sup> )	Amt. Of water in pit in one earth day with one valley flowing (m <sup>3</sup> )	Amt of water in pit in 7 days with all valleys flowing (m <sup>3</sup> )	Amt. Of water in pit in 7 days with one valley flowing (m <sup>3</sup> )
1W	46214	199897	67.01x10 <sup>8</sup>	15.49x10 <sup>8</sup>	46.91x10 <sup>9</sup>	10.84x10 <sup>9</sup>
1E		173685		17.83x10 <sup>8</sup>		12.48x10 <sup>9</sup>
1S1 (rt. side)		157802		19.62x10 <sup>8</sup>		13.74x10 <sup>9</sup>
1S2 (left side)		220211		14.06x10 <sup>8</sup>		98.44x10 <sup>8</sup>
2W1 (top)	8433	11898	47.54x10 <sup>9</sup>	33.70x10 <sup>9</sup>	33.28x10 <sup>10</sup>	23.59x10 <sup>10</sup>
2W2 (mid.)		63439		63.20x10 <sup>8</sup>		44.24x10 <sup>9</sup>
2W2 (bottom)		53281		75.25x10 <sup>8</sup>		52.68x10 <sup>9</sup>
3N Right	3710	15369	77.92x10 <sup>8</sup>	18.72x10 <sup>7</sup>	54.54x10 <sup>9</sup>	13.11x10 <sup>8</sup>
3N Mid.		115065		25.01x10 <sup>6</sup>		17.51x10 <sup>7</sup>
3N Left		38621		74.51x10 <sup>6</sup>		52.16x10 <sup>7</sup>
3NW		31968		90.02x10 <sup>6</sup>		63.01x10 <sup>7</sup>

3W dn.		17022		$16.91 \times 10^7$		$11.83 \times 10^8$
3W Mid.		29836		$96.45 \times 10^6$		$67.51 \times 10^7$
3 W Upper		27495		$10.47 \times 10^7$		$73.26 \times 10^7$
3S		100453		$28.65 \times 10^6$		$20.05 \times 10^7$
4NE	1640	11893	$80.51 \times 10^9$	$11.05 \times 10^8$	$56.35 \times 10^{10}$	$77.36 \times 10^8$
4SW (top)		12313		$10.67 \times 10^8$		$74.71 \times 10^8$
4SW (dn.)		3433		$38.29 \times 10^8$		$26.80 \times 10^9$
4W		9948		$13.21 \times 10^8$		$92.48 \times 10^8$
4E		19013		$69.12 \times 10^7$		$48.39 \times 10^8$
5SW uppermost	7705	42119	$11.55 \times 10^{10}$	$21.03 \times 10^8$	$80.83 \times 10^{10}$	$14.72 \times 10^9$
5SW 2nd		138803		$63.80 \times 10^7$		$44.66 \times 10^8$
5SW 3rd		86278		$10.26 \times 10^8$		$71.85 \times 10^8$
5SW 4th		183822		$48.18 \times 10^7$		$33.72 \times 10^8$
5NE Uppermost		50920		$17.39 \times 10^8$		$12.17 \times 10^9$
5NE 2nd		678362		$13.05 \times 10^7$		$91.38 \times 10^7$
5 NE 3rd		95384		$92.84 \times 10^7$		$64.99 \times 10^8$

5NE 4th+5th		44528		$19.89 \times 10^8$		$13.92 \times 10^9$
5NE 6th		298887		$29.63 \times 10^7$		$20.74 \times 10^8$
5SE upper		57816		$15.32 \times 10^8$		$10.72 \times 10^9$
5SE 2nd		170823		$51.84 \times 10^7$		$36.29 \times 10^8$
5S		154629		$57.27 \times 10^7$		$40.09 \times 10^8$
5 N.Breach Val.		141865		$62.42 \times 10^7$		$43.70 \times 10^8$

Crater number and network name is combined in this table to conserve space.

**Table 7: Valley Flux Type-2 Results (Sand)**

Valley Network	Time required to fill pit with all valleys flowing (s)	Time required to fill pit with a single valley flowing (s)	Amt. Of water in pit in one earth day with all valleys flowing ( $m^3$ )	Amt. Of water in pit in one earth day with one valley flowing ( $m^3$ )	% of pit volume filled in 1 earth day by a single valley	Amt of water in pit in 7 days with all valleys flowing ( $m^3$ )	Amt. Of water in pit in 7 days with one valley flowing ( $m^3$ )
1W	38809	169962	$79.79 \times 10^8$	$18.22 \times 10^8$	50.83	$55.86 \times 10^9$	$12.75 \times 10^9$
1E		146591		$21.12 \times 10^8$	58.94		$14.79 \times 10^9$
1S1 (rt. side)		131269		$23.59 \times 10^8$	65.82		$16.51 \times 10^9$
1S2 (left side)		183699		$16.86 \times 10^8$	47.03		$11.80 \times 10^9$

2W1 (top)	8705	13299	$46.06 \times 10^9$	$30.15 \times 10^9$	649.68	$32.24 \times 10^{10}$	$21.10 \times 10^{10}$
2W2 (mid.)		54806		$73.16 \times 10^8$	157.65		$51.21 \times 10^9$
2W2 (bottom)		46653		$85.94 \times 10^8$	185.20		$60.16 \times 10^9$
3N Right	3159	13022	$91.51 \times 10^8$	$22.20 \times 10^8$	663.48	$64.06 \times 10^9$	$15.54 \times 10^9$
3N Mid.		91640		$31.54 \times 10^7$	94.27		$22.08 \times 10^8$
3N Left		31928		$90.55 \times 10^7$	270.61		$63.38 \times 10^8$
3NW		26339		$10.98 \times 10^8$	328.03		$76.83 \times 10^8$
3W dn.		15925		$18.15 \times 10^8$	542.53		$12.71 \times 10^9$
3W Mid.		24665		$11.72 \times 10^8$	350.29		$82.05 \times 10^8$
3 W Upper		22732		$12.72 \times 10^8$	380.09		$89.03 \times 10^8$
3S		81791		$35.35 \times 10^7$	105.63		$24.74 \times 10^8$
4NE	1436	10352	$91.92 \times 10^9$	$12.76 \times 10^9$	834.64	$64.34 \times 10^{10}$	$89.29 \times 10^9$
4SW (top)		10660		$12.39 \times 10^9$	810.53		$86.71 \times 10^9$
4SW (dn.)		3038		$43.46 \times 10^9$	2843.83		$30.42 \times 10^{10}$
4W		8662		$15.24 \times 10^9$	997.51		$10.67 \times 10^{10}$
4E		16352		$80.75 \times 10^8$	528.38		$56.52 \times 10^9$

5SW uppermost	7705	37278	$11.55 \times 10^{10}$	$23.87 \times 10^9$	231.77	$80.83 \times 10^{10}$	$16.71 \times 10^{10}$
5NE 2nd		120816		$73.64 \times 10^8$	71.51		$51.55 \times 10^9$
5 NE 3rd		75097		$11.85 \times 10^9$	115.05		$82.93 \times 10^9$
5NE 4th+5th		157691		$56.42 \times 10^8$	54.79		$39.49 \times 10^9$
5NE 6th		45067		$19.74 \times 10^9$	191.71		$13.82 \times 10^{10}$
5SE upper		567326		$15.68 \times 10^8$	15.23		$10.98 \times 10^9$
5SE 2nd		83023		$10.72 \times 10^9$	104.07		$75.01 \times 10^9$
5S		39410		$22.58 \times 10^9$	219.23		$15.80 \times 10^{10}$
5 Northern Breach Val.		254128		$35.01 \times 10^8$	34.00		$24.51 \times 10^9$
Valley Network		50624		$17.57 \times 10^9$	170.67		$12.30 \times 10^{10}$
1W		146910		$60.56 \times 10^8$	58.81		$42.39 \times 10^9$
1E		131896		$67.46 \times 10^8$	65.51		$47.22 \times 10^9$
1S1 (rt. side)		123868		$71.83 \times 10^8$	69.75		$50.28 \times 10^9$

Crater number and network name is combined in this table to conserve space.

**Table 8: Valleys Flux Type-3 Results**

Valley Network	Time required to fill pit with all valleys flowing (s)	Time required to fill pit with a single valley flowing (s)	Amt. Of water in pit in one earth day with all valleys flowing (m <sup>3</sup> )	Amt. Of water in pit in one earth day with one valley flowing (m <sup>3</sup> )	Amt of water in pit in 7 days with all valleys flowing (m <sup>3</sup> )	Amt. Of water in pit in 7 days with one valley flowing (m <sup>3</sup> )
1W	1610857	5076710	19.22x10 <sup>7</sup>	61.00x10 <sup>6</sup>	13.46x10 <sup>8</sup>	42.70x10 <sup>7</sup>
1E		5973595		51.84x10 <sup>6</sup>		36.29x10 <sup>7</sup>
1S1 (rt. side)		8018248		38.62x10 <sup>6</sup>		27.03x10 <sup>7</sup>
1S2 (left side)		7593553		40.78x10 <sup>6</sup>		28.55x10 <sup>7</sup>
2W1 (top)	918567	1862200	43.65x10 <sup>7</sup>	21.53x10 <sup>7</sup>	30.55x10 <sup>8</sup>	15.07x10 <sup>8</sup>
2W2 (mid.)		4457832		89.94x10 <sup>6</sup>		62.96x10 <sup>7</sup>
2W2 (bottom)		3055038		13.12x10 <sup>7</sup>		91.87x10 <sup>7</sup>
3N Right	31428	41748	91.99x10 <sup>7</sup>	69.25x10 <sup>7</sup>	64.39x10 <sup>8</sup>	48.47x10 <sup>8</sup>
3N Mid.		1570933		18.40x10 <sup>6</sup>		12.88x10 <sup>7</sup>
3N Left		840726		34.39x10 <sup>6</sup>		24.07x10 <sup>7</sup>
3NW		894676		32.31x10 <sup>6</sup>		22.62x10 <sup>7</sup>

3W dn.		610600		$47.35 \times 10^6$		$33.14 \times 10^7$
3W Mid.		840726		$34.39 \times 10^6$		$24.07 \times 10^7$
3 W Upper		840726		$34.39 \times 10^6$		$24.07 \times 10^7$
3S		1104319		$26.18 \times 10^6$		$18.33 \times 10^7$
4NE	226536	1197656	$58.29 \times 10^7$	$11.02 \times 10^7$	$40.80 \times 10^8$	$77.17 \times 10^7$
4SW (top)		1390545		$94.95 \times 10^6$		$66.47 \times 10^7$
4SW (dn.)		708160		$18.65 \times 10^7$		$13.05 \times 10^8$
4W		1187420		$11.12 \times 10^7$		$77.84 \times 10^7$
4E		1650334		$80.01 \times 10^6$		$56.00 \times 10^7$
5SW uppermos t	660904	4771797	$11.55 \times 10^{10}$	$18.65 \times 10^7$	$80.83 \times 10^{10}$	$13.05 \times 10^8$
5SW 2nd		8070171		$11.02 \times 10^7$		$77.17 \times 10^7$
5SW 3rd		8070171		$11.02 \times 10^7$		$77.17 \times 10^7$
5SW 4th		11822662		$75.25 \times 10^6$		$52.68 \times 10^7$
5NE Upper-		4771797		$18.65 \times 10^7$		$13.05 \times 10^8$

most					
5NE 2nd		20719393		$42.94 \times 10^6$	$30.06 \times 10^7$
5 NE 3rd		8070171		$11.02 \times 10^7$	$77.17 \times 10^7$
5NE 4th+5th		4771797		$18.65 \times 10^7$	$13.05 \times 10^8$
5NE 6th		14585748		$61.00 \times 10^6$	$42.70 \times 10^7$
5SE upper		6779156		$13.12 \times 10^7$	$91.87 \times 10^7$
5SE 2nd		11120452		$80.01 \times 10^6$	$56.00 \times 10^7$
5S		13549393		$65.66 \times 10^6$	$45.96 \times 10^7$
5 N. Breach Val.		7371180		$12.07 \times 10^7$	$84.49 \times 10^7$

Crater number and network name is combined in this table to conserve space.

**Table 9: Channel Flux Type-1 Results**

Valley Network	Time required to fill pit with all channels flowing (s)	Time required to fill pit with a single channel flowing (s)	Amt. Of water in pit in one earth day with all channels flowing (m <sup>3</sup> )	Amt. Of water in pit in one earth day with one channel flowing (m <sup>3</sup> )	Amt of water in pit in 7 days with all channels flowing (m <sup>3</sup> )	Amt. Of water in pit in 7 days with one channel flowing (m <sup>3</sup> )
1W	218054	453978	14.20x10 <sup>8</sup>	68.21x10 <sup>7</sup>	99.41x10 <sup>8</sup>	47.75x10 <sup>8</sup>
1E		815693		37.96x10 <sup>7</sup>		26.57x10 <sup>8</sup>
1S1 (rt. side)		2501156		12.38x10 <sup>7</sup>		86.67x10 <sup>7</sup>
1S2 (left side)		1320131		23.46x10 <sup>7</sup>		16.42x10 <sup>8</sup>
2W1 (top)	81303	140966	49.32x10 <sup>8</sup>	28.44x10 <sup>8</sup>	34.52x10 <sup>9</sup>	19.91x10 <sup>9</sup>
2W2 (mid.)		544864		73.59x10 <sup>7</sup>		51.51x10 <sup>8</sup>
2W2 (bottom)		296695		13.51x10 <sup>8</sup>		94.60x10 <sup>8</sup>
3N Right	14986	123792	19.29x10 <sup>8</sup>	23.35x10 <sup>7</sup>	13.50x10 <sup>9</sup>	16.35x10 <sup>8</sup>
3N Mid.		197177		14.66x10 <sup>7</sup>		10.26x10 <sup>8</sup>
3N Left		259387		11.15x10 <sup>7</sup>		78.02x10 <sup>7</sup>
3NW		2158766		13.39x10 <sup>6</sup>		93.74x10 <sup>6</sup>
3W dn.		73091		39.55x10 <sup>7</sup>		27.69x10 <sup>8</sup>

3W Mid.		81692		$35.39 \times 10^7$		$24.77 \times 10^8$
3 W Upper		52728		$54.83 \times 10^7$		$38.38 \times 10^8$
3S		228714		$12.64 \times 10^7$		$88.48 \times 10^7$
4NE	8499	25027	$15.54 \times 10^9$	$52.76 \times 10^8$	$10.88 \times 10^{10}$	$36.93 \times 10^9$
4SW (top)		216890		$60.88 \times 10^7$		$42.61 \times 10^8$
4SW (dn.)		48495		$27.23 \times 10^8$		$19.06 \times 10^9$
4W		410809		$32.14 \times 10^7$		$22.50 \times 10^8$
4E		19983		$66.08 \times 10^8$		$46.25 \times 10^9$
5SW uppermost	60269	365927	$14.76 \times 10^9$	$24.31 \times 10^8$	$10.33 \times 10^{10}$	$17.02 \times 10^9$
5SW 2nd		21364188		$41.64 \times 10^6$		$29.15 \times 10^7$
5SW 3rd		1526919		$58.27 \times 10^7$		$40.79 \times 10^8$
5SW 4th		6797055		$13.09 \times 10^7$		$91.63 \times 10^7$
5NE Uppermost		334021		$26.64 \times 10^8$		$18.65 \times 10^9$
5NE 2nd		7402975		$12.02 \times 10^7$		$84.13 \times 10^7$
5 NE 3rd		432288		$20.58 \times 10^8$		$14.41 \times 10^9$
5NE 4th+5 <sup>th</sup>		161100		$55.23 \times 10^8$		$38.66 \times 10^9$

5NE 6th		4310397		$20.64 \times 10^7$		$14.45 \times 10^8$
5SE upper		1493263		$59.58 \times 10^7$		$41.71 \times 10^8$
5SE 2nd		2950584		$30.15 \times 10^7$		$21.11 \times 10^8$
5S		8284424		$10.74 \times 10^7$		$75.18 \times 10^7$
5 N. Breach Val.		4180893		$21.28 \times 10^7$		$14.90 \times 10^8$

Crater number and network name is combined in this table to conserve space.

**Table 10: Channel Flux Type-2 Results (Gravel)**

Valley Network	Time required to fill pit with all channels flowing (s)	Time required to fill pit with a single channel flowing (s)	Amt. Of water in pit in one earth day with all channels flowing ( $m^3$ )	Amt. Of water in pit in one earth day with one channel flowing ( $m^3$ )	Amt of water in pit in 7 days with all channels flowing ( $m^3$ )	Amt. Of water in pit in 7 days with one channel flowing ( $m^3$ )
1W	219523	429395	$14.11 \times 10^8$	$72.12 \times 10^7$	$98.75 \times 10^8$	$50.48 \times 10^8$
1E		771616		$40.13 \times 10^7$		$28.09 \times 10^8$
1S1 (rt. side)		7577499		$40.87 \times 10^6$		$28.61 \times 10^7$
1S2 (left side)		1252326		$24.73 \times 10^7$		$17.31 \times 10^8$
2W1 (top)	77140	133901	$51.98 \times 10^8$	$29.94 \times 10^8$	$36.38 \times 10^9$	$20.96 \times 10^9$

2W2 (mid.)		515165		$77.83 \times 10^7$		$54.48 \times 10^8$
2W2 (bottom)		281368		$14.25 \times 10^8$		$99.75 \times 10^8$
3N Right	14201	117242	$20.36 \times 10^8$	$24.66 \times 10^7$	$14.25 \times 10^9$	$17.26 \times 10^8$
3N Mid.		187771		$15.40 \times 10^7$		$10.78 \times 10^8$
3N Left		246944		$11.71 \times 10^7$		$81.95 \times 10^7$
3NW		2131266		$13.56 \times 10^6$		$94.95 \times 10^6$
3W dn.		69134		$41.82 \times 10^7$		$29.27 \times 10^8$
3W Mid.		77366		$37.37 \times 10^7$		$26.16 \times 10^8$
3 W Upper		49882		$57.96 \times 10^7$		$40.57 \times 10^8$
3S		216997		$13.32 \times 10^7$		$93.26 \times 10^7$
4NE	8078	23813	$16.35 \times 10^9$	$55.45 \times 10^8$	$11.44 \times 10^{10}$	$38.81 \times 10^9$
4SW (top)		205184		$64.35 \times 10^7$		$45.05 \times 10^8$
4SW (dn.)		45954		$28.73 \times 10^8$		$20.11 \times 10^9$
4W		389254		$33.92 \times 10^7$		$23.74 \times 10^8$
4E		19013		$69.44 \times 10^8$		$48.61 \times 10^9$
5SW uppermost	57355	347573	$15.51 \times 10^9$	$25.60 \times 10^8$	$10.86 \times 10^{10}$	$17.92 \times 10^9$

5SW 2nd		20431624		$43.55 \times 10^6$		$30.48 \times 10^7$
5SW 3rd		1443648		$61.63 \times 10^7$		$43.14 \times 10^8$
5SW 4th		6472369		$13.75 \times 10^7$		$96.22 \times 10^7$
5NE Uppermost		317825		$27.99 \times 10^8$		$19.60 \times 10^9$
5NE 2nd		7048281		$12.62 \times 10^7$		$88.36 \times 10^7$
5 NE 3rd		409624		$21.72 \times 10^8$		$15.20 \times 10^9$
5NE 4th+5th		153970		$57.78 \times 10^8$		$40.45 \times 10^9$
5NE 6th		4089570		$21.76 \times 10^7$		$15.23 \times 10^8$
5SE upper		1411976		$63.01 \times 10^7$		$44.11 \times 10^8$
5SE 2nd		2794447		$31.84 \times 10^7$		$22.29 \times 10^8$
5S		7860716		$11.32 \times 10^7$		$79.23 \times 10^7$
5 N. Breach Val.		3954508		$22.50 \times 10^7$		$15.75 \times 10^8$

Crater number and network name is combined in this table to conserve space.

**Table 11: Channel Flux Type-2 Results (Sand)**

Valley Network	Time required to fill pit with all channels flowing (s)	Time required to fill pit with a single channel flowing (s)	Amt. Of water in pit in one earth day with all channels flowing (m <sup>3</sup> )	Amt. Of water in pit in one earth day with one channel flowing (m <sup>3</sup> )	% of pit volume filled in 1 earth day by a single channel	Amt of water in pit in 7 days with all channels flowing (m <sup>3</sup> )	Amt. Of water in pit in 7 days with one channel flowing (m <sup>3</sup> )
1W	180154	359134	17.19x10 <sup>8</sup>	86.23x10 <sup>7</sup>	24.06	12.03x10 <sup>9</sup>	60.36x10 <sup>8</sup>
1E		628248		49.29x10 <sup>7</sup>	13.75		34.50x10 <sup>8</sup>
1S1 (rt. side)		5818437		53.22x10 <sup>6</sup>	1.48		37.26x10 <sup>7</sup>
1S2 (left side)		997261		31.05x10 <sup>7</sup>	8.66		21.74x10 <sup>8</sup>
2W1 (top)	65541	114552	61.18x10 <sup>8</sup>	35.00x10 <sup>8</sup>	75.42	42.82x10 <sup>9</sup>	24.50x10 <sup>9</sup>
2W2 (mid.)		425900		94.14x10 <sup>7</sup>	20.29		65.90x10 <sup>8</sup>
2W2 (bottom)		239231		16.76x10 <sup>8</sup>	36.12		11.73x10 <sup>9</sup>
3N Right	11440	94496	25.27x10 <sup>8</sup>	30.59x10 <sup>7</sup>	91.43	17.69x10 <sup>9</sup>	21.42x10 <sup>8</sup>
3N Mid.		147210		19.64x10 <sup>7</sup>	58.69		13.75x10 <sup>8</sup>
3N Left		193639		14.93x10 <sup>7</sup>	44.62		10.45x10 <sup>8</sup>
3NW		1514067		19.09x10 <sup>6</sup>	5.71		13.37x10 <sup>7</sup>

3W dn.		56284		$51.36 \times 10^7$	153.51		$35.96 \times 10^8$
3W Mid.		62357		$46.36 \times 10^7$	138.56		$32.45 \times 10^8$
3 W Upper		40613		$71.18 \times 10^7$	212.74		$49.83 \times 10^8$
3S		172835		$16.73 \times 10^7$	49.99		$11.71 \times 10^8$
4NE	6903	20480	$19.13 \times 10^9$	$64.47 \times 10^8$	421.88	$13.39 \times 10^{10}$	$45.13 \times 10^9$
4SW (top)		167036		$79.05 \times 10^7$	51.73		$55.33 \times 10^8$
4SW (dn.)		38935		$33.91 \times 10^8$	221.91		$23.74 \times 10^9$
4W		312389		$42.27 \times 10^7$	27.66		$29.59 \times 10^8$
4E		16352		$80.75 \times 10^8$	528.38		$56.52 \times 10^9$
5SW uppermost	48933	297359	$18.18 \times 10^9$	$29.92 \times 10^8$	29.06	$12.73 \times 10^{10}$	$20.94 \times 10^9$
5SW 2nd		15697467		$56.68 \times 10^6$	0.55		$39.67 \times 10^7$
5SW 3rd		1185124		$75.07 \times 10^7$	7.29		$52.55 \times 10^8$
5SW 4th		5075179		$17.53 \times 10^7$	1.70		$12.27 \times 10^8$
5NE Uppermost		273333		$32.55 \times 10^8$	31.61		$22.79 \times 10^9$

5NE 2nd		5527396		$16.10 \times 10^7$	1.56		$11.27 \times 10^8$
5 NE 3rd		347069		$25.63 \times 10^8$	24.89		$17.94 \times 10^9$
5NE 4th+5th		133790		$66.50 \times 10^8$	64.58		$46.55 \times 10^9$
5NE 6th		3256654		$27.32 \times 10^7$	2.65		$19.12 \times 10^8$
5SE upper		1159111		$76.76 \times 10^7$	7.45		$53.73 \times 10^8$
5SE 2nd		2252798		$39.49 \times 10^7$	3.84		$27.65 \times 10^8$
5S		6256099		$14.22 \times 10^7$	1.38		$99.55 \times 10^7$
5 N.Breach Val.		3219993		$27.63 \times 10^7$	2.68		$19.34 \times 10^8$

Crater number and network name is combined in this table to conserve space.

**Table 12: Channel Flux Type-3 Results**

Valley Network	Time required to fill pit with all channels flowing (s)	Time required to fill pit with a single channel flowing (s)	Amt. Of water in pit in one earth day with all channels flowing ( $m^3$ )	Amt. Of water in pit in one earth day with one channel flowing ( $m^3$ )	Amt of water in pit in 7 days with all channels flowing ( $m^3$ )	Amt. Of water in pit in 7 days with one channel flowing ( $m^3$ )
1W	3135745	7211583	$98.76 \times 10^6$	$42.94 \times 10^6$	$69.13 \times 10^7$	$30.06 \times 10^7$
1E		11828901		$26.18 \times 10^6$		$18.33 \times 10^7$
1S1 (rt.		27570438		$11.23 \times 10^6$		$78.62 \times 10^6$

side)						
1S2 (left side)		16827028		$18.40 \times 10^6$		$12.88 \times 10^7$
2W1 (top)	2418240	5693991	$16.58 \times 10^7$	$70.42 \times 10^6$	$11.61 \times 10^8$	$49.29 \times 10^7$
2W2 (mid.)		11659806		$34.39 \times 10^6$		$24.07 \times 10^7$
2W2 (bottom)		6573092		$61.00 \times 10^6$		$42.70 \times 10^7$
3N Right	193304	1301980	$14.96 \times 10^7$	$22.20 \times 10^6$	$10.47 \times 10^8$	$15.54 \times 10^7$
3N Mid.		1956776		$14.77 \times 10^6$		$10.34 \times 10^7$
3N Left		1956776		$14.77 \times 10^6$		$10.34 \times 10^7$
3NW		5975156		$48.38 \times 10^5$		$33.87 \times 10^6$
3W dn.		1104319		$26.18 \times 10^6$		$18.33 \times 10^7$
3W Mid.		1301980		$22.20 \times 10^6$		$15.54 \times 10^7$
3 W Upper		1104319		$26.18 \times 10^6$		$18.33 \times 10^7$
3S		1570933		$18.40 \times 10^6$		$12.88 \times 10^7$
4NE	600004	3587346	$22.01 \times 10^7$	$36.81 \times 10^6$	$15.40 \times 10^8$	$25.76 \times 10^7$

4SW (top)		5043595		$26.18 \times 10^6$		$18.33 \times 10^7$
4SW (dn.)		2343879		$56.33 \times 10^6$		$39.43 \times 10^7$
4W		6367539		$20.74 \times 10^6$		$14.52 \times 10^7$
4E		1650334		$80.01 \times 10^6$		$56.00 \times 10^7$
5SW uppermo st	1786526	12635016	$49.80 \times 10^7$	$70.42 \times 10^6$	$34.86 \times 10^8$	$49.29 \times 10^7$
5SW 2nd		79211834		$11.23 \times 10^6$		$78.62 \times 10^6$
5SW 3rd		15842367		$56.16 \times 10^6$		$39.31 \times 10^7$
5SW 4th		60219523		$14.77 \times 10^6$		$10.34 \times 10^7$
5NE Uppermo st		11120452		$80.01 \times 10^6$		$56.00 \times 10^7$
5NE 2nd		60219523		$14.77 \times 10^6$		$10.34 \times 10^7$
5 NE 3rd		15793771		$56.33 \times 10^6$		$39.43 \times 10^7$
5NE 4th+5th		8468370		$10.51 \times 10^7$		$73.54 \times 10^7$
5NE 6th		48345251		$18.40 \times 10^6$		$12.88 \times 10^7$

5SE upper		29421538		$30.24 \times 10^6$		$21.17 \times 10^7$
5SE 2nd		40068243		$22.20 \times 10^6$		$15.54 \times 10^7$
5S		48345251		$18.40 \times 10^6$		$12.88 \times 10^7$
5 N. Breach Val.		33985275		$26.18 \times 10^6$		$18.33 \times 10^7$

Crater number and network name is combined in this table to conserve space.

## 9. REFERENCES

- Alzate, N., Barlow, N. G., 2011. Central pit craters on Ganymede. *Icarus* 211, 1274-1283.
- Barlow, N. G., 2010. Central pit craters: observations from Mars and Ganymede and implications for formation models. In: Gibson, R. L., and Reimold, W. U. (Eds.), *Large Meteorite Impacts and Planetary Evolution IV: Geological Society of America Special Paper 465*, P. 15-27, doi: 10.1130/2010.2465(02).
- Burr, D. M., Williams, R. M. E., Nussbaumer, J., Zimbelman, J. R., 2006. Multiple, distinct, (glacio?)fluvial paleochannels throughout the western Medusae Fossae formation, Mars. 37<sup>th</sup> Lunar and Planetary Science Conference, abs. no. 1367.
- Carr, M. H., 1996. *Water on Mars*. New York: Oxford University Press, 248 pp.
- Carr, M. H., Crumpler, L. S., Cutts, J. A., Greeley, R., Guest, J. E., Masursky, H., 1977. Martian Impact Craters and Emplacement of Ejecta by Surface Flow. *Journal of Geophysical Research* 82, 4055-4065.
- Carr, M. H., Head, J. W., 2003. Basal melting of snow on early Mars: a possible origin of some valley networks. *Geophysical Research Letters* 30(24), 2245, doi: 10.1029/2003GL018575.
- Carr, M. H., Schaber, G. G., 1977. Martian permafrost features. *Journal of Geophysical Research* 82, 4039-4054.
- Christensen, P. R., 2003. Formation of recent martian gullies through melting of extensive water-rich snow deposits. *Nature* 422, 45-48.
- Costard, F., Forget, F., Mangold, N., Peulvast, J. P., 2002. Formation of recent martian debris flows by melting of near-surface ground ice at high obliquity. *Science* 295, 110-113.
- Craddock, R. A., Howard, A. D., 2002. The case for rainfall on a warm, wet early Mars. *Journal of Geophysical Research* 107(E11), 5111, doi: 10.1029/2001JE001505.
- Craddock, R. A., Maxwell, T. A., Howard, A. D., 1997. Crater morphometry and modification in the Sinus Sabaeus and Margaritifer Sinus regions of Mars. *Journal of Geophysical Research* 102, 13,321-13,340.
- Croft, S. K. 1981. On the origin of pit craters. 7<sup>th</sup> Lunar and Planetary Science Conference, 196-198 (abstract).

- Croft, S. K., 1983. A proposed origin for palimpsests and anomalous pit craters on Ganymede and Callisto. Proceedings of the Fourteenth Lunar and Planetary Science Conference, Part 1. Journal of Geophysical Research 88, supplement B71-B89.
- Di Achille, G., Ori, G. G., Reiss, D., 2007. Evidence for late Hesperian lacustrine activity in Shalbatana Vallis, Mars. Journal of Geophysical Research 112, E07007, doi: 10.1029/2006JE002858.
- Dickson, J. L., Fassett, C. I., Head, J. W., 2009. Amazonian-aged fluvial valley systems in a climatic microenvironment on Mars: melting of ice deposits on the interior of Lyot Crater. Geophysical Research Letters 36, L08201, doi: 10.1029/2009GL037472.
- Dickson, J. L., Head, J. W., 2009. The formation and evolution of youthful gullies on Mars: Gullies as the late-stage phase of Mars' most recent ice age. Icarus 204, 63-86.
- Dickson, J. L., Head, J. W., Kreslavsky, M., 2007. Martian gullies in the southern mid-latitudes of Mars: evidence for climate-controlled formation of young fluvial features based upon local and global topography. Icarus 188, 315-323. Doi: 10.1016/j.icarus.2006.11.020
- Dohm, J. M., Tanaka, K. L., 1999. Geology of the Thaumasia region, Mars: plateau development, valley origins, and magmatic evolution. Planetary and Space Science 47, 411-431.
- Elder, C. M., Bray, V. J., Melosh, H. J., 2010. Central pit formation in Ganymede craters via melt drainage. 41<sup>st</sup> Lunar and Planetary Science Conference, abs. no. 2519.
- Farmer, C. B., Davies, D. W., Holland, A. L., 1977. Mars: Water Vapor Observations From the Viking Orbiters. Journal of Geophysical Research, 82, 4225-4248.
- Fassett, C. I., Dickson, J. L., Head, J. W., Levy, J. S., Marchant, D. R., 2010. Supraglacial and proglacial valleys on Amazonian Mars. Icarus 208, 86-100.
- Fassett, C. I., Head, J. W., 2005. Fluvial sedimentary deposits on Mars: ancient deltas in a crater lake in the Nili Fossae region. Geophysical Research Letters 32, L14201, doi: 10.1029/2005GL023456.
- Fassett, C. I., Head, J. W. III, 2008. Valley network-fed, open-basin lakes on Mars: Distribution and implications for Noachian surface and subsurface hydrology. Icarus 198, 37-56.
- Foster, M. A., Kelsey, H. M., 2012. Knickpoint and knickzone formation and propagation, South Fork Eel River, northern California. Geosphere 8, 403-416. Doi: 10.1130/GES00700.

- Garner, K. M. L., Barlow, N. G., 2012. Distribution of rimmed, partially rimmed, and non-rimmed central floor pits on Mars. 43<sup>rd</sup> Lunar and Planetary Science Conference, abs. no. 1256.
- Grant, J. A., Wilson, S. A., 2011. Late alluvial fan formation in southern Margaritifer Terra, Mars. *Geophysical Research Letters* 38, L08201, doi:10.1029/2001GL046844.
- Grin, E. A., Cabrol, N. A., 1997. Limnologic Analysis of Gusev Crater Paleolake, Mars. *Icarus* 130, 461-474.
- Gulick, V. C., 2001. Origin of the valley networks on Mars: a hydrological perspective. *Geomorphology* 37, 241-268.
- Gulick, V. C., Baker, V. R., 1989. Fluvial valleys and martian paleoclimates. *Nature* 341, 514-516.
- Hale, W. S., Head, J. W., 1981. Central structures in martian craters: preliminary implications for substrate volatile effects. 3<sup>rd</sup> International Colloquium on Mars, p. 104.
- Head, J. W., Mustard, J. F., Kreslavsky, M. A., Milliken, R. E., Marchant, D.R., 2003. Recent ice ages on Mars. *Nature* 426, 797-802.
- Head, J. W., Neukum, G., Jaumann, R., Hiesinger, H., Hauber, E., Carr, M., Masson, P., Foing, B., Hoffman, H., Kreslavsky, M., Werner, S., Milkovich, S., van Gasselt, The HRSC Co-Investigator Team, 2005. Tropical to mid-latitude snow and ice accumulation, flow and glaciations on Mars. *Nature* 434, 346-351.
- Heldmann, J. L., Mellon, M. T., 2004. Observations of martian gullies and constraints on potential formation mechanisms. *Icarus* 168, 285-304.
- Hodges, C. A., 1978a. Central pit craters on Mars. 9<sup>th</sup> Lunar and Planetary Science Conference, 521-522 (abstract).
- Hodges, C. A., 1978b. Central pit craters, peak rings, and the Argyre Basin. In: Strom, R., Boyce, J. M., (Eds). *Reports of Planetary Geology Program, 1977-1978*, pp. 169-171.
- Hodges, C. A., Shew, N. B., Clow, G., 1980. Distribution of central pit craters on Mars. 11<sup>th</sup> Lunar and Planetary Science Conference, 450-452 (abstract).
- Holt, J. W., Safaeinili, A., Plaut, J. J., Head, J. W., Phillips, R. J., Seu, R., Kempf, S. D., Choudhary, P., Young, D. A., Putzig, N. E., Biccari, D., Gim, Yonggyu, 2008. Radar sounding evidence for buried glaciers in the southern mid-latitudes of Mars. *Science* 332, 1235-1238.
- Hynek, B. M., Beach, M., Hoke, M. R. T., 2010. Updated global map of Martian valley networks and implications for climate and hydrological processes. *Journal of Geophysical Research* 115, E09008, doi: 10.1029/2009JE003548.

- Irwin III, R. P., Craddock, R. A., Howard, A. D., 2005. Interior channels in Martian valley networks: Discharge and runoff production. *Geology* 33, 489-492, doi: 10.1130/G21333.
- Jakosky, B. M., Farmer, C. B., 1982. The seasonal and global behavior of water vapor in the Mars atmosphere: complete global results of the Viking atmospheric water detector experiment. *Journal of Geophysical Research* 87, 2999-3019.
- Jerolmack, D. J., Mohrig, D., Zuber, M. T., Byrne, S., 2004. A minimum time for the formation of Holden Northeast fan, Mars. *Geophysical Research Letters* 31, L21701, doi: 10.1029/2004GL021326.
- Jones, A. P., McEwen, A. S., Tornabene, L. L., Baker, V. R., Melosh, H. J., Berman, D. C., 2011. A geomorphic analysis of Hale crater, Mars: The effects of impact into ice-rich crust. *Icarus* 211, 259-272.
- Kite, E. S., Michaels, T. I., Rafkin, S., Manga, M., Dietrich, W. E., 2011. Localized precipitation and runoff on Mars. *Journal of Geophysical Research* 116, E07002, doi: 10.1029/2010JE003783.
- Kraal, E. R., Asphaug, E., Moore, J. M., Howard, A., Brecht, A., 2008. Catalogue of large alluvial fans in martian impact craters. *Icarus* 194, 101-110.
- Malin, M. C., Bell III, J. F., Cantor, B. A., Caplinger, M. A., Calvin, W. M., Clancy, R. T., Edgett, K. S., Edwards, L., Haberle, R. M., James, P. B., Lee, S. W., Ravine, M. A., Thomas, P. C., Wolff, M. J., 2007. Context camera investigation on board the Mars Reconnaissance Orbiter. *Journal of Geophysical Research* 112, E05S04, doi: 10.1029/2006JE002808.
- Malin, M. C., Carr, M. H., 1999. Groundwater formation of Martian valleys. *Nature* 397, 589-591.
- Malin, M. C., Edgett, K. S., 2000. Evidence for Recent Groundwater Seepage and Surface Runoff on Mars. *Science* 288, 2330-2335.
- Malin, M. C., Edgett, K. S., 2003. Evidence for Persistent Flow and Aqueous Sedimentation on Early Mars. *Science* 302, 1931-1934.
- Mangold, N., Ansan, V., 2006. Detailed study of an hydrological system of valleys, a delta and lakes in the Southwest Thaumasia region, Mars. *Icarus* 180, 75-87.
- Mangold, N., Quantin, C., Ansan, V., Delacourt, C., Allemand, P., 2004. Evidence for Precipitation on Mars from Dendritic Valleys in the Valles Marineris Area. *Science* 305, 78-81. DOI: 10.1126/science.1097549.
- Mars Channel Working Group, 1983. Channels and Valleys on Mars. *Geological Society of America Bulletin* 94, 1035-1054.

- Mellon, M. T., Jakosky, B. M., 1995. The distribution and behavior of Martian ground ice during past and present epochs. *Journal of Geophysical Research* 100, 11,781-11,799.
- Montgomery, D. R., Gillespie, A., 2005. Formation of Martian outflow channels by catastrophic dewatering of evaporate deposits. *Geology* 33, 625-628.
- Moore, J. M., Howard, A. D., 2005. Large alluvial fans on Mars. *Journal of Geophysical Research* 110, E04005, doi: 10.1029/2004JE002352.
- Moore, J. M., Howard, A. D., Dietrich, W. E., Schenk, P. M., 2003. Martian layered fluvial deposits: implications for Noachian climate scenarios. *Geophysical Research Letters* 30(24), 2292, doi: 10.1029/2003GL019002.
- Moore, J. M., Malin, M. C., 1988. Dome craters on Ganymede. *Geophysical Research Letters* 15, 225-228.
- Moratto, Z. M., Brozton, M. J., Beyer, R. A., Lundy, M., and K. Husmann, 2010. Ames Stereo Pipeline, NASA's Open Source Automated Stereogrammetry Software. 41<sup>st</sup> Lunar and Planetary Science Conference, 2364 (abstract).
- Morgan, G. A., Head III, J. W., 2009. Sinton crater, Mars: evidence for impact into a plateau icefield and melting to produce valley networks at the Hesperian-Amazonian boundary. *Icarus* 202, 39-59.
- Morris, A. R., Mouginiis-Mark, P. J., Garbeil, H., 2010. Possible impact melt and debris flows at Tooting Crater, Mars. *Icarus* 209, 369-389.
- Mouginiis-Mark, P. J., Tornabene, L. L., Boyce, J. M., McEwen, A. S., 2007. Impact melt and water release at tooting crater, Mars. *Seventh International Conference on Mars*, abs. no. 3039.
- Mustard, J. F., Cooper, C. D., Rifkin, M. K., 2001. Evidence for recent climate change on Mars from the identification of youthful near-surface ground ice. *Nature* 412, 411-414.
- Neukum, G. et al., 2004. HRSC: the High Resolution Stereo Camera of Mars Express, ESA Sp. Pub. 1240, 17-36.
- Pain, C. F., Clarke, J. D. A., Thomas, M., 2007. Inversion of relief on Mars. *Icarus* 190, 478-491.
- Parker, G., Andrews, E. D., 1986. On the time development of meander bends. *Journal of Fluid Mechanics* 162, 139-156.
- Pierazzo, E., Artemieva, N. A., Ivanov, B. A., 2005. Starting conditions for hydrothermal systems underneath Martian craters: Hydrocode modeling. In: Kenkmann, T., Hörz, F., and Deutsch, A., (Eds.). *Large meteorite impacts III: Geological Society of America Special Paper 384*, p. 443-457.
- Pieri, D. C., 1980. Martian valley: morphology, distribution, age, and origin. *Science* 210, 895-897.

- Pilkington, M., Grieve, R. A. F., 1992. The geophysical signature of terrestrial impact craters. *Reviews of Geophysics* 30, 161-181.
- Plaut, J. J., Safaeinili, A., Holt, J. W., Phillips, R. J., Head III, J. W., Seu, R., Putzig, N. E., Frigeri, A., 2009. Radar evidence for ice in lobate debris aprons in the mid-northern latitudes of Mars. *Geophysical Research Letters* 36, L02203, doi:10.1029/2008GL036379.
- Pondrelli, M., Rossi, A. P., Marinangeli, L., Hauber, E., Gwinner, K., Baliva, A., Di Lorenzo, S., 2008. Evolution and depositional environments of the Eberswalde fan delta, Mars. *Icarus* 197, 429-451.
- Rice, J. W., Mollard, J. D., 1994. Analogs and interpretations for the martian thumbprint terrain and sinuous ridges. 25<sup>th</sup> Lunar and Planetary Science Conference, 1127-1128 (abstract).
- Richey, J. E., Nobre, C., Deser, C., 1989. Amazon River Discharge and Climate Variability: 1903 to 1985. *Science* 246, 101-103.
- Ritter, D. F., Kochel, R. C., Miller, J. R., 2006. *Process Geomorphology*; 4th ed. Long Grove, Illinois: Waveland Press, Inc. 560 pp.
- Schenk, P. M., 1993. Central pit and dome craters: exposing the interiors of Ganymede and Callisto. *Journal of Geophysical Research* 98, 7475-7498.
- Segura, T. L., Toon, O. B., Colaprete, A., Zahnle, K., 2002. Environmental effects of large impacts on Mars. *Science* 298, 1977-1980.
- Senft, L. E., Stewart, S. T., 2009. The role of phase changes during impact cratering on icy satellites. 40<sup>th</sup> Lunar and Planetary Science Conference, abs. no. 2130.
- Smith, E. I., 1976. Comparison of the crater morphology-size relationship for Mars, Moon and Mercury. *Icarus* 28, 543-550.
- Smith, M. D., 2004. Interannual variability in TES atmospheric observations of Mars during 1999-2003. *Icarus* 167, 148-165.
- Soderblom, L. A., Kreidler, T. J., Masursky, H., 1973. Latitudinal distribution of a debris mantle on the Martian surface. *Journal of Geophysical Research* 78, 4117-4122.
- Spinrad, H., Munch, G., Kaplan, L. D. 1963. The detection of water vapor on Mars. *Astrophysics Journal* 137, 1319-1321.
- Squyres, S. W., 1978. Martian fretted terrain: flow of erosional debris. *Icarus* 34, 600-613.
- Squyres, S. W., 1979. The distribution of lobate debris aprons and similar flows on Mars. *Journal of Geophysical Research* 84, 8087-8096.

- Squyres, S. W., Carr, M. H., 1986. Geomorphic evidence for the distribution of ground ice on Mars. *Science* 231, 249-252.
- Stewart, S. T., Ahrens, T. J., O'Keefe, J. D., 2004. Impact-induced melting of near-surface water ice on Mars. In: Furnish, M. D., Gupta, Y. M., Forbes, J. W., (Eds.). *Shock Compression of Condensed Matter—2003*. AIP, New York, pp. 1484-1487.
- Tanaka, K. L., Kolb, E. J., 2001. Geologic history of the polar regions of Mars based on Mars Global Surveyor Data. *Icarus* 154, 3-21.
- Titus, T. N., Kieffer, H. H., Christensen, P. R., 2003. Exposed water ice discovered near the south pole of Mars. *Science* 299, 1048-1051.
- Toon, O. B., Segura, T., Zahnle, K., 2010. The formation of martian river valleys by impacts. *Annual Review Earth Planetary Science* 38, 303-322.
- Wang, C., Manga, M., Wong, A., 2005. Floods on Mars released from groundwater by impact. *Icarus* 175, 551-555.
- Weitz, C. M., Irwin III, R. P., Chuang, F. C., Bourke, M. C., Crown, D. A., 2006. Formation of a terraced fan deposit in Coprates Catena, Mars. *Icarus* 184, 436-451.
- Williams, R. M. E., Edgett, K. S., 2005. Valleys in the Martian record. 36th Lunar and Planetary Science Conference, abs. no. 1099.
- Williams, R. M. E., Edgett, K. S., Malin, M. C., 2004. Young fans in an equatorial crater in Xanthe Terra, Mars. 35<sup>th</sup> Lunar and Planetary Science Conference, abs. no. 1415.
- Williams, R. M. E., Malin, M. C., 2008. Sub-kilometer fans in Mojave Crater, Mars. *Icarus* 198, 365-383.
- Williams, R. M. E., Phillips, R. J., 2001. Morphometric measurements of martian valley networks from Mars Orbiter Laser Altimeter (MOLA) data. *Journal of Geophysical Research* 106, 23737-23751.
- Williams, K. E., Toon, O. B., Heldmann, J. L., Mellon, M. T., 2009. Ancient melting of mid-latitude snowpacks on Mars as a water source for gullies. *Icarus* 200, 418-425.
- Wilson, L., Ghatan, G. J., Head III, J. W., Mitchell, K. L., 2004. Mars outflow channels: A reappraisal of the estimation of water flow velocities from water depths, regional slopes, and channel floor properties. *Journal of Geophysical Research* 109, E09003, doi: 10.1029/2004JE002281.
- Wood, C. A., Head, J. W., Cintala, M. J., 1978. Interior morphology of fresh martian craters: the effects of target characteristics. *Proc. Lunar Planet. Sci. Conf.* 9, 3691-3709.

Zuber, M. T., Smith, D. E., Solomon, S. C., Muhleman, D. O., Head, J. W., Garvin, J. B., Abshire, J. B., Bufton, J. L., 1992. The Mars Observer Laser Altimeter Investigation. *Journal of Geophysical Research* 97, 7781-7797.